REFERENCE ONLY

UNIVERSITY OF LONDON THESIS

Degree PhD Year 2006 Name of Author HOLLANDS R.

The orexins and their involvement in the modulation of trigeminovascular nociceptive transmission

Philip Robert Holland

Thesis submitted for the Degree of Doctor of Philosophy at the faculty of Medicine, University of London.

Headache Group
Institute of Neurology
University College London
Queen Square
London
WC1N 3BG

2006

ProQuest LLC
789 East Eisenhower Parkway
P.O. Box 1346
Ann Arbor, MI 48106-1346

Abstract

Migraine is a common and disabling condition that affects up to 15% of the population. This thesis sought to explore a possible role of the orexins in migraine by investigating aspects of their effect on trigeminovascular physiology. The orexins are two neuropeptides synthesised in the lateral and posterior hypothalamic nuclei that have recently been implicated in the modulation of nociceptive processing.

To investigate a possible role of the orexins in the pathophysiology of migraine, different animal models of trigeminovascular activation were used to identify possible modulatory functions. Intravital microscopy uses dilation of dural blood vessel as a measure of trigeminal nerve activation, and thus compounds inhibiting the vasodilator response have the potential to inhibit trigeminovascular nociceptive transmission. Orexin A, but not B was able to significantly inhibit the observed dilation, an effect reversed by the selective orexin 1 (OX_1) receptor antagonist SB-334867.

Central modulatory roles of the orexins were investigated using electrophysiological methods. Orexin A and B and SB-334867 were given intravenously, or microinjected into the ventrolateral PAG (vlPAG) of the anaesthetised rat, and the responses of trigeminocervical complex (TCC) neurons to a variety of stimuli examined. Orexin A inhibited trigeminal neurons in the TCC when given intravenously or microinjected into the vlPAG, via activation of the OX_1 receptor. Orexin B demonstrated a differential effect, resulting in a facilitation of trigeminal neuronal firing when microinjected into the vlPAG.

The orexinergic system was also investigated in the feline model of trigeminovascular activation via stimulation of the SSS. Double-labelled immunohistochemistry for Fos and orexin A or B was utilised to identify orexinergic neurons that are activated in the hypothalamus in response to trigeminovascular activation. A subpopulation of orexin synthesising neurons were shown to be activated in response to SSS stimulation, demonstrating that either efferent or afferent nociceptive transmission from the hypothalamus may involve orexinergic systems.

Contents

Figures and Tables

Published Papers and Abstract

Papers

Holland PR, Akerman S and Goadsby PJ. Orexin 1 receptor activation attenuates neurogenic dural vasodilation in an animal model of trigeminovascular activation. The Journal of Pharmacology and Experimental Therapeutics 2005; 315 (3): 1380–1385.

Abstracts

Holland PR, Akerman S and Goadsby PJ. Hypothalamic neuropeptides orexin A and B: modulation of central and peripheral pathways in the pathophysiology of migraine. Cephalalgia 2005; 25 (10): 857.

Holland PR, Akerman S, Lasalandra M, Van der Gucht E, Classey J and Goadsby PJ. Hypothalamic neurones that contain orexin A and B express *c-fos* in response to superior sagittal sinus (SSS) stimulation in the cat. Cephalalgia 2005; 25 (12): 1194–1195.

Holland PR, Akerman S and Goadsby PJ. Modulation of nociceptive dural input to orexin A and B receptor activation in the rat. Cephalalgia 2005; 25 (10): 872.

Acknowledgements

I would like to thank my parents, Philip and Elizabeth, and my family for their support over the years. I would also like to thank Laura Easton, my long suffering fiancée and and her parents, William and Morag for their support throughout the past few years.

I would like to thank Professor Peter Goadsby and Dr Simon Akerman, for their excellent supervision and guidance, enabling me to complete this thesis. I am also indebted to all the remaining members of the Headache Group and the Denny-Brown Laboratories for their assistance. I am particularly thankful to Ria Bhola, Andreas Gantenbein, Paul Hammond, Holger Kaube, Michele Lasalandra, Kevin Shields and Ben Townsend for their help and friendship over the past three years.

I would finally like express my sincere thanks to the Wellcome Trust for their financial support over the past three years.

Chapter 1 – General Introduction

History of Migraine

The following historical review is adapted from cited sources (Pearce, 1986; Rosner, 1993; Silberstein et al., 1998; Isler and Rose, 2000).

Headache is not a modern phenomenon; evidence suggests that Neolithic man performed trepanation around 7000 years BC (Lyons and Petrucelli, 1978). This form of treatment was widely used until the seventeenth century and was initially thought to release demons and evil spirits from the head and thus relieve the pain. The ancient Egyptians mentioned headaches as far back as 1200 BC in the Ebers Papyrus, which is thought to be based on older text dating back to 1550 BC (Edmeads, 1990; Karenberg and Leitz, 2001).

Figure 1: The treatment of Headache in 1200 BC.

The Egyptians believed in placing herbs in the mouth of a clay crocodile and securing it to the patients head with a linen strip to relieve head pain (Silberstein et al., 1998).

The Egyptians described symptoms similar to that of migraine and believed in binding a clay crocodile holding grain to the patients head as a cure (figure 1). It was not until 400 BC that the first definite association with migraine could be drawn, when Hippocrates described the visual aura that can precede migraine and could be relieved by vomiting. 'A shining light, usually in the right eye, followed by violent pain beginning in the temples and eventually reaching the entire head and neck area' (Lance, 1982; Edmeads, 1990). At this time numerous hypotheses for the cause of migraine were suggested and this reflected a move from the spiritual demons to intrinsic causes. Hippocrates correctly believed that headache could be triggered by exercise and sexual intercourse (Lance, 1982) although he was incorrect in his belief that it was caused by vapours rising from the stomach to the head (Lance, 1982; Edmeads, 1990). Plato also noticed that headaches could be triggered and he reasoned that a preoccupation with the body was the main cause (Plato, 1961).

Celsus in 215–300 AD also recognised some well established triggers for headaches such as the drinking of wine and heat or cold. However, it is Aretaeus of Cappadocia who is generally credited with the discovery of migraine due to his classic descriptions of one sided pain accompanied by gastrointestinal distress and visual disturbances (Critchley, 1967). It is not until the late 1700s (Willis, 1672), that vascular theories for migraine were proposed and this led to Erasmus Darwin suggesting that patients should be centrifuged to force blood to the feet, away from the head (Lance, 1982; Edmeads, 1990).

Liveing was the first to postulate the neural theory of migraine in his monograph 'On Megrim, Sick-headache and Some Allied Disorders: A Contribution to the Pathology of Nerve-Storms' in 1873 (Liveing, 1873). William Gowers published his famous two volume work "Diseases of the Nervous System" in 1886 (Gowers, 1886), which contained a substantial chapter on 'Migraine: Paroxysmal Headache'. Gowers referred to the two main theories of migraine postulated at the time; neural storm and vascular. He sided more with the neural hypothesis and favoured the cortex as the site of neural disturbances with the involvement of lower centres (Pearce, 1984, 1985).

It was not until the late 1930s, that Harold Wolff carried out the first laboratory studies of headache. In his widely cited book 'Wolff's Headache and Other Head Pain' (Wolff, 1948) he identified the need to know which structures of the head are sensitive to pain. Wolff identified that most of the intracranial structures including the dura mater and blood vessels are pain sensitive and thus he added great support to the vascular theory of migraine.

Liveing's neural theory gained substantially from the work of Leao, who published work on cortical spreading depression (SD) in the rabbit (Leao, 1944). Leao was the first to propose the neurogenic theory of migraine, which hypothesises that alterations of blood flow develop as a consequence of a neuronal event. Leao's SD manifested itself as a marked decrease in spontaneous activity which slowly spreads in all directions over the ipsilateral cortex.

The remaining historical perspective from this point is synonymous with the current understanding and beliefs of the pathophysiology and treatment of migraine, and as such will be integrated with the main body of this thesis.

Epidemiology of Migraine

Migraine is one of the most common neurological disorder affecting humans. Epidemiological studies carried out after the International Headache Society classification of 1988 (updated in 2004) (Headache Classification Committee of the International Headache Society, 2004), suggest a lifetime prevalence of 16% with a female to male ratio of approximately 3:1. The one year overall prevalence was 6% in males and 15% in females. Another study carried out in France found 4% and 11.9% prevalence in male and females respectively (Henry et al., 1992; Henry et al., 2002; Henry, 2004), with an overall population prevalence of 8.1%. The male to female ratio in Europe is similar to that in America and Africa although the exact percentages differ. America has a prevalence of 5.9% and 17.6% respectively (Lipton et al., 2001; Lipton et al., 2002; Lipton and Bigal, 2005), while Africa has a much lower prevalence of 1.7% in

males and 4.2% in females (Tekle Haimanot et al., 1995). A recent survey carried out over five countries across Europe and America found an overall prevalence of between 5% and 12% in agreement with previous epidemiologic studies (MacGregor et al., 2003).

As well as the gender differences in migraine, age, race, geography, and socio-economic status play an important role in the prevalence of the disease state (Stewart et al., 1995). Gender differences in the occurrence of migraine attacks are not seen in pre-pubescent children, however with the onset of puberty it becomes more common in women (Epstein et al., 1975; Lipton et al., 2001). This rise in the prevalence of migraine in women which peaks with a one year prevalence of about 30% in 30 to 39 year olds (Lipton et al., 2001) declines after the onset of menopause (Neri et al., 1993; Fettes, 1999), indicating the influence of hormonal changes on migraine occurrence.

Menstrual Migraine

The normal female hormonal cycle experiences many influences during life, including menarche, pregnancy, contraception, hormone replacement therapy and the menopause. During menstrual cycles attacks of migraine without aura, but not with aura, are more likely to occur 2 days before onset and on the first 2 days of menses (Mannix, 2003). This form of attack is most likely to be a result of oestrogen withdrawal (Somerville, 1972, 1975a, b). Oestrogen and progestin's are known to have potent effects on both central serotonergic and opioid neurons, thus providing a possible central modulatory explanation for menstrual migraine. The use of oral contraceptives can improve, worsen or have no effect on migraine occurrence (Silberstein, 1995, 2000). Pregnancy can provide relief for some women who generally suffer from menstrual migraine, thought to be due to stabilisation of oestrogen levels (Silberstein, 1997).

Migraine Triggers

Hormonal changes as seen in menstrual migraine (Silberstein, 1995; MacGregor, 2000; Silberstein, 2000) are the most reliable triggers of attacks in females, however there are a number of other well characterised triggers. Triggers can be both external and internal stimuli that the migraineur is abnormally responsive to, resulting in the onset of an attack. As migraine triggers vary greatly from one patient to another, much of the evidence is anecdotal as opposed to scientific. Common well accepted triggers are summarised in table 1, and any single trigger may not be enough to illicit an attack on its own. It is important to bear in mind that certain migraine triggers may not be a causative factor, but a result of the migraine premonitory symptoms, giving the appearance of a triggering role.

Table 1: Potential migraine triggers.

It is important to remember that certain 'triggers' may actually be caused as a result of the impending attack and not be a causative factor for that attack (Headache Classification Committee of the International Headache Society, 2004).

Diet:	**Head or neck pain:**
Hunger	Of a different cause
Alcohol	**Physical exertion:**
Additives	Exercise
Certain food types	Sex
Chronobiologic:	**Stress and anxiety:**
Sleep disruption	Letdown
Schedule	**Head trauma**
Hormonal changes:	
Menstruation	
Environmental factors:	
Light Intensity	
Odours	
Altitude	

Migraine Attack & Classification

Migraine is defined as a common, chronic, incapacitating neurovascular disorder which results in severe, normally unilateral, pulsating headaches which can involve neurological symptoms resulting in aura. Aura symptoms are typically seen in about 15–20% of patients (Rasmussen and Olesen, 1992). Migraine without aura is the most common form and a typical attack if left untreated lasts between 4–72 hours and can be accompanied by nausea, photophobia and phonophobia (Headache Classification Committee of the International Headache Society, 2004). Migraine diagnosis requires that a patient's symptoms must fulfil certain criteria (table 2) set out by the International Headache Society (Headache Classification Committee of the International Headache Society, 2004).

Table 2: Diagnostic criteria for migraine.

Diagnostic criteria for migraine:	
A.	At least 5 attacks fulfilling criteria B–D
B.	Headache attacks lasting 4–72 hours
C.	Headache has at least two of the following characteristics: 1. unilateral location 2. pulsating quality 3. moderate or severe pain intensity 4. aggravation by or causing avoidance of routine physical activity
D.	During headache at least one of the following: 1. nausea and / or vomiting 2. photophobia and phonophobia
E.	Not attributed to another disorder

(Headache Classification Committee of the International Headache Society, 2004)

Table 3: International Headache Society (IHS) classification system.

1 Migraine		
1.1		Migraine without aura
1.2		Migraine with aura
	1.2.1	Typical aura with migraine headache
	1.2.2	Typical aura with non-migraine headache
	1.2.3	Typical aura without headache
	1.2.4	Familial hemiplegic migraine (FHM)
	1.2.5	Sporadic hemiplegic migraine
	1.2.6	Basilar-type migraine
1.3		Childhood periodic syndromes that are commonly precursors of migraine
	1.3.1	Cyclical vomiting
	1.3.2	Abdominal migraine
	1.3.3	Benign paroxysmal vertigo of childhood
1.4		Retinal migraine
1.5		Complications of migraine
	1.5.1	Chronic migraine
	1.5.2	Status Migrainous
	1.5.3	Persistent aura without infarction
	1.5.4	Migrainous infarction
	1.5.5	Migraine-triggered seizure
1.6		Probable migraine
	1.6.1	Probable migraine without aura
	1.6.2	Probable migraine with aura
	1.6.3	Probable chronic migraine

(Headache Classification Committee of the International Headache Society, 2004)

The migraine attack is typically divided into three or four phases depending on the presence of aura, the premonitory phase, the aura, the headache phase and finally the postdrome.

The Premonitory phase

Premonitory symptoms, those neurological symptoms occurring prior to the onset of headache have been recognised for many years (Gowers, 1888). These symptoms (table 4) are reported in up to 60% of migraineurs and can vary from psychological/neurological disturbances to general feelings of unrest. The exact symptoms are variable depending on the patient, however a study carried out by Giffin and colleagues demonstrated reproducible headache predictive symptoms (Giffin et al., 2003).

Table 4: Premonitory symptoms of migraine.

Psychologic	Neurologic	General
Depressed	Photophobia	Stiff neck
Hyperactive	Phonophobia	Food cravings/Anorexia
Euphoric	Difficulty concentrating	Cold feeling
Talkative	Dysphasia	Sluggish
Irritable	Hyperosmia	Diarrhoea/Constipation
Drowsy	Yawning	Thirst
Restless		Urination/Fluid retention

(Headache Classification Committee of the International Headache Society, 2004)

The exact cause of the premonitory symptoms observed in the majority of migraineurs are not yet fully known, however evidence suggests a link with a disturbance of the hypothalamus (Zurak, 1997). The hypothalamus is the main centre for the integration of endocrine functions, autonomic responses and behaviour, and governs the rythmicity of

many bodily functions (Saper, 1990; Swaab, 1997). This may account for the periodicity of migraine attacks.

The Aura

Wolff originally proposed that migraine aura was caused by a rebound vasoconstriction of the blood vessels (Wolff, 1948). However work carried out by Leao (1944) in the rabbit, identified a spreading depression of activity in the cerebral cortex that moved at a rate of about 2–3 mm/min. This work, backed up by Grafstein's discovery that at the margin of the advancing cortical depression neurons become highly active (Grafstein, 1956a, b), identified a neuronal phenomena which could be the cause of aura in humans. Lashley, who himself suffered migraine plotted the course of his visual aura (Fig 2.) and calculated that it spread across the cortex at the same rate as Leao's spreading depression (Lashley, 1941). Thus the aura is now thought to be a wave of cortical spreading depression (CSD) which spreads out from the occipital lobe across the cortex, resulting in an initial hyperaemic phase followed by a oligaemic phase (Olesen et al., 1990; Lauritzen, 1994; Olesen, 1998). The aura symptoms typically develop over 5–20 minutes and last for less than 1 hour (Headache Classification Committee of the International Headache Society, 2004). Migraine aura can result in many neurological phenomena including visual, sensory and motor symptoms and may also result in language problems and brain stem dysfunctions. Headache follows aura about 80% of the time and usually commences while cerebral blood flow remains diminished (Olesen et al., 1990).

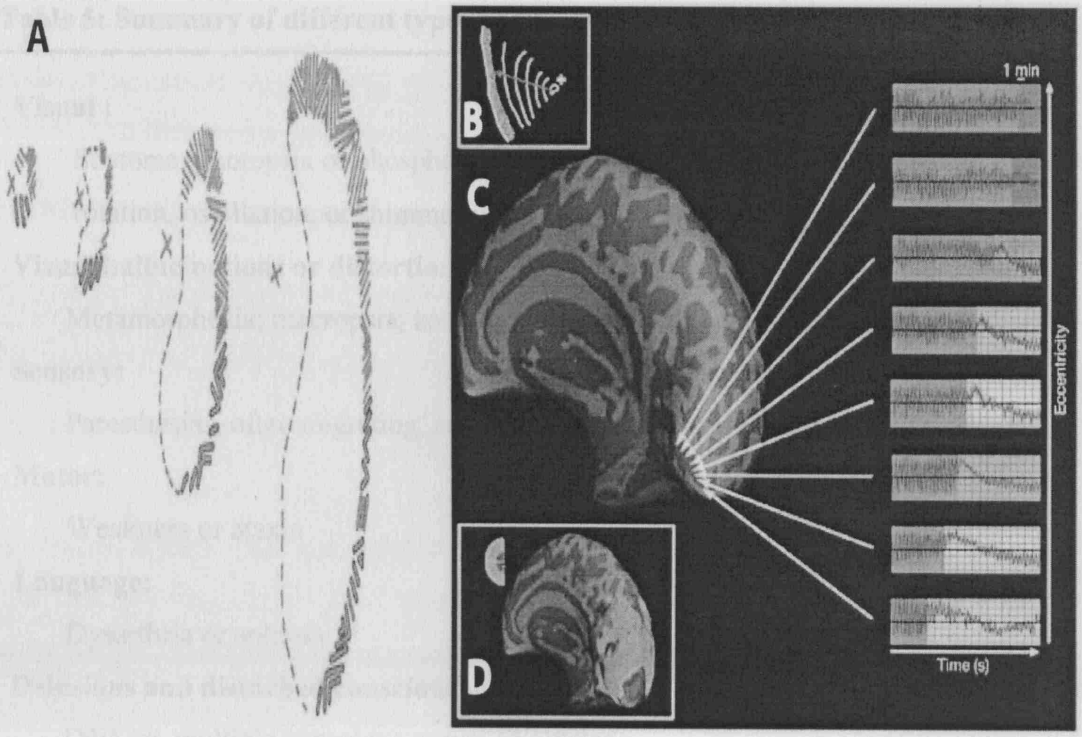

Figure 2: Lashley's visual aura and a visual field defect of a patient studied with brain imaging.

(A) Lashley's visual aura progressing across his visual field (Lashley, 1941). (B) Visual field defect of a patient studied with brain imaging. The red arrow shows the overall direction of progression of the visual percept. (C) Reconstruction of the patient's brain on the basis of anatomical data. Signal changes over time are shown to the right. Each time course was recorded from one in a sequence of voxels that were sampled along the primary visual cortex, from the posterior pole to a more anterior location, as indicated by arrowheads. A similar blood oxygenation level-dependent response was found within all of the extrastriate areas, differing only in the time of onset of the magnetic resonance perturbations. The perturbations developed earlier in the foveal representation, compared with more eccentric representations of retinotopic visual cortex. This finding was consistent with the progression of the aura from central to peripheral eccentricities in the corresponding visual field (B and D). (D) The maps of retinotopic eccentricity from the same subject as in B and C, acquired during interictal scans. As shown in the logo in the upper left, voxels that show retinotopically specific activation in the fovea are coded in red. Parafoveal eccentricities are shown in blue, and more peripheral eccentricities are shown in green (Hadjikhani et al., 2001).

Table 5: Summary of different types of aura.

Visual :

Scotoma; photopsia or phosphenes: geometric forms; fortification spectra; rotation, oscillation, or shimmering of objects; excessive brightness

Visual hallucinations or distortions:

Metamorphosia; macropsia; zoom or mosaic vision

Sensory:

Paresthesias, often migrating, and can become bilateral olfactory hallucinations

Motor:

Weakness or ataxia

Language:

Dysarthria or aphasia

Delusions and disturbed consciousness:

Déjà vu, multiple conscious trance-like states.

(Silberstein et al., 2001)

The Headache

Migraine headache is typically unilateral, with a throbbing quality of moderate to marked severity that exacerbates over time and can be aggravated by movement. The pain may be bilateral in about one third of cases and can move from one side to the other during an attack (Selby and Lance, 1960; Lance and Anthony, 1966). The attack commonly occurs in the morning and can last for 4–72 hours with a gradual onset which peaks and then slowly subsides (Silberstein et al., 1998). The attack is normally combined with other clinical features including nausea, vomiting, anorexia and sensory disturbances such as photophobia and phonophobia (Headache Classification Committee of the International Headache Society, 2004).

Resolution phase

After the headache has subsided many patients report varying symptoms. Lethargy, lack of concentration and a washed out and irritable sensation are among the most common reported (Blau, 1991). However some patients report feelings of euphoria and freshness commonly combined with food cravings. The headache can still be felt if excessive movement is undertaken and this can last for several days (Lance, 1982).

Migraine Treatment

Migraine treatments akin to the migrainous symptoms are variable depending on the individual patient. Once a correct diagnosis has been made, any coexisting disorders and biological conditions need to be considered. In general migraine therapy can be split into two modalities; prophylactic or acute depending on the frequency and severity of attacks and in severe cases both approaches may be employed.

Prophylactic Treatment

Prophylactic treatment is given when the incidence of attack is greater than 2–3 per month, the severity of attack is sufficient to impair normal function or when the patient is unable to cope and only in the event of acute therapy failing or causing serious side effects. Prophylaxis should be carefully considered if pregnancy is a possibility. Possible prophylactic therapies include anticonvulsants, antidepressants, β-blockers, calcium channel antagonists, serotonin antagonists and nonsteroidal anti-inflammatory drugs (NSAID, table 6).

Table 6: Prophylactic migraine treatments.

Anticonvulsants:	
	Valproate, gabapentin, topiramate
Antidepressants:	
	Tricyclic antidepressants, selective serotonin reuptake inhibitors, monoamine oxidase inhibitors
β-Adrenergic blockers:	
	Propranolol, nadolol, metoprolol, atenolol
Calcium channel antagonists:	
	Verapamil, flunarazine
Serotonin antagonists:	
	Methysergide, methergine
Others:	
	Nonsteroidal anti-inflammatory drugs, riboflavin, magnesium, neuroleptics, coenzyme Q10, feverfew,

(Silberstein et al., 2001)

The available prophylactic drugs are taken even when the headache is not present in an attempt to reduce the frequency of attacks and if one single drug is ineffective combination therapies can be utilised.

Acute Treatment

As with the prophylactic treatment, the frequency and severity of a patient's migraine determines the acute medication. Acute intervention is recommended at an early stage as this may prevent the attack worsening and increases the effectiveness of the drug (Burstein et al., 2004). Two forms of acute treatment are available, the non-specific analgesics and the specific acute headache treatments (table 7). Non-specific therapies are utilised for the treatment of migraine pain as well as that of other disorders, whereas

the specific acute headache treatments have no general analgesic properties and only treat the migraine attack.

Table 7: Different types of medication for acute attacks.

Non-specific acute medications	Specific acute treatments
Analgesics (NSAID and combination analgesics)	Ergotamine
Antiemetics	Dyhydroergotamine
Opiods	Triptans (5-HT receptor agonists)
Corticosteroids	
Dopamine antagonists	

Adapted from (Silberstein et al., 2001).

Since the 1980's and the discovery of the 5-$HT_{1B/1D}$ receptor agonists the acute treatment of migraine has been revolutionised. The triptans were developed on the basis of clinical observations that 5-hydroxyindoleacetic acid (the main metabolite of serotonin) was increased in the urine of patients during migraine attack (Curran et al., 1965). Further research also identified that platelet 5-HT levels decreased at the onset of migraine (Curran et al., 1965) and that intravenous 5-HT could abort headache (Kimball et al., 1960; Anthony, 1968; Anthony et al., 1968). The triptans target specific subclasses of the 5-HT_1 receptors that show a differential distribution in the central and peripheral pathways of migraine. 5-HT_{1B}, 5-HT_{1D} and 5-HT_{1F} receptor mRNA are expressed in the human trigeminal ganglia and afferents, however only 5-HT_{1D} immunoreactivity is found on trigeminal sensory nerve endings and only 5-HT_{1B} immunoreactivity on the cranial blood vessels (Beer et al., 1993; Longmore et al., 1997). The localisation of the 5-HT_{1F} receptor to the trigeminal nucleus caudalis (TNC) and the differential distribution of the 5-$HT_{1B/1D}$ receptors make them prime candidates for involvement in the pathophysiology of migraine (figure 3).

Migraine Attack & Classification

Migraine is defined as a common, chronic, incapacitating neurovascular disorder which results in severe, normally unilateral, pulsating headaches which can involve neurological symptoms resulting in aura. Aura symptoms are typically seen in about 15–20% of patients (Rasmussen and Olesen, 1992). Migraine without aura is the most common form and a typical attack if left untreated lasts between 4–72 hours and can be accompanied by nausea, photophobia and phonophobia (Headache Classification Committee of the International Headache Society, 2004). Migraine diagnosis requires that a patient's symptoms must fulfil certain criteria (table 2) set out by the International Headache Society (Headache Classification Committee of the International Headache Society, 2004).

Table 2: Diagnostic criteria for migraine.

Diagnostic criteria for migraine:	
A.	At least 5 attacks fulfilling criteria B–D
B.	Headache attacks lasting 4–72 hours
C.	Headache has at least two of the following characteristics: 1. unilateral location 2. pulsating quality 3. moderate or severe pain intensity 4. aggravation by or causing avoidance of routine physical activity
D.	During headache at least one of the following: 1. nausea and / or vomiting 2. photophobia and phonophobia
E.	Not attributed to another disorder

(Headache Classification Committee of the International Headache Society, 2004)

Table 3: International Headache Society (IHS) classification system.

1 Migraine		
1.1		Migraine without aura
1.2		Migraine with aura
	1.2.1	Typical aura with migraine headache
	1.2.2	Typical aura with non-migraine headache
	1.2.3	Typical aura without headache
	1.2.4	Familial hemiplegic migraine (FHM)
	1.2.5	Sporadic hemiplegic migraine
	1.2.6	Basilar-type migraine
1.3		Childhood periodic syndromes that are commonly precursors of migraine
	1.3.1	Cyclical vomiting
	1.3.2	Abdominal migraine
	1.3.3	Benign paroxysmal vertigo of childhood
1.4		Retinal migraine
1.5		Complications of migraine
	1.5.1	Chronic migraine
	1.5.2	Status Migrainous
	1.5.3	Persistent aura without infarction
	1.5.4	Migrainous infarction
	1.5.5	Migraine-triggered seizure
1.6		Probable migraine
	1.6.1	Probable migraine without aura
	1.6.2	Probable migraine with aura
	1.6.3	Probable chronic migraine

(Headache Classification Committee of the International Headache Society, 2004)

The migraine attack is typically divided into three or four phases depending on the presence of aura, the premonitory phase, the aura, the headache phase and finally the postdrome.

The Premonitory phase

Premonitory symptoms, those neurological symptoms occurring prior to the onset of headache have been recognised for many years (Gowers, 1888). These symptoms (table 4) are reported in up to 60% of migraineurs and can vary from psychological/neurological disturbances to general feelings of unrest. The exact symptoms are variable depending on the patient, however a study carried out by Giffin and colleagues demonstrated reproducible headache predictive symptoms (Giffin et al., 2003).

Table 4: Premonitory symptoms of migraine.

Psychologic	Neurologic	General
Depressed	Photophobia	Stiff neck
Hyperactive	Phonophobia	Food cravings/Anorexia
Euphoric	Difficulty concentrating	Cold feeling
Talkative	Dysphasia	Sluggish
Irritable	Hyperosmia	Diarrhoea/Constipation
Drowsy	Yawning	Thirst
Restless		Urination/Fluid retention

(Headache Classification Committee of the International Headache Society, 2004)

The exact cause of the premonitory symptoms observed in the majority of migraineurs are not yet fully known, however evidence suggests a link with a disturbance of the hypothalamus (Zurak, 1997). The hypothalamus is the main centre for the integration of endocrine functions, autonomic responses and behaviour, and governs the rythmicity of

many bodily functions (Saper, 1990; Swaab, 1997). This may account for the periodicity of migraine attacks.

The Aura

Wolff originally proposed that migraine aura was caused by a rebound vasoconstriction of the blood vessels (Wolff, 1948). However work carried out by Leao (1944) in the rabbit, identified a spreading depression of activity in the cerebral cortex that moved at a rate of about 2–3 mm/min. This work, backed up by Grafstein's discovery that at the margin of the advancing cortical depression neurons become highly active (Grafstein, 1956a, b), identified a neuronal phenomena which could be the cause of aura in humans. Lashley, who himself suffered migraine plotted the course of his visual aura (Fig 2.) and calculated that it spread across the cortex at the same rate as Leao's spreading depression (Lashley, 1941). Thus the aura is now thought to be a wave of cortical spreading depression (CSD) which spreads out from the occipital lobe across the cortex, resulting in an initial hyperaemic phase followed by a oligaemic phase (Olesen et al., 1990; Lauritzen, 1994; Olesen, 1998). The aura symptoms typically develop over 5–20 minutes and last for less than 1 hour (Headache Classification Committee of the International Headache Society, 2004). Migraine aura can result in many neurological phenomena including visual, sensory and motor symptoms and may also result in language problems and brain stem dysfunctions. Headache follows aura about 80% of the time and usually commences while cerebral blood flow remains diminished (Olesen et al., 1990).

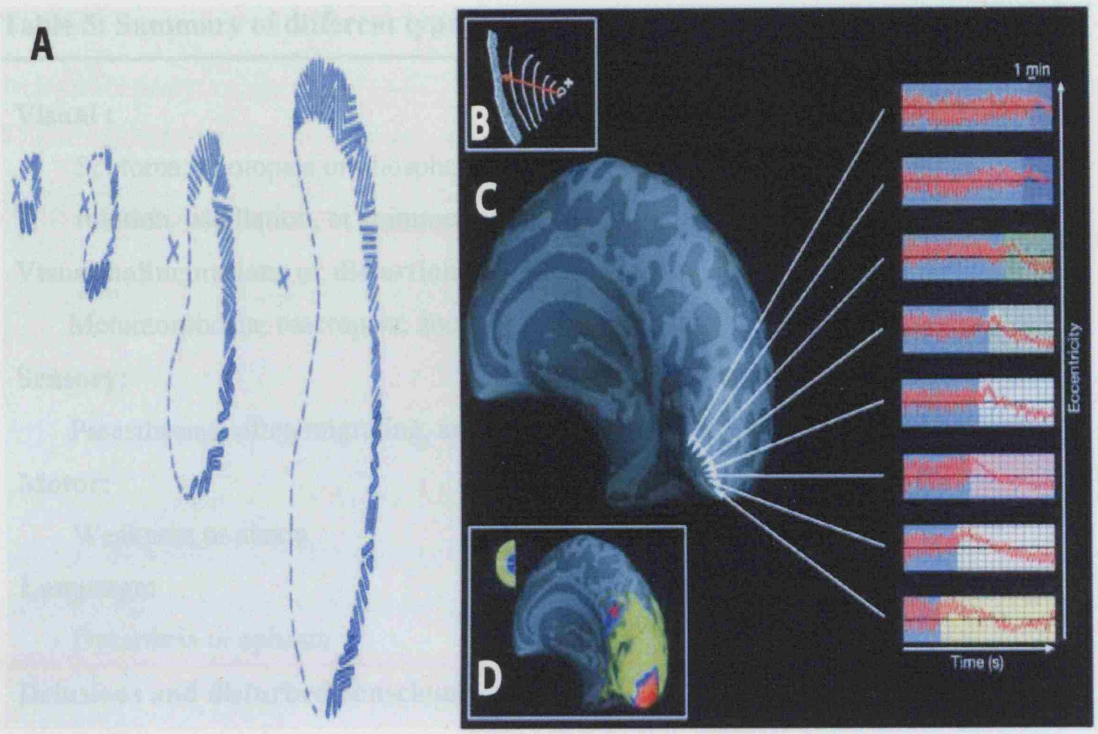

Figure 2: Lashley's visual aura and a visual field defect of a patient studied with brain imaging.

(A) Lashley's visual aura progressing across his visual field (Lashley, 1941). (B) Visual field defect of a patient studied with brain imaging. The red arrow shows the overall direction of progression of the visual percept. (C) Reconstruction of the patient's brain on the basis of anatomical data. Signal changes over time are shown to the right. Each time course was recorded from one in a sequence of voxels that were sampled along the primary visual cortex, from the posterior pole to a more anterior location, as indicated by arrowheads. A similar blood oxygenation level-dependent response was found within all of the extrastriate areas, differing only in the time of onset of the magnetic resonance perturbations. The perturbations developed earlier in the foveal representation, compared with more eccentric representations of retinotopic visual cortex. This finding was consistent with the progression of the aura from central to peripheral eccentricities in the corresponding visual field (B and D). (D) The maps of retinotopic eccentricity from the same subject as in B and C, acquired during interictal scans. As shown in the logo in the upper left, voxels that show retinotopically specific activation in the fovea are coded in red. Parafoveal eccentricities are shown in blue, and more peripheral eccentricities are shown in green (Hadjikhani et al., 2001).

Table 5: Summary of different types of aura.

Visual :

Scotoma; photopsia or phosphenes: geometric forms; fortification spectra; rotation, oscillation, or shimmering of objects; excessive brightness

Visual hallucinations or distortions:

Metamorphosia; macropsia; zoom or mosaic vision

Sensory:

Paresthesias, often migrating, and can become bilateral olfactory hallucinations

Motor:

Weakness or ataxia

Language:

Dysarthria or aphasia

Delusions and disturbed consciousness:

Déjà vu, multiple conscious trance-like states.

(Silberstein et al., 2001)

The Headache

Migraine headache is typically unilateral, with a throbbing quality of moderate to marked severity that exacerbates over time and can be aggravated by movement. The pain may be bilateral in about one third of cases and can move from one side to the other during an attack (Selby and Lance, 1960; Lance and Anthony, 1966). The attack commonly occurs in the morning and can last for 4–72 hours with a gradual onset which peaks and then slowly subsides (Silberstein et al., 1998). The attack is normally combined with other clinical features including nausea, vomiting, anorexia and sensory disturbances such as photophobia and phonophobia (Headache Classification Committee of the International Headache Society, 2004).

Resolution phase

After the headache has subsided many patients report varying symptoms. Lethargy, lack of concentration and a washed out and irritable sensation are among the most common reported (Blau, 1991). However some patients report feelings of euphoria and freshness commonly combined with food cravings. The headache can still be felt if excessive movement is undertaken and this can last for several days (Lance, 1982).

Migraine Treatment

Migraine treatments akin to the migrainous symptoms are variable depending on the individual patient. Once a correct diagnosis has been made, any coexisting disorders and biological conditions need to be considered. In general migraine therapy can be split into two modalities; prophylactic or acute depending on the frequency and severity of attacks and in severe cases both approaches may be employed.

Prophylactic Treatment

Prophylactic treatment is given when the incidence of attack is greater than 2–3 per month, the severity of attack is sufficient to impair normal function or when the patient is unable to cope and only in the event of acute therapy failing or causing serious side effects. Prophylaxis should be carefully considered if pregnancy is a possibility. Possible prophylactic therapies include anticonvulsants, antidepressants, β-blockers, calcium channel antagonists, serotonin antagonists and nonsteroidal anti-inflammatory drugs (NSAID, table 6).

Table 6: Prophylactic migraine treatments.

Anticonvulsants:	
	Valproate, gabapentin, topiramate
Antidepressants:	
	Tricyclic antidepressants, selective serotonin reuptake inhibitors, monoamine oxidase inhibitors
β-Adrenergic blockers:	
	Propranolol, nadolol, metoprolol, atenolol
Calcium channel antagonists:	
	Verapamil, flunarazine
Serotonin antagonists:	
	Methysergide, methergine
Others:	
	Nonsteroidal anti-inflammatory drugs, riboflavin, magnesium, neuroleptics, coenzyme Q10, feverfew,

(Silberstein et al., 2001)

The available prophylactic drugs are taken even when the headache is not present in an attempt to reduce the frequency of attacks and if one single drug is ineffective combination therapies can be utilised.

Acute Treatment

As with the prophylactic treatment, the frequency and severity of a patient's migraine determines the acute medication. Acute intervention is recommended at an early stage as this may prevent the attack worsening and increases the effectiveness of the drug (Burstein et al., 2004). Two forms of acute treatment are available, the non-specific analgesics and the specific acute headache treatments (table 7). Non-specific therapies are utilised for the treatment of migraine pain as well as that of other disorders, whereas

the specific acute headache treatments have no general analgesic properties and only treat the migraine attack.

Table 7: Different types of medication for acute attacks.

Non-specific acute medications	Specific acute treatments
Analgesics (NSAID and combination analgesics)	Ergotamine
Antiemetics	Dyhydroergotamine
Opiods	Triptans (5-HT receptor agonists)
Corticosteroids	
Dopamine antagonists	

Adapted from (Silberstein et al., 2001).

Since the 1980's and the discovery of the 5-$HT_{1B/1D}$ receptor agonists the acute treatment of migraine has been revolutionised. The triptans were developed on the basis of clinical observations that 5-hydroxyindoleacetic acid (the main metabolite of serotonin) was increased in the urine of patients during migraine attack (Curran et al., 1965). Further research also identified that platelet 5-HT levels decreased at the onset of migraine (Curran et al., 1965) and that intravenous 5-HT could abort headache (Kimball et al., 1960; Anthony, 1968; Anthony et al., 1968). The triptans target specific subclasses of the 5-HT_1 receptors that show a differential distribution in the central and peripheral pathways of migraine. 5-HT_{1B}, 5-HT_{1D} and 5-HT_{1F} receptor mRNA are expressed in the human trigeminal ganglia and afferents, however only 5-HT_{1D} immunoreactivity is found on trigeminal sensory nerve endings and only 5-HT_{1B} immunoreactivity on the cranial blood vessels (Beer et al., 1993; Longmore et al., 1997). The localisation of the 5-HT_{1F} receptor to the trigeminal nucleus caudalis (TNC) and the differential distribution of the 5-$HT_{1B/1D}$ receptors make them prime candidates for involvement in the pathophysiology of migraine (figure 3).

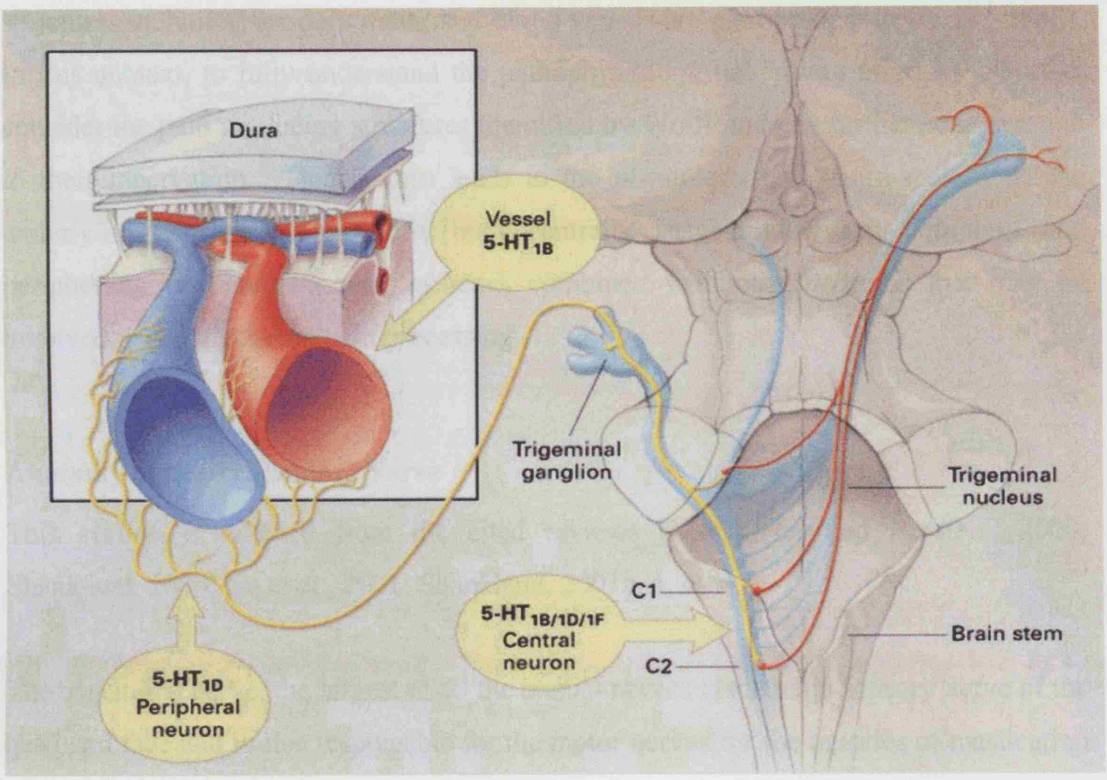

Figure 3: Possible sites of triptan action.

Triptans have four potential mechanisms of action: cranial vasoconstriction (Humphrey et al., 1990), peripheral neuronal inhibition (Moskowitz and Cutrer, 1993), inhibition of transmission through second-order neurons of the trigeminocervical complex (Goadsby, 2000), and the proposed activation of descending pain modulatory pathways from the periaqueductal gray, not shown in diagram (Bartsch et al., 2004a). Which mechanism is the most important is as yet unclear. These actions inhibit the effects of activated nociceptive trigeminal afferents and, in this way, control acute attacks of migraine (Goadsby et al., 2002a)

Pathophysiology of migraine

In order to appreciate the pathophysiology of migraine, we must first understand the anatomy of the headache pain producing structures. In 1684 Thomas Willis was the first to postulate that headache was due to the distension of the blood vessels which "pulls the nervous fibres one from another and so brings to them painful corrugations or wrinkling's" (Lance and Goadsby, 1993). Wolff also identified the need to know which structures of the head are sensitive to pain, identifying that most of the intracranial

structures including the dura mater and blood vessels are pain producing (Wolff, 1948). In this context, to fully understand the pathophysiology underlying migraine we must consider the pain producing structures identified by Wolff and pay further consideration to their innervation. This in turn leads to the physiology and pharmacology of the underlying neuronal connections both centrally (trigeminocervical complex) and peripherally (trigeminovascular system), combined with other systems that may be involved in the trigeminal pain processing.

Anatomy of the Trigeminal Nerve

This section is adapted from the cited reviews (Messlinger and Burstein, 2000; Shankland, 2000; Go et al., 2001; Shankland, 2001b, a, c).

The trigeminal nerve, the largest of all the cranial nerves is the main sensory nerve of the head and face and is also responsible for the motor nerves for the muscles of mastication (figure. 4).

The motor root arises from two nuclei; the superior nucleus, which consists of a strand of cells occupying the length of the lateral portion of the gray substance of the cerebral aqueduct at the level of the pons; and the inferior nucleus, which is situated in the upper pons and runs along the lateral margin of the rhomboid fossa. The motor root passes under the trigeminal ganglion and leaves the skull via the foramen ovale and joins the mandibular nerve.

The sensory root arises from the trigeminal ganglion (semilunar ganglion) which occupies a cavity (*cavum Meckelii*) in the dura mater covering the trigeminal impression. Three large branches enter the trigeminal ganglion; the ophthalmic, maxillary and mandibular.

The ophthalmic or first division (V_1) innervates the most superior region of the face including the skin, eye, mucous membrane of the nasal cavity, ethmoid and sphenoid sinuses, the dura mater of the tentorium cerebelli and falx cerebri along with portions of

the dura mater surrounding the middle meningeal artery (MMA) and the superior sagittal sinus (SSS).

The maxillary or second division (V_2) leaves the skull via the foramen rotundum and crosses the pterygopalatine fossa before entering the orbit via the inferior orbital fissure and appears on the face at the infraorbital foramen. It then splits into branches and innervates part of the oral cavity, nose, lower eyelid, cutaneous structures of the middle portion of the face, the tongue, maxillary and paranasal sinuses, the dura of the middle cranial fossa and portions of the dura surrounding the MMA.

The mandibular or third division (V_3) is the only branch of the trigeminal nerve to have a sensory and motor component. It innervates the teeth and gums of the mandible, cutaneous structures overlying the mandible, the auricular, the lower lip, the mucous membrane of the anterior two thirds of the tongue, the muscles of mastication, the external surface of the eardrum and a small portion of the dura mater supplied by the MMA.

In addition to the trigeminal innervation, oral-facial innervation is also obtained from the Facial (VII), Glossopharyngeal (IX) and Vagus (X) cranial nerves.

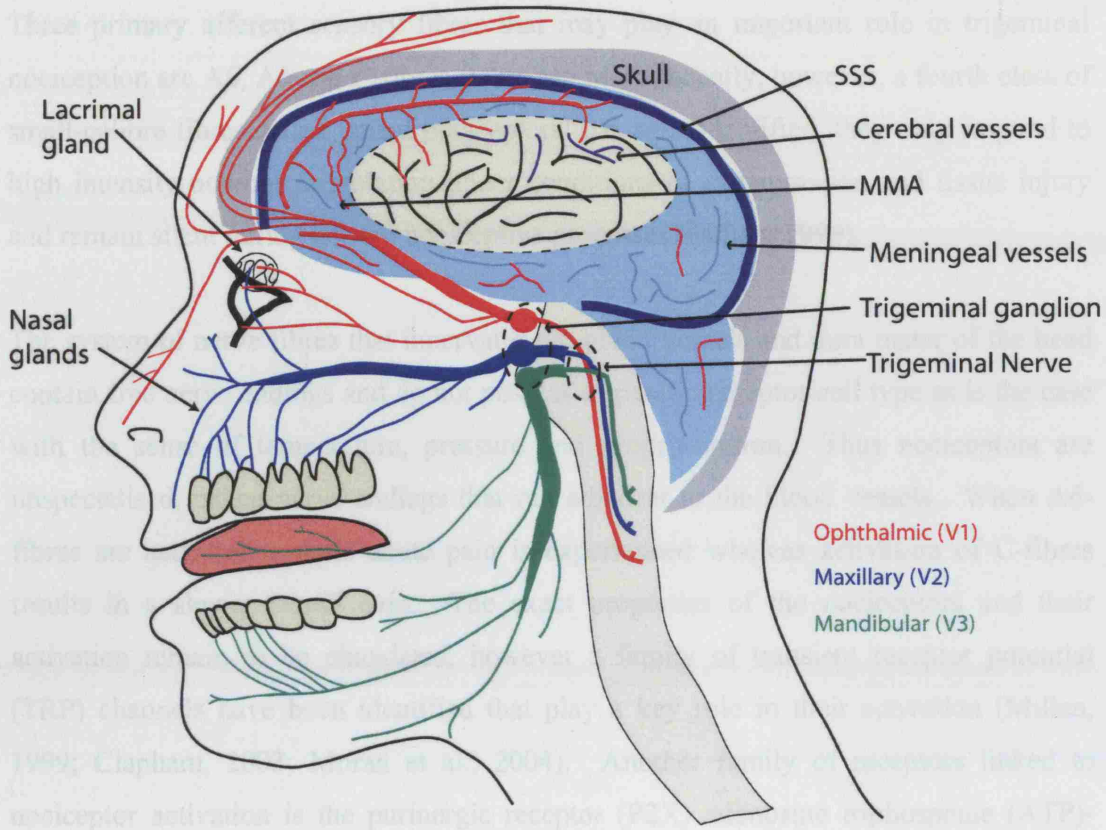

Figure 4: Trigeminal innervation of the Head.

The trigeminal nerve is the largest of all the cranial nerves and innervates the head and face as well as the motor output to the muscles of mastication.

Neuronal Afferent Fibres

The trigeminal nerve gives rise to the majority of the afferent fibres innervating the head and face as previously described (Messlinger and Burstein, 2000; Go et al., 2001). The importance of the trigeminal system in migraine is related to its rich innervation of the vasculature and meninges of the brain. A large plexus of mainly unmyelinated fibres that arise from the trigeminal ganglion are found surrounding the cerebral vasculature, pial vessels, venous sinuses and the dura mater (Messlinger and Burstein, 2000; Go et al., 2001). The area of the posterior fossa is also surrounded by a plexus of unmyelinated fibres, which arise from the upper cervical dorsal roots (Messlinger and Burstein, 2000; Go et al., 2001).

Three primary afferent sensory fibres that may play an important role in trigeminal nociception are Aβ, Aδ and C-fibres (table 8). More recently, however, a fourth class of small-calibre fibres called 'silent nociceptors' has been identified, they only respond to high intensity noxious stimulation under conditions of inflammation and tissue injury and remain silent during normal nociceptive processes (Millan, 1999).

The system of nerve fibres that innervates the blood vessels and dura mater of the head contain free nerve endings and do not possess a specific receptor cell type as is the case with the sense of temperature, pressure and proprioception. Thus nociceptors are unspecialised, naked nerve endings that run adjacent to the blood vessels. When Aδ-fibres are activated a rapid acute pain is experienced whereas activation of C-fibres results in a slower "dull" pain. The exact properties of the nociceptors and their activation remain to be elucidated, however a family of transient receptor potential (TRP) channels have been identified that play a key role in their activation (Millan, 1999; Clapham, 2003; Moran et al., 2004). Another family of receptors linked to nociceptor activation is the purinergic receptor (P2X) adenosine triphosphate (ATP)-gated cation channel. Seven different P2X receptors have been cloned and the mRNA of six has been identified in sensory neurons, however only P2X3 is expressed in small diameter sensory neurons that generally subserve a nociceptive function.

Although the exact mechanisms of nociceptor activation remain to be elucidated, in general; the opening of mechanically sensitive membrane channels [large prokaryotic mechanosensitive channel (MscL)] (Perozo et al., 2002), non-specific actions of chemicals on nociceptor membranes, and the action of G-protein coupled receptor which initiate second messenger events and alter nociceptor thresholds can all activate nociceptive transduction. The activation of nociceptors results in a depolarisation, which if above the threshold will result in the activation of a nerve impulse.

Table 8: Fibre types and properties.

Fibre type	Aβ	Aδ	C
Diameter (μm)	> 10	2–6	0.4–1.2
Conduction (m/sec)	30–100	12–30	0.5–1.2
Myelination	Thickly	Thinly	Unmyelinated
Threshold	Low	High	High
Principal neurotransmitters released	Excitatory amino acids (EAA's)	Substance P, NKA, CGRP, EAA's	Substance P, NKA, CGRP, EAA's
Receptors activated post-synaptically	AMPA	NK_{1+2}, $CGRP_{1+2}$, NMDA/AMPA, mGLU	NK_{1+2}, $CGRP_{1+2}$, NMDA/AMPA, mGLU
Laminae in which neurons terminate	IIi, III, IV, V	I/IIo, V	I/IIo, V, X
Types of second order neurons contacted	Light touch, Wide dynamic range (WDR)	Nociceptive specific, WDR, Light touch	Nociceptive specific, WDR
Sensory modality transmitted	Innocuous: light touch, vibration and pressure	Noxious: sharp, pricking pain Sharp, stinging pain	Noxious: thermal, mechanical and chemical irritation Dull, burning pain

AMPA: α-amino-3-hydroxy-5-methylisoxazole-4-proprionic acid, CGRP: calcitonin gene-related peptide, mGLU: metabotropic glutamate, NK: neurokinin, NMDA: *N*-methyl-*D*-aspartic acid, WDR: wide dynamic range (Millan, 1999).

Table 9: Summary of the different channels involved in nociceptor activation.

Channel Name	Major Tissue Distribution	Sensory Modality
TRPV1	DRG, TG, bladder	Temp ≥43°C, acid, capsaicin
TRPV2	DRG, SC, brain, spleen, intestine	Temp ≥ 52°C
TRPV3	DRG, TG, SC, brain, tongue	Temp ≥ 30–39°C, camphor
TRPV4	DRG, TG, brain, kidney, lung, spleen, testis, heart, liver, inner-ear hair cells	Temp ≥ 25°C, hypotonicity, noxious mechanical stimuli, acid, endocannabinoids
TRPM8	DRG, TG, prostate	Temp ≤ 23–28°C, menthol
TRPA1	DRG, fibroblasts, hair cells	Temp ≤ 18°C, cannabinoids, mustard oil, mechanical stimuli (hair cells)
$P2X_{2,3}$	DRG, TG (small diameter sensory neurons)	ATP
$P2Y_1$	Large-fibre DRG neurons	Mechanical stimuli
Mscl	Brain, heart, inner-ear hair cells	Mechanical stimuli
TREK	Brain, heart	Mechanical stimuli, arachidonic acid
TRAAK	Brain, SC, retina	Mechanical stimuli, arachidonic acid, colchicine

DRG, dorsal root ganglion; TG, trigeminal ganglion; SC, spinal cord; ATP, adenosine triphosphate; TRPV, transient receptor potential vanilloid family; TRPM, transient receptor potential melastatin family; TRPA, transient receptor potential ankyrin family; P2, purinergic receptors; Mscl, large prokaryotic mechanosensitive channel; TREK, two-pore domain weak inward rectifying K^+ channels-related K^+ channel; TRAAK, two-pore domain weak inward rectifying K^+ channels -related arachidonic acid-stimulated K^+ channel.

Trigeminal Brainstem Nuclear Complex

Trigeminal primary afferents are psudo-unipolar neurons which originate in the trigeminal ganglion (semilunar ganglion) and project via the three divisions of the trigeminal nerve as summarised previously to innervate the head, dura mater and blood vessels of the brain. In turn the psudo-unipolar neurons project centrally terminating on second order neurons in the trigeminal brainstem nuclear complex (TBNC) or trigeminocervical complex (TCC).

The sensory root of the trigeminal nerve enters the lateral pons where it terminates in the trigeminal nucleus on second order neurons. The TBNC extends from the rostral pons down to the upper cervical spinal cord levels and consists of a complex of sub nuclei divided into the principal (Vp) and spinal nucleus (Vsp). The TBNC is organised somatotopically, with the three trigeminal divisions being represented in a sequence from ventrolateral to dorsomedial (Strassman et al., 1994a), (figure 5).

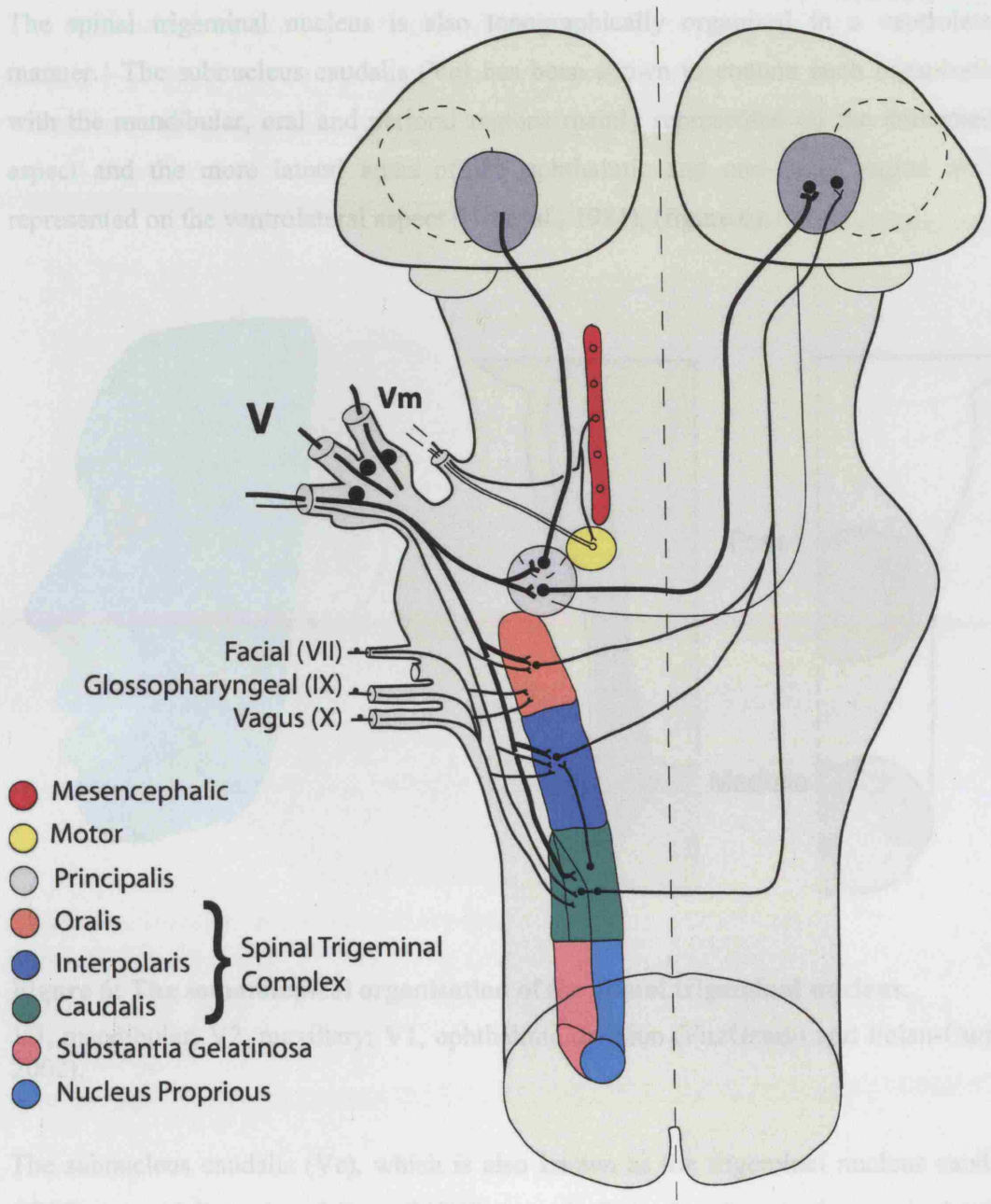

Figure 5: Cytoarchitecture of the trigeminal brainstem nuclear complex.
Adapted from (Wilkinson, 1986).

The spinal nucleus or spinal trigeminal complex is further subdivided into three sub-nuclei; the nucleus oralis (Vo), interpolaris (Vi) and caudalis (Vc) arranged in a rostrocaudal manner.

The spinal trigeminal nucleus is also topographically organised in a ventrolateral manner. The subnucleus caudalis (Vc) has been shown to contain such organisation, with the mandibular, oral and perioral regions mainly represented on the dorsomedial aspect and the more lateral areas of the ophthalmic and oral-facial region mainly represented on the ventrolateral aspect (Hu et al., 1981), (figure 6).

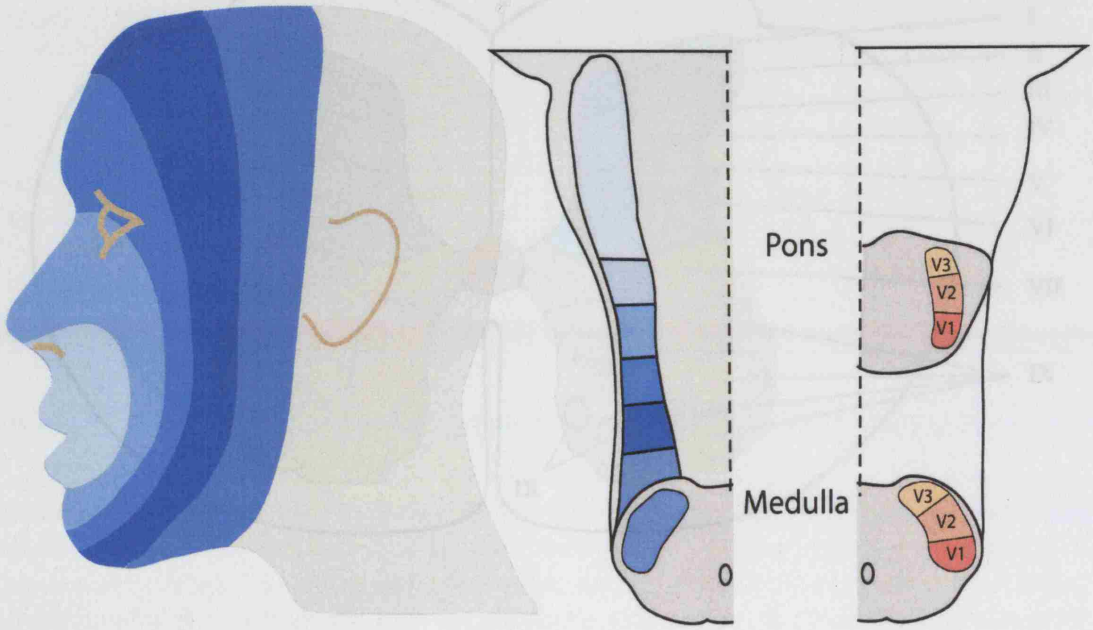

Figure 6: The somatotopical organisation of the spinal trigeminal nucleus.
V3, mandibular; V2, maxillary; V1, ophthalmic division (FitzGerald and Folan-Curran, 2002).

The subnucleus caudalis (Vc), which is also known as the trigeminal nucleus caudalis (TNC) or medullary dorsal horn (MDH) extends from the obex to the cervical spinal cord and is a continuation of the spinal dorsal horn (Olszewski, 1950). It is composed of separate layers similar in appearance to the spinal cord dorsal horn with the outermost layer, the subnucleus marginalis corresponding to lamina I. Ventral to this lies the subnucleus gelatinosus (lamina II), and the subnucleus magnocellularis corresponds to lamina III and IV. The corresponding structure to lamina V, the subnucleus reticularis dorsalis is however less defined in the Vc than in the dorsal horn (Olszewski, 1950).

The organisation of the Vc and spinal dorsal horn are depicted in fig. 7–8, basically lamina I–VI receive sensory input and constitute the dorsal horn. Lamina VII–IX contain the motor neurons and form the ventral horn, while lamina X surrounds the central canal and receives afferent input similar to lamina I and II.

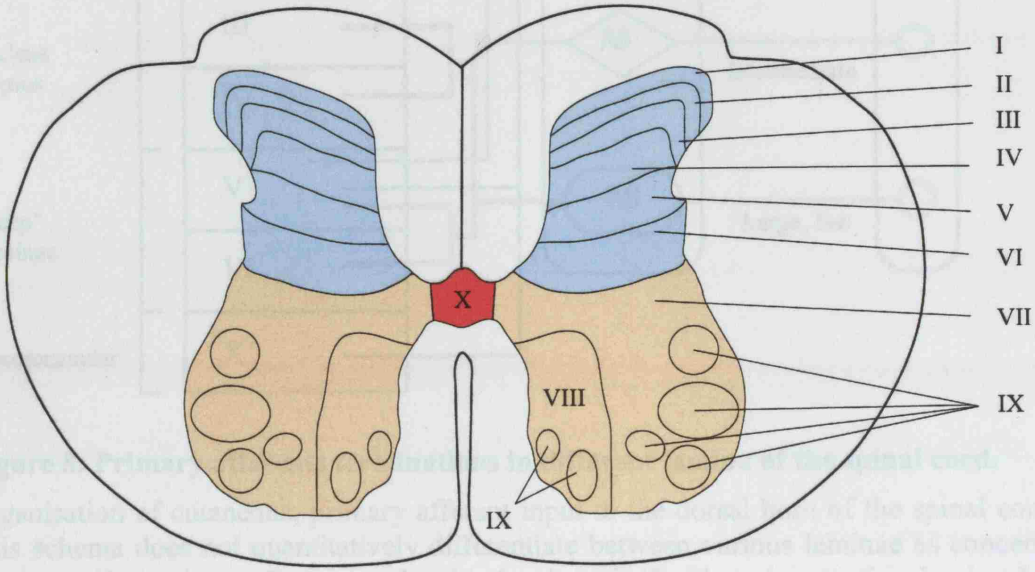

Figure 7: Laminations of the spinal cord.

An example of the Rexed lamina of the 1st cervical segment of the spinal cord in man. Laminae I–VI, dorsal horn; Laminae VII–IX, ventral horn; Lamina X, central gray.

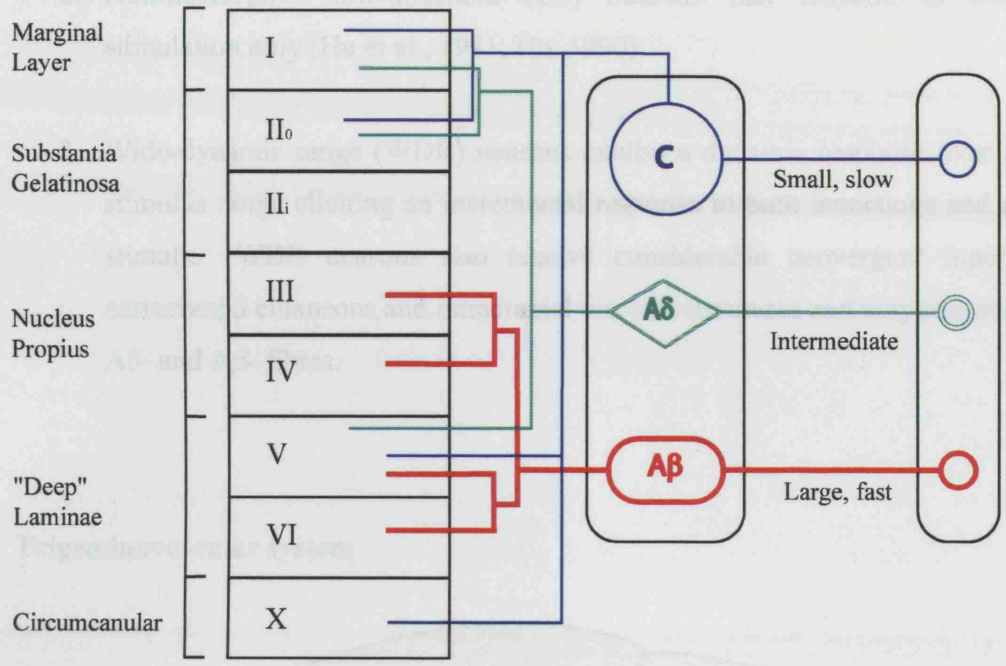

Figure 8: Primary afferents terminations in different lamina of the spinal cord.

Organisation of cutaneous, primary afferent input to the dorsal horn of the spinal cord. This schema does not quantitatively differentiate between various laminae as concerns primary afferent input. For example, the density of *Aδ*- fibres innervating lamina I is considerably greater than that projecting to lamina II_0, a principal target of C fibre input. Unmyelinated fibres from muscle, viscera and joints appear to preferentially innervate laminae I/II_0 and V/X. Lamina VI, which functionally complements lamina V, is clearly identifiable only at the level of the cervical and thoracic cord. Lamina X corresponds to the grey matter surrounding the central canal (Leem et al., 1993; Belemonte and Cervero, 1996; Hendry et al., 1999; Millan, 1999; Woodbury et al., 2000; Woodbury and Koerber, 2003).

Primary afferent sensory fibres converge on second order neurons in the medullary dorsal horn (figure 8). These second order neurons have been classified into three categories depending on the properties they exhibit.

1. Nociceptive-specific (NS) neurons are silent at rest and become activated in response to high intensity, noxious stimuli and receive inputs from Aδ- and C-fibres.

2. Non-nociceptive low-threshold (LT) neurons that respond to innocuous stimulation only (Hu et al., 1981; Hu, 1990).

3. Wide-dynamic range (WDR) neurons exhibit a dynamic response over a broad stimulus range eliciting an incremental response to both innocuous and noxious stimuli. WDR neurons also receive considerable convergent inputs from extracranial cutaneous and intracranial visceral structures and may respond to C-, Aδ- and Aβ- fibres.

Trigeminovascular system

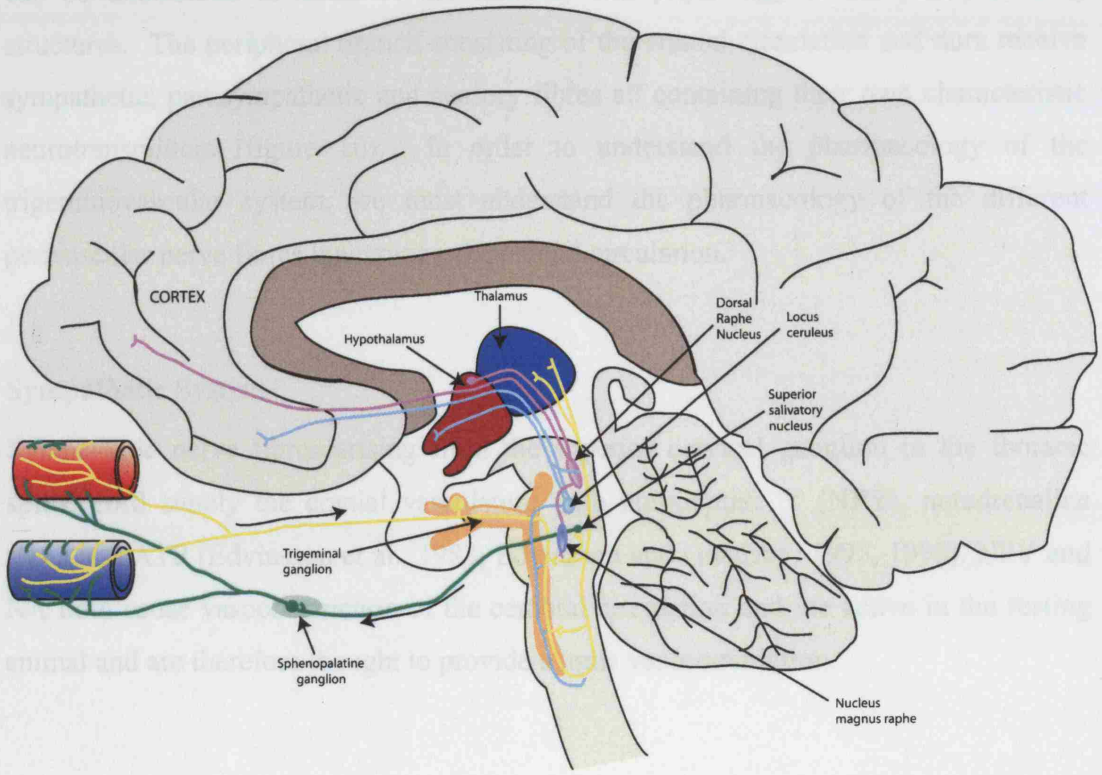

Figure 9: Pathophysiology of the trigeminovascular system.
Adapted from (Goadsby et al., 2002b).

Sensory fibres innervating the cranial vessels arise from neurons which have their cell bodies within the trigeminal ganglion. Sensory inputs from the dural blood vessels (such as the superior sagittal sinus and middle meningeal artery) synapse on second order neurons in the trigeminocervical complex. These in turn project to the thalamus in the quinto/trigemino-thalamic tract. There are also connections between pontine neurons and the superior salivatory nucleus which results in a reflex activation of parasympathetic fibres (with resultant vasodilation), these are relayed in the sphenopalatine ganglion (Goadsby et al., 2002b), (figure 9).

Pharmacology of Trigeminovascular system

The pharmacology of the trigeminovascular system is complex in an overall sense but can be understood in terms of the anatomy and physiology of the pain-producing structures. The peripheral branch consisting of the cranial circulation and dura receive sympathetic, parasympathetic and sensory fibres all containing their own characteristic neurotransmitters (figure 10). In order to understand the pharmacology of the trigeminovascular system, we must understand the pharmacology of the different perivascular nerve fibres innervating the cranial circulation.

Sympathetic System

Sympathetic nerve fibres arising from the superior cervical ganglion in the thoracic spinal cord supply the cranial vasculature with nuropeptide Y (NPY), noradrenaline (NA) and ATP (Edvinsson et al., 1983; Edvinsson and Goadsby, 1995, 1998). NPY and NA both cause vasoconstriction of the cerebral circulation and are active in the resting animal and are therefore thought to provide a tonic vasoconstriction.

Parasympathetic system

Parasympathetic nerve fibres arising from the sphenopalatine and otic ganglia as well as the carotid miniganglia (Edvinsson and Goadsby, 1998) supply the cranial vasculature with vasoactive intestinal peptide (VIP), peptide histidine isoleucine (PHI),

acetylcholinesterase (AChE), peptide histidine methionine 27 (PHM) and pituitary adenylate cyclase-activating peptide (PACAP) as well as other VIP-related peptides (Olesen and Edvinsson, 2000). The parasympathetic innervation of the cranial circulation is a vasodilatory pathway, with VIP, acetylcholine and PHM all being potent vasodilators in human cranial arteries.

Sensory system

Sensory nerve fibres arising from the trigeminal ganglion supply the cranial vasculature with substance P (SP), calcitonin gene-related peptide (CGRP) and neurokinin A (NKA) (Olesen and Edvinsson, 2000). Trigeminovascular afferents innervating the cranial vasculature are psudo-unipolar, also projecting via the trigeminal ganglion to the trigeminal nucleus caudalis (TNC), which is the key relay centre for the transmission of nociceptive information to higher brain centres (Moskowitz, 1984).

It is important when dealing with the pathophysiology of migraine to consider that it is most likely to involve a combination of factors, including the potential activation of any of the three divisions of the perivascular nerve fibres innervating the cranial circulation as well as alterations in sensory processing pathways that modulate trigeminovascular signals (Goadsby et al., 1991).

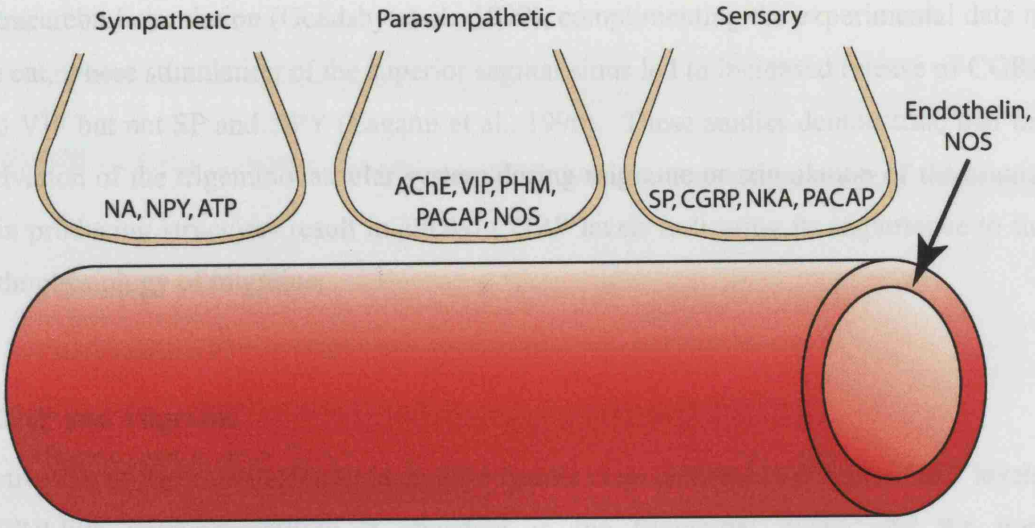

Figure 10: The three separate systems of perivascular nerve fibres innervating the cranial circulation.

1. Sympathetic fibres containing noradrenaline (NA), nuropeptide Y (NPY), and adenosine triphosphate (ATP) project from the superior cervical ganglion.

2. Parasympathetic fibres containing vasoactive intestinal peptide (VIP), peptide histidine isoleucine (PHI, animal version), acetylcholinesterase (AChE), peptide histidine methionine 27 (PHM, human version), pituitary adenylate cyclase-activating peptide (PACAP) and nitric oxide synthase (NOS) project from the sphenopalatine/pterygopalatine and otic ganglia as well as the carotid miniganglia.

3. Sensory fibres containing substance P (SP), calcitonin gene-related peptide (CGRP) and neurokinin A (NKA) project from the trigeminal ganglion.

Neuropeptide studies in migraine

Activation of the trigeminovasular system via electrical stimulation of the trigeminal ganglion in cats and thermocoagulation of the trigeminal ganglion in humans results in facial flushing and causes the local release of both SP and CGRP in human and cat into the extracerebral circulation (Drummond et al., 1983; Lambert et al., 1984; Goadsby et al., 1986; Goadsby et al., 1988; Goadsby and Edvinsson, 1993). However, during

migraine attack in humans CGRP but not SP, NPY and VIP levels are elevated in the extracerebral circulation (Goadsby et al., 1990), complimenting the experimental data in the cat, where stimulation of the superior sagittal sinus led to increased release of CGRP and VIP but not SP and NPY (Zagami et al., 1990). These studies demonstrate that the activation of the trigeminovascular system during migraine or stimulation of the cranial pain producing structures result in altered CGRP levels indicating its importance to the pathophysiology of migraine.

CGRP and Migraine

Activation of the trigeminovascular system results in an increase in cranial CGRP levels. CGRP-like immunoreactivity is abundant in the trigeminal nuclei and the non-myelinated trigeminal afferents (Welch, 2003), demonstrating an innervation by CGRP containing nerves (Edvinsson, 2004). Intravenous infusion of CGRP is known to cause a delayed migraine-like headache in patients (Lassen et al., 2002) and a correlation has been shown between increased plasma CGRP levels and migraine headache (Juhasz et al., 2003). In an animal model of trigeminovascular activation induced by trigeminal nerve stimulation the observed neurogenic dural vasodilation was inhibited by a CGRP receptor antagonist, suggesting that blockade of the CGRP receptor may be a possible therapeutic target in the treatment of migraine (Williamson and Hargreaves, 2001). Recent advances in the study of CGRP receptor antagonism have led to the discovery of a potent non-peptide CGRP receptor antagonist, BIBN4096BS (Doods et al., 2000), which shows high affinity for the human α-CGRP receptor. Initial clinical trial results have shown that BIBN4096BS is effective in the treatment of migraine without significant side effects (Olesen et al., 2004).

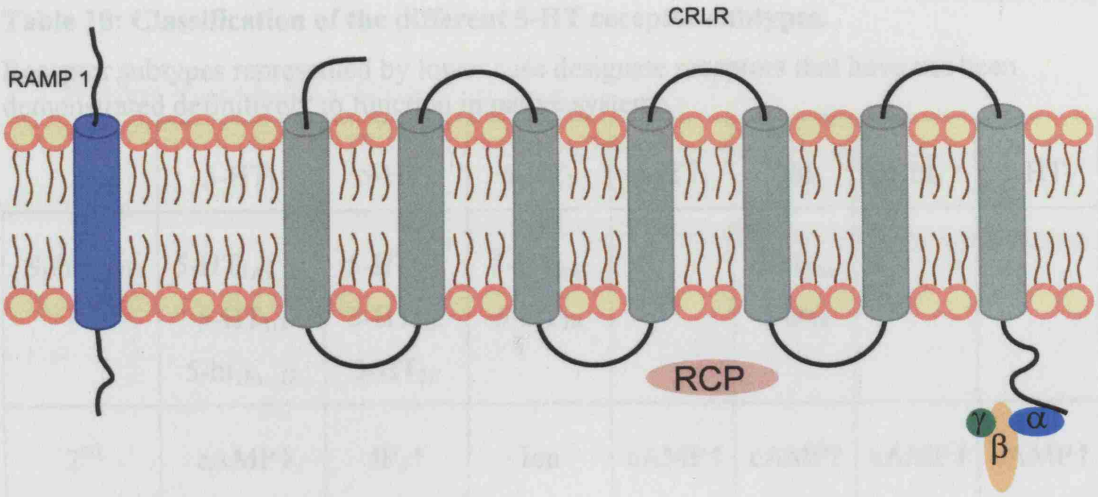

Figure 11: Structure of the CGRP receptor.

The CGRP receptor consists of a seven-transmembrane G-protein-coupled calcitonin receptor-like receptor (CRLR) linked to the receptor activity modifying protein 1 (RAMP1). RCP, receptor component protein.

Serotonin and migraine

The initial argument for the involvement of serotonin in migraine was first postulated over 40 years ago. Studies carried out in the 1960's demonstrated that the main metabolite of serotonin, 5-hydroxyindoleacetic acid, was increased in association with migraine attacks (Curran et al., 1965; Sicuteri et al., 1965). It was also shown that 5-HT platelet levels decreased rapidly at the onset of migraine (Anthony, 1968) and that intravenous injection of 5-HT could abort both reserpine-induced (Kimball et al., 1960) or spontaneous headache (Lance et al., 1967). Thus it was initially believed that migraine was a result of chronically low serotonin levels. This data led to the belief that serotonin receptors may be a possible therapeutic target in the treatment of migraine.

The discovery of the triptans ($5\text{-HT}_{1B/1D}$ receptor agonists) has driven an interest in the classification of the 5-HT receptors and there are currently 7 classes identified (table 10).

Table 10: Classification of the different 5-HT receptor subtypes.

Receptor subtypes represented by lower case designate receptors that have not been demonstrated definitively to function in native systems.

	5-HT_1	5-HT_2	5-HT_3	5-HT_4	5-ht_5	5-ht_6	5-HT_7
Subtypes	$5\text{-HT}_{1A, 1B,}$ 5-HT_{1D} $5\text{-ht}_{1E, 1F}$	$5\text{-HT}_{2A,}$ $5\text{-HT}_{2B,}$ 5-HT_{2C}	$5\text{-HT}_{3A,}$ 5-HT_{3B}		$5\text{-ht}_{5A,}$ 5-ht_{5B}		
2^{nd} messenger	cAMP↓	IP_3↑	Ion channels	cAMP↑	cAMP?	cAMP↑	cAMP↑

cAMP, cyclic adenosine monophosphate; IP_3, inositol-3-phosphate.

Understanding the 5-HT receptor systems has allowed the mechanisms of the triptans to be partially understood in relation to receptor localisation and function. The current concepts of the pharmacological actions of the acute-migraine drugs related to 5-HT are listed below in table 11.

Table 11: Current concepts of the pharmacology of acute anti-migraine drugs.

Target	**Receptor**
Large cranial vessels	5-HT_{1B}
Peripheral terminal of the trigeminal nerve	
• Inhibits plasma protein extravasation	$5\text{-HT}_{1D/1F}$
• Blocks dural vasodilation	5-HT_{1D}
• Inhibits release of trigeminal neuropeptides	5-HT_{1D}
Trigeminal nucleus inhibition	$5\text{-HT}_{1B/1D}$, 5-HT_{1F}

(Goadsby, 1997)

Plasma Protein Extravasation in Migraine

It is now widely accepted that activation of nociceptors, causes release of neuropeptides and other mediators from their central and peripheral terminals. Release from the peripheral terminal is thought to promote inflammation, manifesting as vasodilation, plasma extravasation (the leakage of blood plasma from a vessel out into surrounding tissue) and hypersensitivity. Neurogenic inflammation is the inflammatory response resulting from release of vasoactive substances by a nerve into the area surrounding the vasculature that results in increased blood flow and extravasation. It was strongly implicated in the pathogenesis of migraine following experiments that indicated that stimulation of the trigeminal ganglion causes the release of SP, CGRP and NKA, resulting in plasma protein extravasation (PPE) (Moskowitz, 1990). Further studies identified that PPE could also be triggered by intravenous injection of SP, NKA and the vanilloid found in hot peppers capsaicin, but not CGRP (Markowitz et al., 1987).

The small unmyelinated C-fibres sensitive to capsaicin are now known to be of major importance in the generation of neurogenic inflammation (Markowitz et al., 1987), along with the neuropeptides SP and CGRP. Neurogenic plasma extravasation has been shown to be blocked by a series of migraine treatments including, the triptans (Buzzi and Moskowitz, 1990; Buzzi et al., 1991; Buzzi and Moskowitz, 1991), the ergot alkaloids (Markowitz et al., 1988; Saito et al., 1988; Buzzi and Moskowitz, 1991) and indomethacin (Buzzi et al., 1989), thought to be via the blockade of the release of pro-inflammatory mediators from trigeminal fibres. Substance P antagonists (Shepheard et al., 1993; Lee et al., 1994; Shepheard et al., 1995; Polley et al., 1997) are also able to prevent neurogenic inflammation; however they are not effective in the treatment of migraine (May and Goadsby, 2001), or in the SSS stimulation model (Goadsby et al., 1998) used in this thesis, suggesting it is a more appropriate model of migraine. This is also true of the conformationally restricted analogues of sumatriptan and zolmitriptan, CP122, 228 (Lee and Moskowitz, 1993; Gupta et al., 1995; Roon et al., 2000) and 4991w93, respectively, both of which were ineffective in clinical trials. Further evidence indicating the absence of any pathology of an inflammatory response in humans during migraine (Nissila et al., 1996) and the absence of extravasation in the

retina of humans during migraine (May et al., 1998b) cast limitations over the proposed involvement of neurogenic inflammation in migraine.

Genetics of migraine

Migraine is a complex, polygenic, multifactorial disorder with an array of potential genetic factors (table 12) which interact with each other and environmental influences to produce the clinical heterogeneity observed. Several possible loci have been identified for migraine with and without aura including 19p13, 1q21-23 and Xq, see table 12.

One rare form of migraine, Familial Hemiplegic Migraine (FHM) has been mapped to three different loci:

A) FHM 1 locus affecting the CACNA1A calcium channel gene has been mapped to chromosome 19p13 (Ophoff et al., 1998).

B) FHM 2 affecting the ATP1A2 gene on chromosome 1q23 (De Fusco et al., 2003).

C) FHM 3 affecting the SCN1A gene on chromosome 2q24 (Dichgans et al., 2005; Schwedt and Dodick, 2005).

The FHM1 locus accounts for about half of all families demonstrating FHM (Estevez and Gardner, 2004) and causes mutations in the α1A pore forming unit of P/Q-type voltage dependent calcium channels (VDCCs) resulting in a neuronal channelopathy. CACNA1A mutations have been shown to alter the density and gating of P/Q-type currents, thus resulting in a gain of function mutation which causes altered calcium currents. The first *in vivo* studies on the effects of CACNA1A mutations have demonstrated enhanced neurotransmission at the neuromuscular junction, with reduced thresholds for triggering and increased velocity of propagation of cortical spreading depression (CSD) (van den Maagdenberg et al., 2004). Knockout mice that do not carry

the CACNA1A gene are born with severe ataxia and die within a few days (Jun et al., 1999) however mice carrying CACNA1A mutations display distinct phenotypes indicating a role of the P/Q-type channels in the control of neurotransmitter release and neuronal development.

Table 12: Susceptibility loci identified in familial hemiplegic migraine and in migraine with aura.

Migraine subtype	Chromosome	Gene
FHM with cerebellar symptoms	19p13	CACNA1A
Pure FHM	19p13	CACNA1A
Pure FHM	1q21-23, 1q31	ATP1A2
FHM	2q24	SCN1A
Migraine with aura	19p13.2	Distinct from CACNA1A? INSR?
Migraine with aura	4q24	Unknown
Migraine with aura	Xq	Unknown

INSR: Insulin Receptor Gene (Ducros et al., 2002).

Brain regions involved in migraine

Ascending nociceptive pathways related to migraine

Sensory information relayed in the trigeminal ganglion to the TNC is then conducted via second order projection neurons to other centres in the brain including the thalamus, hypothalamus and brainstem sites (Goadsby et al., 2002a). The ascending pathways distribute sensory information to multiple cortical regions and may produce antinociception as well as nociception (Messlinger and Burstein, 2000). Two types of pathway are known to exist and these are classified as monosynaptic and polysynaptic depending on their neuroanatomical organisation. Monosynaptic pathways project directly to target structures and include the trigeminothalamic and trigeminohypothalamic tract, polysnaptic pathways project to other brain regions en route to higher centres. Thus there is a complex pattern of direct and indirect projections to higher structures via multiple ascending pathways that also interact with descending modulatory pathways. Three ascending pathways that are of major importance in the processing of nociceptive information from the trigeminal brainstem nuclear complex are:

A) The trigeminothalamic tract (monosynaptic projections to the thalamus).

B) The spinomesencephalic and spinoreticular (projections to bulbar and mesenchephalic nuclei that integrate homeostatic control and monoaminergic modulatory centres).

C) The trigeminohypothalamic tract (monosynaptic projections to the hypothalamus).

The ascending pathways and supraspinal mechanisms play an important role in the modulation and experience of pain, and can be divided into two fundamental components, processed by distinctive, interconnected circuits:

A) The sensory-discriminative circuit, which facilitates the perception and detection of noxious stimuli.

B) The affective-cognitive circuit, which integrates pain and mood, the attention to and memory of pain as well as the tolerance of pain (Craig, 1994).

The sensory and affective aspects of the ascending pathways combine to form the overall experience of pain (Jones and Derbyshire, 1995, 1996), however the individual properties have implications for the induction and treatment of pain.

Descending nociceptive pathways related to migraine

The trigeminal nucleus has been shown to receive projections from other nociceptive modulatory structures some of which are discussed briefly below.

Nucleus Raphe Magnus

Fibres from the nucleus raphe magnus (NRM) project to both the trigeminal nucleus oralis and caudalis. Other raphe nuclei (obscurus and pallidus) do not project to the trigeminal nucleus caudalis (Lovick and Robinson, 1983; Lovick and Wolstencroft, 1983). NRM is known to control sensory responses of neurons in the spinal trigeminal nucleus (Lovick and Wolstencroft, 1979; Sessle et al., 1981) and has been shown to send branches to the spinal cord in the cat and rat (Lovick and Robinson, 1983) thus allowing sensory control of both spinal and trigeminal responses simultaneously. Stimulation of the NRM has been shown to produce potent inhibition of TNC nociceptive and non-nociceptive neuronal responses (Chiang et al., 1994).

Parabrachial Area

The parabrachial area (PBA) situated within the dorsolateral pontomesencephalic tegmentum of the brainstem plays a major role in the integration of autonomic and somatosensory information. Sub-divisions of the PBA including the Kölliker-Fuse

nucleus and nucleus cuneiformis project to the trigeminal nucleus targeting predominantly neurons located in the superficial laminae of the dorsal horn. Stimulation of the PBA has been shown to produce potent inhibition of TNC nociceptive and non-nociceptive neuronal responses (Chiang et al., 1994).

Cortex

Evidence is accumulating that cortical structures play a more pivotal role in nociceptive processing. The cortex can produce antinociceptive effects via relays in the PAG (Zhang et al., 1997; Millan, 1999) and other cerebral structures and the somatosensory cerebral cortex produces descending modulation of trigeminal somatosensory neurones (Chiang et al., 1990).

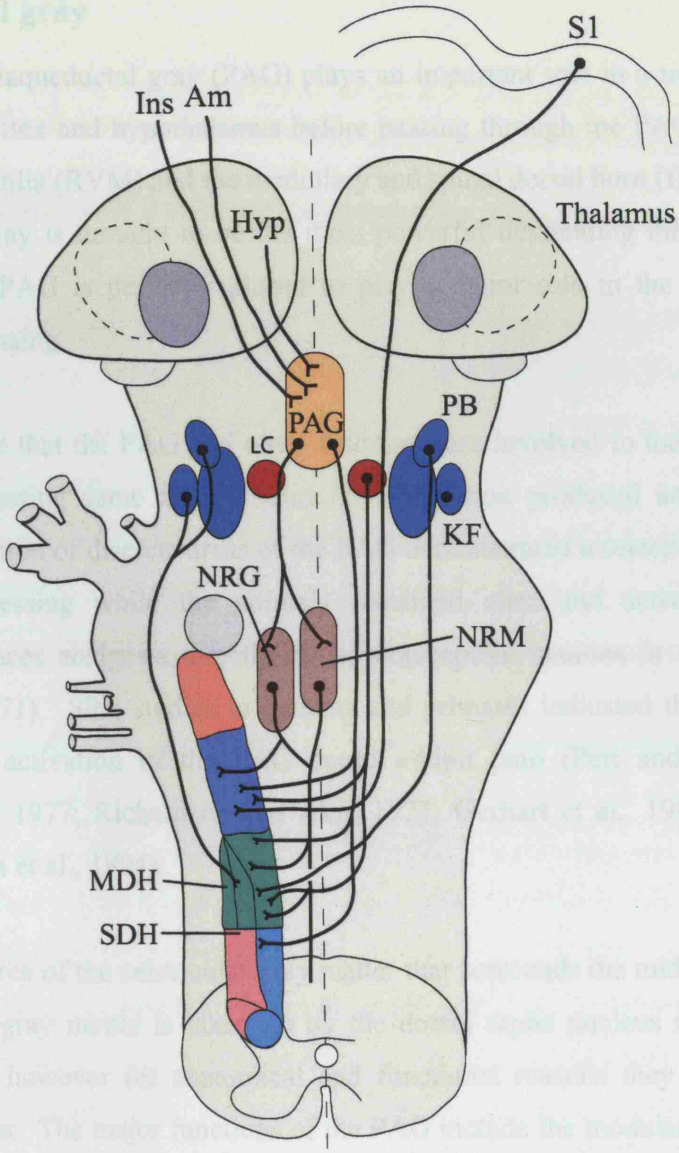

Figure 12: Schematic representation of the descending inhibitory pathways to the trigeminal nucleus caudalis related to nociception.

The periaqueductal gray (PAG) receives input from the insular cortex (Ins), the amygdala (Am), and the hypothalamus (Hyp) and projects to the nucleus raphe magnus (NRM) and the adjacent reticular formation, including the nucleus reticularis gigantocellularis (NRG) within the rostral ventromedial medulla. Serotonergic pathways then descend to the medullary dorsal horn (MDH) and spinal dorsal horn (SDH). Other descending pathways arise bilaterally from the parabrachial (PB). Locus coeruleus (LC) and Kölliker-Fuse (KF) nuclei, and there is a direct projection from the somatosensory cortex (SI) to the subnucleus interpolaris. Adapted from (Messlinger and Burstein, 2000)

Periaqueductal gray

The midbrain periaqueductal gray (PAG) plays an important role in a neuronal circuit, initiated in the cortex and hypothalamus before passing through the PAG to the rostral ventromedial medulla (RVM) and the medullary and spinal dorsal horn (figure 12). This descending pathway is thought to be the most powerful descending inhibitory system and as such the PAG is perfectly placed to play a major role in the modulation of nociceptive processing.

The first evidence that the PAG and other structures are involved in the modulation of nociceptive processing came from studies on stimulation produced analgesia (SPA). Electrical stimulation of discrete areas of the PAG demonstrated a selective inhibition of nociceptive processing while the animals remained alert and active. Brainstem stimulation produces analgesia directly at the nociceptive neurons in the spinal cord (Mayer et al., 1971). SPA studies in humans and primates indicated that electrical or pharmacological activation of the PAG could inhibit pain (Pert and Yaksh, 1974; Hosobuchi et al., 1977; Richardson and Akil, 1977; Gerhart et al., 1984; Gybels and Kupers, 1990; Lin et al., 1994).

The PAG is the area of the ventricular gray matter that surrounds the midbrain aqueduct, a portion of the gray matter is taken up by the dorsal raphe nucleus and oculomotor group of nuclei, however for anatomical and functional reasons they are considered separate structures. The major functions of the PAG include the modulation of pain and analgesia, fear and anxiety, vocalisation, lordosis and cardiovascular control (Carrive, 1993; Rossi et al., 1994; Behbehani, 1995).

The PAG is a complex structure consisting of numerous longitudinal neuronal columns that terminate at varying levels throughout the extent of the PAG (figure 13) and have been shown to be similarly conserved across species (Shipley et al., 1991; Behbehani, 1995; Bandler and Keay, 1996).

A) Dorsolateral

B) Dorsomedial

C) Lateral

D) Ventrolateral

The dorsolateral column extends along the rostral and intermediate sections of the PAG before diminishing in the caudal portion, has robust projections to the cuneiform nucleus and periabducens region and receives afferent inputs from the nucleus prepositis hypoglossi, cuneiform nucleus and deep layers of the superior colliculus. The dorsomedial column extends along the entire length of the PAG and receives inputs from the cortical and subcortical forebrain. The dorsomedial column has projections to the rostral ventromedial and rostroventrolateral medulla. The dorsolateral and dorsomedial columns combine to form the dorsal column.

The lateral column extends along the rostral and intermediate sections of the PAG (figure 13), and has projections to the ventromedial, ventrolateral and dorsal medulla (particularly the nucleus tractus solitarius). The different rostrocaudal sections of the lateral column receive afferents from different sources, with the rostral portion receiving significant input from the spinal trigeminal nucleus (STN), the intermediate portion receiving inputs from the anterior hypothalamic/medial preoptic region, the central nucleus of the amygdala and the anterior cingulate cortex, and the caudal portion receiving significant input from the cervical enlargement of the spinal cord. The ventrolateral (vl) column extends along the intermediate and caudal portion of the PAG and sits adjacent to the dorsal raphe nucleus. The ventrolateral column is anatomically similar to the lateral column (figure 13); however stimulation of the two columns produces different responses.

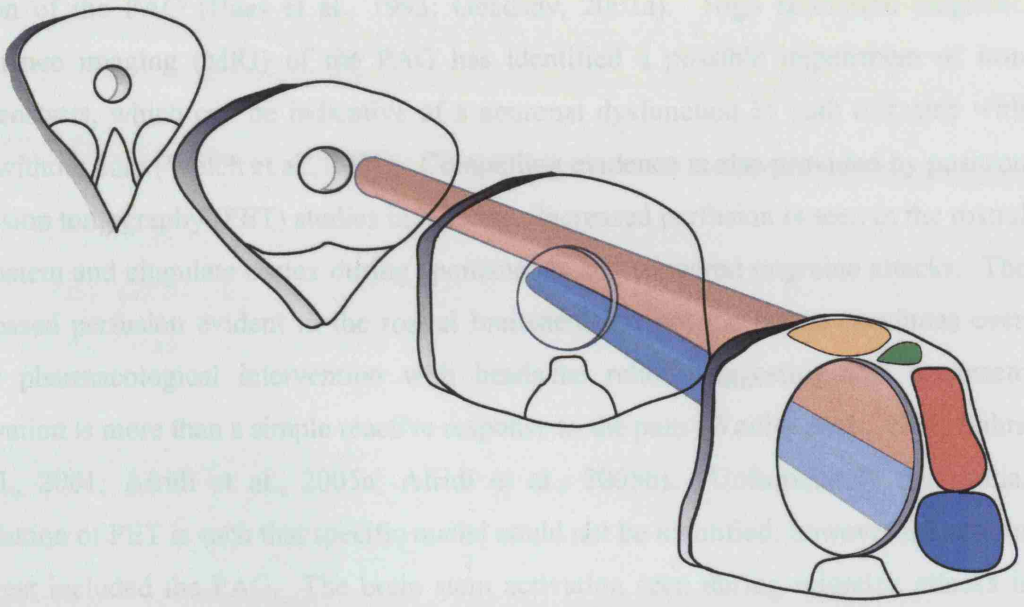

Figure 13: Schematic illustration of the columnar organisation of the periaqueductal gray.

Extent of the lateral (red) and ventrolateral (blue) neuronal columns within the rostral (far left) and caudal (far right) extent of the PAG. The caudal ends of the dorsomedial (orange) and dorsolateral (green) neuronal columns are also shown, both of which extend along the whole length of the PAG.

Periaqueductal gray and migraine

Investigations into the PAG as an anti-nociceptive modulatory structure are widely documented in many animal models of pain (Reynolds, 1969; Behbehani, 1995). The first evidence for brainstem modulation of descending inhibition was undertaken in the rat where it was found that electrical stimulation of the PAG produced analgesia sufficient for abdominal surgery (Reynolds, 1969). In humans PAG electrical stimulation can be used for the treatment of intractable somatic pain, and in some cases this has been shown to trigger head pain in previously headache-free individuals. The headaches are similar to migraine and include many of the characteristics including: unilateral location, throbbing quality and associated nausea and vomiting (Raskin et al., 1987; Veloso et al., 1998). Further evidence for a role of the PAG in migraine was

obtained from the development of a migraine-like headache attributed to lesions in the region of the PAG (Haas et al., 1993; Goadsby, 2002a). High resolution magnetic resonance imaging (MRI) of the PAG has identified a possible impairment of iron homeostasis, which can be indicative of a neuronal dysfunction in both migraine with and without aura (Welch et al., 2001). Compelling evidence is also provided by positron emission tomography (PET) studies in humans. Increased perfusion is seen in the rostral brainstem and cingulate cortex during spontaneous and triggered migraine attacks. The increased perfusion evident in the rostral brainstem but not the cortex continues even after pharmacological intervention with headache relief, suggesting that brainstem activation is more than a simple reactive response to the pain (Weiller et al., 1995; Bahra et al., 2001; Afridi et al., 2005a; Afridi et al., 2005b). Unfortunately the spatial resolution of PET is such that specific nuclei could not be identified; however the area of interest included the PAG. The brain stem activation seen during migraine attacks is also thought to be specific as it is not seen in experimentally induced or atypical facial pain (Derbyshire et al., 1994; May et al., 1998c), acute cluster headache (May et al., 1998a) and short-lasting, unilateral, neuralgiform headache attacks with conjunctival injection and tearing (SUNCT) (May et al., 1999a).

The ventrolateral column of the PAG (vlPAG) is of particular relevance to migraine as it selectively receives input from trigeminovascular afferents (Oliveras et al., 1974; Keay and Bandler, 1998; Hoskin et al., 2001) and stimulation of the vlPAG affects the nociceptive trigeminal-mediated jaw-opening reflex (Oliveras et al., 1974; Dostrovsky et al., 1982) in the cat. Recent research has identified that both electrical and chemical activation of the vlPAG can inhibit trigeminovascular specific nociception in the cat and rat (Knight and Goadsby, 2001; Knight et al., 2002; Knight et al., 2003), supporting the findings that vlPAG stimulation can inhibit MMA afferents (Strassman et al., 1986). Interestingly it has also been demonstrated that microinjection of the 5-$HT_{1B/1D}$ receptor agonist naratriptan into the vlPAG selectively inhibits A- and C-fibre responses to dural electrical stimulation raising the possibility that the triptans may exert part of there anti-migraine efficacy within the PAG (Bartsch et al., 2004a).

Hypothalamus

The hypothalamus surrounds the third ventricle and contains many individual nuclei (figure 14), the boundaries of which are not precise. The hypothalamus is known to have a multitude of functions including hormone synthesis, regulation of sympathetic and parasympathetic branches of the autonomic nervous system which control visceral functions, regulation of temperature and electrolyte balance, it contains a biological clock which determines biological rhythms, controls emotional behaviour, mediates motivational arousal, and regulation of the cardiovascular system (table 14).

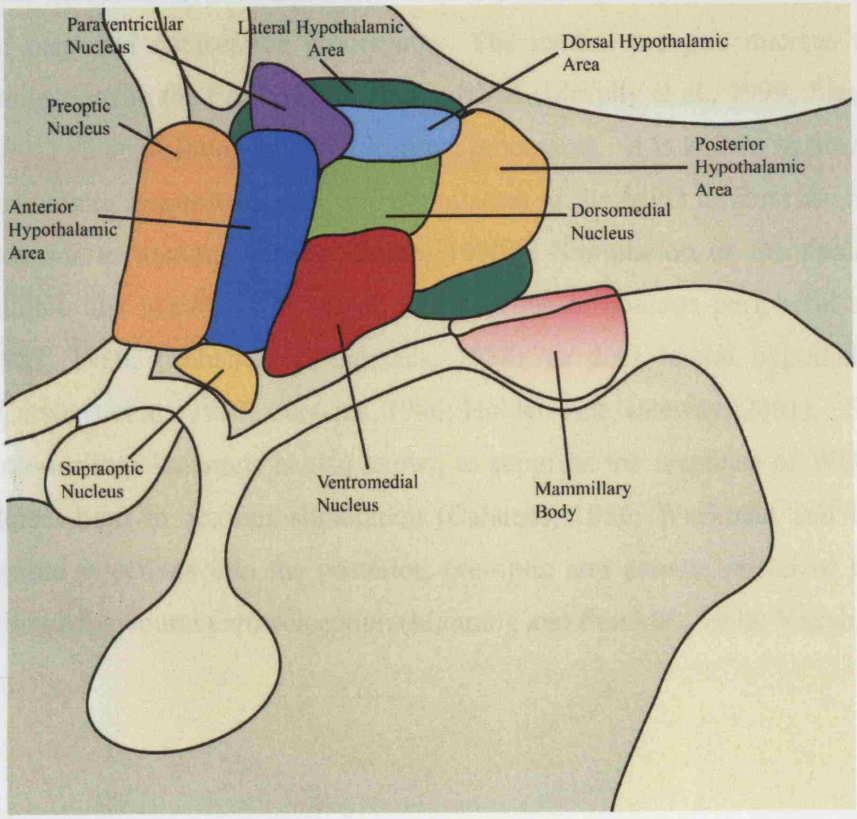

Figure 14: Hypothalamic nuclei.

Afferent and efferent nerve fibres connect the hypothalamus to a variety of structures including the cerebral cortex, thalamus, hippocampus, amygdala, septum, PAG and the spinal cord. The hypothalamus also receives a dense blood supply and individual nuclei

can be influenced by a wide variety of chemical messengers from the blood and cerebro-spinal fluid and neurotransmitters from other neurons.

The hypothalamus is not traditionally associated with nociceptive processing, however it does receive a direct ascending pathway form the dorsal horn (Giesler, 1995; Millan, 1999). As mentioned the hypothalamus has afferent and efferent connections with many structures, including the nucleus tractus solitarius (NTS), rostroventromedial medulla (RVM), PAG and nucleus raphe magnus (NRM) as well as some corticolimbic structures implicated in the affective and cognitive aspects of pain (Millan, 1999). To date numerous hypothalamic nuclei have been implicated in the descending modulation of pain and nociceptive processing. The medial preoptic nucleus (MPO) has clear projections to the PAG, NRM and the RVM (Murphy et al., 1999; Jiang and Behbehani, 2001) all areas involved in nociceptive processing. It is known to play a key role in the autonomic response to pain, and stimulation of the MPO inhibits the response of spinal neurons to noxious stimuli (Lumb, 1990). Stimulation of the medial hypothalamus inhibits the responses of spinal cord neurons to noxious peripheral stimuli (Carstens, 1982, 1986; Culhane and Carstens, 1988), as does lateral hypothalamic stimulation (Carstens et al., 1983; Carstens, 1986; Holden and Naleway, 2001). Stimulation of the anterior hypothalamus is also known to suppress the response of WDR neurons in the dorsal horn to noxious stimulation (Carstens, 1986; Workman and Lumb, 1997) and opioid injections into the posterior, pre-optic and arcuate nuclei of the hypothalamus elicit behavioural antinociception (Manning and Franklin, 1998; Yaksh, 1999).

Table 13: Selected hypothalamic nuclei and their known functions.

Nuclei
Preoptic area (POA) and anterior hypothalamus (AH)
Synthesis of LHRH and TRH
Coordinates parasympathetic nervous system functions
Temperature regulation; vasodilation responses to heat
Suprachiasmatic nuclei (SCN)
Biological clock, regulates rhythmic release of certain hormones
Regulates sleep-wake cycle and other body rhythms
Supraoptic nuclei (SON)
Synthesis of vasopressin (ADH)
Regulation of thirst and drinking
Lateral Hypothalamus (LH)
Control of hunger
Regulation of sodium balance
Dorsomedial nuclei (DMN)
Regulates autonomic nervous system activity
Control of aggression
Posterior hypothalamus (PH)
Temperature regulation- response to cold
Regulates sympathetic nervous system and visceral functions
Regulates fight or flight response
Influences sleep and arousal

ADH: antidiuretic hormone.

Trigeminohypothalamic tract

The presence of a trigeminohypothalamic tract, the trigeminal equivalent of the spinohypothalamic tract, has been known for some time. Retrograde tracing studies using injection of flouro-gold into the hypothalamus of rats labelled numerous neurons throughout the extent of the TNC, with the majority of cells labelling contralaterally (Burstein et al., 1991). Direct projections from the TNC to the posterior and lateral hypothalamus have also been demonstrated (Iwata et al., 1992) in the rat.

The Hypothalamus and Migraine

It is now widely accepted that the hypothalamus plays a major role in the group of primary headaches resulting in pain and autonomic involvement termed trigeminal autonomic cephalgias (TAC's) (Goadsby and Lipton, 1997). Initial observations indicating a seasonal and circadian rythmicity to the onset of attacks points firmly at the involvement of the suprachiasmatic nucleus (Zurak, 1997). Further evidence is gained from the close correlation with sleep (Dodick et al., 2003) and the presence of cranial autonomic symptoms. Clinical evidence indicating endocrine abnormalities have identified altered production of melatonin, cortisol, testosterone, lutenising-hormone and prolactin during cluster headache. Similar findings in chronic migraine support the involvement of the hypothalamus in the pathophysiology of both cluster headache and chronic migraine (Peres et al., 2001).

PET and fMRI studies have identified hypothalamic activation during spontaneous, as well as triggered cluster attacks and SUNCT (May et al., 1998a, 2000; Sprenger et al., 2004a; Sprenger et al., 2004b) and permanent subtle structural abnormalities have been identified using MRI (May et al., 1999b). In response to the imaging evidence the use of deep brain stimulation in the posterior hypothalamus for the treatment of chronic cluster headache has proved a successful intervention strategy providing strong evidence for the involvement of the hypothalamus in cluster headache (Leone et al., 2001; Franzini et al., 2003; Leone et al., 2003).

As mentioned the hypothalamus is known to play an important role in the pathophysiology of cluster headache and other TAC's as well as chronic migraine. The same may be true for migraine. The presence of premonitory symptoms up to 48 hours preceding the onset of an attack indicate an underlying hypothalamic dysfunction (Giffin et al., 2003; Kelman, 2004) as does recent research indicating the presence of similar symptoms following glyceryl trinitrate (GTN) triggered attacks (Afridi et al., 2004). As with cluster headache, migraine attacks demonstrate a striking circadian rythmicity (Solomon, 1992; Fox and Davis, 1998) and link to hormonal fluctuation (MacGregor, 2000) further implicating the hypothalamus.

Experimental evidence for a role of the hypothalamus in migraine has been provided from a variety of studies. Malick *et al.* (2001) demonstrated that stimulation of the dura mater in the rat produced Fos expression in the ventromedial, paraventricular and dorsomedial hypothalamic nuclei resulting in suppression of appetite and increases in arterial blood pressure. The findings indicate a complex relationship between nociceptive trigeminal neuron activation and suppression of food intake at the level of the hypothalamus, consistent with clinical observations of loss of appetite in migraine (Malick et al., 2001). Stimulation of the superior sagittal sinus (SSS) in the cat has also demonstrated hypothalamic activation with up-regulation of Fos protein-like immunoreactivity in the supra-optic and posterior hypothalamic nucleus consistent with a role for hypothalamic structures in modulation of nociceptive (Benjamin et al., 2004).

The Orexins

The orexins are two neuropeptides derived from the same 130 amino acid precursor peptide, prepro-orexin, by proteolytic cleavage. A single gene located on chromosome 17q21 in humans is responsible for encoding prepro-orexin (Sakurai et al., 1998; Sakurai, 2005). Following proteolytic cleavage both orexin peptides are post-transationally modified, with the addition of N-terminal pyroglutamyl cyclisation and C-terminal amidation for orexin A and only C-terminal amidation for orexin B (figure 15) (Lee et al., 1999). Mature orexin A is a 33-residue neuropeptide containing two

disulfide bridges, Cys6-Cys12 and Cys7-Cys14 (Soll and Beck-Sickinger, 2000) which are essential for functional potency (Darker et al., 2001; Okumura et al., 2001) as are the 19 C-terminal residues (Darker et al., 2001). Mature orexin B is a 28-residue neuropeptide containing 2 α-helices linked by a flexible loop (Lee et al., 1999). Orexin A and B are 46% homologous, and the sequence of orexin A is fully conserved across rat, mouse, pig, cow and human (Sakurai et al., 1998; Dyer et al., 1999; Shibahara et al., 1999). Orexin B shows a slight variation across species, with the rat/mouse isoforms differing by 2 amino acids compared with the human sequence (Shibahara et al., 1999) and porcine orexin b has a single serine-to-proline substitution (Dyer et al., 1999).

The orexins bind to two G-protein coupled receptors, termed OX_1 and OX_2 (Foord et al., 2005). The two receptors are 64% homologous and are most closely related (26%) to the NPY2 receptor (Sakurai et al., 1998). The rat and human receptors for OX_1 and OX_2 demonstrate a 94% and 95% homology respectively, suggesting a high level of conservation across mammalian species (Sakurai et al., 1998). Orexin A has equal affinity for both the OX_1 and OX_2 receptors, with orexin B demonstrating a 10-fold higher affinity for the OX_2 than the OX_1 receptor. Activation of either OX_1 or OX_2 results in elevated levels of intracellular Ca^{2+} concentrations (Smart et al., 1999; Lund et al., 2000) which results in the enhancement of the G_q-mediated stimulation of phospholipase C.

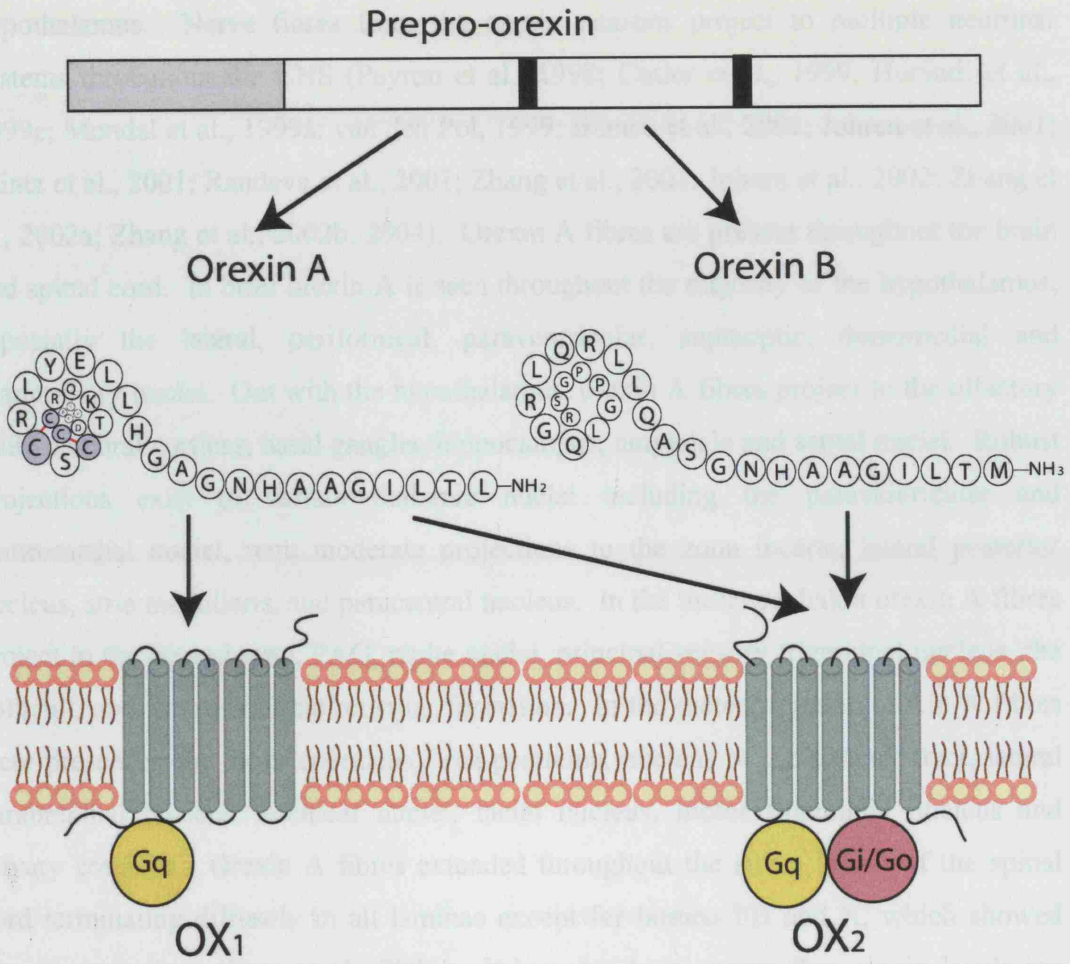

Figure 15: Schematic representation of the orexin system.

Orexin A and B are cleaved from a common precursor peptide, prepro-orexin. The orexins act on two G protein-coupled receptors, OX_1 and OX_2. OX_1 couples exclusively to the G_q subclass of heterotrimeric G proteins, whereas OX_2 couples with $G_{i/o}$ and/or G_q. OX_1 is selective for orexin A, whereas OX_2 is non-selective for both orexin A and B (Sakurai et al., 1998; Lee et al., 1999).

Distribution of the orexinergic system

The orexins are synthesised by neurons located exclusively in the lateral and posterior hypothalamus. Nerve fibres from the orexin neurons project to multiple neuronal systems throughout the CNS (Peyron et al., 1998; Cutler et al., 1999; Horvath et al., 1999c; Mondal et al., 1999a; van den Pol, 1999; Blanco et al., 2001; Johren et al., 2001; Mintz et al., 2001; Randeva et al., 2001; Zhang et al., 2001; Johren et al., 2002; Zhang et al., 2002a; Zhang et al., 2002b, 2004). Orexin A fibres are present throughout the brain and spinal cord. In brief orexin A is seen throughout the majority of the hypothalamus, especially the lateral, perifornical, paraventricular, supraoptic, dorsomedial and mammillary nuclei. Out with the hypothalamus, orexin A fibres project to the olfactory bulb, cerebral cortices, basal ganglia, hippocampus, amygdale and septal nuclei. Robust projections exist to certain thalamic nuclei including the paraventricular and centromedial nuclei, with moderate projections to the zona incerta, lateral posterior nucleus, stria medullaris, and paracentral nucleus. In the mesencephalon orexin A fibres project to the central gray, PAG, raphe nuclei, principal sensory trigeminal nucleus, the colliculi, and throughout the reticular formation. In the metencephalon orexin A fibres were present in the locus coeruleus, area postrema, nucleus of the solitary tract, lateral parabrachial nucleus, cochlear nuclei, facial nucleus, motor trigeminal nucleus and olivary complex. Orexin A fibres extended throughout the entire length of the spinal cord terminating diffusely in all laminae except for lamina I/II and X, which showed denser projections (Date et al., 2000). It has also been shown that orexin levels are highest in the cervical spinal cord and decline along the cephalocaudal axis (Date et al., 2000).

Orexin B fibres follow a similar distribution pattern as orexin A although fewer sites demonstrated orexin B immunoreactivity and were present at much lower densities. One notable difference in distribution was the lack of orexin B fibres from the ventricular surface, suggesting orexin A and not B may be influenced by hormones.

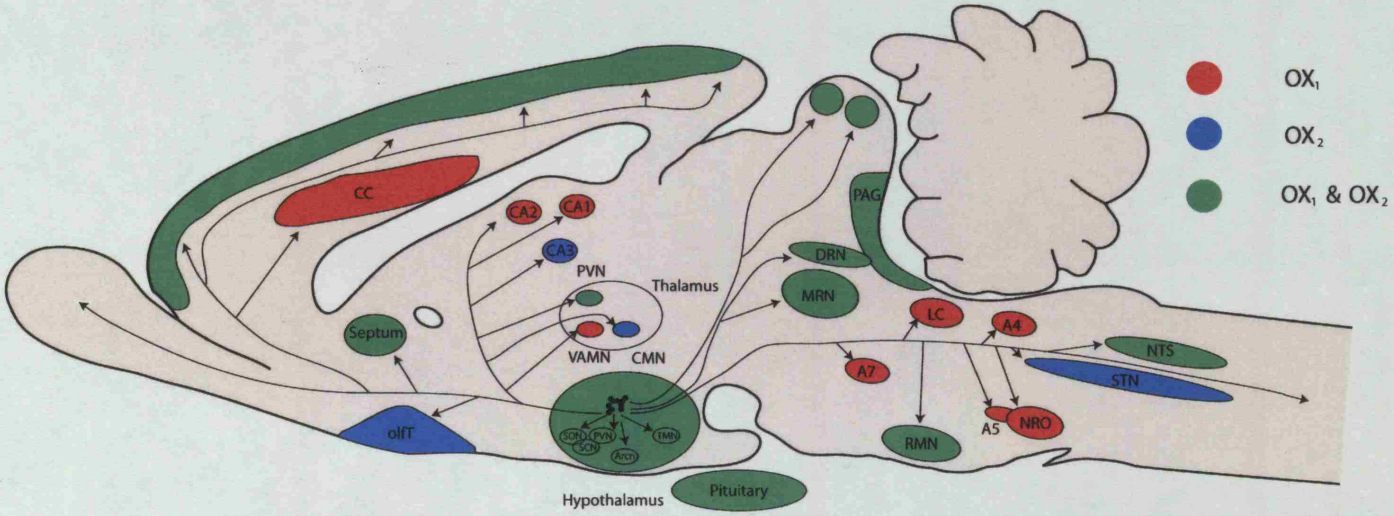

Figure 16: Orexinergic pathways and orexin 1 and 2 receptor mRNA distribution in the rat brain.

A summary of the major orexinergic pathways and receptor mRNA distribution in the rat brain. Not all pathways and sites are shown and the level of expression may be varied between areas, adapted from the references of (de Lecea et al., 1998; Sakurai et al., 1998; Trivedi et al., 1998; Chen et al., 1999; Cutler et al., 1999; Date et al., 1999; Harrison et al., 1999; Horvath et al., 1999a; Horvath et al., 1999c; Horvath et al., 1999b; Mondal et al., 1999b; Mondal et al., 1999a; van den Pol, 1999; Date et al., 2000; Hervieu et al., 2001; Marcus et al., 2001). Arcn, arcuate nucleus; CA1-3, areas of hippocampus; CC, cingulate cortex; CMN, centromedial nucleus; DRN, dorsal raphe; LC, locus coeruleus; MRN, median raphe nucleus; NST, nucleus of solitary tract; olfB, olfactory bulb; olfT, olfactory tubercle; PVN, paraventricular nucleus; NRM, nucleus raphe magnus; RO, nucleus raphe obscurus; SCN, suprachiasmatic nucleus; SON, supraoptic nucleus; STN, spinal trigeminal nucleus; TMN, tuberomamillary nucleus; VAMN, ventral anteromedial nucleus.

Orexin receptor distribution (figure 16) has been most widely investigated in the rat. In general the receptor expression is in agreement with the orexinergic fibre projections and OX_1 and OX_2 receptor distributions are largely distinct and complementary throughout the CNS (Trivedi et al., 1998; van den Pol, 1999; Blanco et al., 2001; Hervieu et al., 2001; Johren et al., 2001; Marcus et al., 2001; Backberg et al., 2002). In brief, OX_1 receptor mRNA is preferentially located in the prelimbic and infralimbic cortices in layers 2–3, whereas OX_2 receptor mRNA is preferentially expressed in the deep layers (5–6). Within the hippocampus OX_1 receptors are densest in the CA2 region and OX_2 receptors the CA3 region. The two receptors are similarly expressed in the thalamus, but show differential staining patterns in the hypothalamus. OX_2 receptors are densest in the dorsomedial, arcuate, paraventricular and tuberomammilary nuclei as well as the lateral hypothalamic area, all areas expressing low levels of OX_1 receptor mRNA. OX_1 receptor mRNA expression was most abundant in the anterior hypothalamic area, dorsomedial, central and ventrolateral parts of the ventromedial hypothalamic nucleus. In the midbrain, pons and medulla OX_1 receptors were preferentially located in the locus coeruleus, A5 and A7 group, the ventral lateral medulla and the laterodorsal and pedunculopontine tegmental nuclei. OX_2 receptor mRNA in contrast was strongest in the tuberomammilary nucleus, parabigeminal nucleus and nucleus of the trapezoid body. Similar expression levels were detected in the ventral tegmental area and the dorsal raphe nucleus. The trigeminal nuclei expressed higher levels of OX_2 receptor mRNA than OX_1.

Functions of the orexins

The orexins in feeding and energy homeostasis

Early studies utilising lesions in the lateral hypothalamus of several species identified a syndrome of decreased food and water intake resulting in lowered body weight (Teitelbaum and Epstein, 1962; Bernardis and Bellinger, 1996). Intracerebroventricular (i.c.v.) injection of orexin A, stimulates feeding in rats and this response has been partially mimicked by orexin B administration (Sakurai et al., 1998; Edwards et al., 1999; Haynes et al., 1999; Yamanaka et al., 2000). In addition, OX_1 receptor

antagonists have been shown to inhibit natural and orexin A induced feeding (Arch, 2000). Central administration of orexin A also increases gastric acid secretion, indicating a possible role in digestion (Takahashi et al., 1999). The orexinergic influence on feeding has been demonstrated to be highly dependant on circadian processes, with the effect of orexin A administration on feeding varying depending on time of day (Haynes et al., 1999). This is further evident, as chronic infusion of orexin A results in disruption of the normal circadian feeding pattern in rats with no subsequent weight loss, indicating total daily food intake was unaltered (Haynes et al., 1999; Yamanaka et al., 1999).

The orexins and sleep wake cycle

Early studies investigating the response of electrical stimulation of the lateral hypothalamic area (LHA) demonstrated an increased level of wakefulness, while destruction of the LHA resulted in somnolence and inattentiveness (Levitt and Teitelbaum, 1975; Danguir and Nicolaidis, 1980; Bernardis and Bellinger, 1996). The initial discovery for an orexinergic function in sleep wake modulation came from the identification of a mutation at the OX_2 receptor, responsible for the canine narcolepsy model (Lin et al., 1999). In addition, orexin knockout mice were reported to suffer from episodes of cataplexy and alteration of sleep/wake cycles during the dark period (Chemelli et al., 1999). Interestingly, OX_1 receptor knockout mice do not demonstrate any behavioural abnormalities, suffering only from fragmentation of the sleep/wake cycle (Kisanuki et al., 2000). Suggesting that both receptor subtypes play a role in the regulation of the sleep/wake cycle. The orexinergic involvement in human narcolepsy has focused mainly on levels of orexin peptides in cerebrospinal fluid. Ninety percent of narcoleptic patients demonstrate a decreased level of orexin A in their cerebrospinal fluid (Mignot et al., 2002b), as well as an 80–90% reduction in the number of prepro-orexin expressing neurons (Peyron et al., 2000; Thannickal et al., 2000).

Histological evidence also implicates the orexinergic system in the regulation of sleep/wakefulness. Robust projections from the hypothalamic orexin neurons to the monoaminergic nuclei including the tuberomammilary nucleus, locus coeruleus, dorsal

raphe, ventral tegmental area, pedunculopontine tegmental area and the laterodorsal tegmental area provide strong anatomical evidence of their involvement.

The orexins and nociception

The orexins have been shown to project to multiple neuronal systems, many of which are involved in nociceptive processing (Peyron et al., 1998; Trivedi et al., 1998; Cutler et al., 1999; van den Pol, 1999; Marcus et al., 2001; Mintz et al., 2001; Zhang et al., 2001; Zhang et al., 2002a; Zhang et al., 2002b, 2004). Robust innervation of the hypothalamus, PAG and lamina I, II and X of the spinal cord demonstrate anatomical evidence for a role in the modulation of nociceptive processing.

Destruction of the posterior hypothalamus in rats results in transient hyperalgesia (Millan et al., 1983) indicating a possible hypothalamic role in the maintenance of a basal nociceptive threshold. Bingham *et al.* (2001) postulated a novel descending orexinergic inhibitory system in the rat raising the possibility that this maintenance of basal nociceptive threshold may be orexin driven.

Experimental evidence on a possible role of the orexins in modulating nociceptive processing is both complimentary and contradictory. Bingham *et al.* (2001) reported that orexin A is anti-nociceptive in the thermal and visceral nociceptive tests in the rat and mouse and anti-hyperalgesic in the mouse carrageenan-induced thermal hyperalgesia test when given intravenously or intracerebroventricularly. N-(2-Methyl-6-benzoxazolyl)-N"-1,5-naphthyridin-4-yl urea (SB-334867) a selective non-peptide OX_1 receptor antagonist reversed the orexin A effects as well as demonstrating hyperalgesic activity when given alone, suggesting the presence of a descending orexinergic inhibitory system that is activated under inflammatory conditions. The responses observed were independent of the endogenous opiate system a finding confirmed by Yamamoto *et al.* (2002) in the rat, despite having similar effects as morphine (Bingham et al., 2001).

Yamamoto *et al.* (2002) also demonstrated the analgesic effects of orexin A and proposed a spinal cord mechanism. Orexin B had no effect on any of the aspects studied and SB-334867 was again able to antagonise the effects of orexin A, however no change was seen when given alone. Thus it is possible that the descending inhibitory system proposed by Bingham *et al.* (2001) is only activated during inflammatory conditions, such as the mouse carrageenan-induced thermal hyperalgesia test and not under resting conditions or acute nociceptive stimuli such as the rat formalin or hot plate test (Yamamoto et al., 2002).

A similar result was observed by Kajiyama *et al.* (2004), with orexin A demonstrating analgesic effects in diabetic but not normal rats. In this model orexin B when given at a higher dose than orexin A produced some antinociceptive effects; however both responses were blocked by SB-334867 suggesting an OX_1 receptor site of action. SB-334867 when administered intrathecally elicited an increase in diabetes-induced mechanical hyperalgesia suggesting that the endogenous spinal cord OX_1 receptors may be responsible for hyperalgesia in diabetes (Kajiyama et al., 2005).

Further discrepancies in the roles of orexin A and B in different models of nociception exist. Suyama *et al.* (2004) demonstrated that only orexin A and not orexin B inhibit heat evoked hyperalgesia in the rat when given intrathecally. Orexin A also reduces mechanical allodynia when given intrathecally or intracerebroventricularly via a spinal or supraspinal mechanism (Suyama et al., 2004) that did not involve any peripheral mechanisms proposed by Bingham *et al.* (2001).

Cheng *et al.* (2003) in agreement with Kajiyama *et al.* (2004) demonstrated an effect of both orexin A and B in a model of postoperative pain. Orexin A demonstrated a more potent effect than orexin B and was exclusively mediated via the OX_1 receptor, whereas the effect of orexin B was only partially mediated by the OX_1 receptor. The study also demonstrated that opioid receptors were not involved in the orexin response; however the possibility of a role for the glycine and P2X receptors was raised (Cheng et al., 2003).

The variety of results with regards to the differing roles of orexins and the modulation of pain are most likely due to the experimental model being utilised. Clear evidence for a state dependant role of the orexins has been demonstrated in prepro-orexin knockout mice (Watanabe et al., 2005). Under normal baseline conditions there was no difference in pain thresholds between knockout and wild type mice. However following the induction of peripheral inflammation prepro-orexin knock out mice demonstrated a greater degree of hyperalgesia and lowered stress-induced analgesia than their wild type counterparts. It would appear that the orexinergic system facilitates an increase in pain thresholds under inflammatory conditions and this is likely to be mediated within the CNS (Watanabe et al., 2005). Peripheral inflammation is known to activate ascending pain pathways, which as previously described project to higher structures including the hypothalamus. Watanabe et al. (2005) demonstrated that under inflammatory conditions orexinergic hypothalamic neurons are activated, however this may be as a result of the ascending nociceptive input or as a result of the activation of endogenous descending inhibitory pathways (Millan, 2002). The distribution of the orexinergic system from the hypothalamus to the PAG and spinal cord present the possibility for both the modulation of descending inhibitory pathways or the direct release of orexin at the spinal cord, suppressing nociceptive inputs at the second order relay neurons as demonstrated by the antinociceptive effects of spinal as well as intracerebroventricularly administration (Bingham et al., 2001; Yamamoto et al., 2002; Cheng et al., 2003; Yamamoto et al., 2003b; Yamamoto et al., 2003a; Mobarakeh et al., 2005).

The orexins and a possible role in migraine

The orexins have only very recently been linked with a possible role in migraine and the evidence as such is circumstantial. An obvious generic link is the anatomical distribution of the orexins and the discovery that they could influence nociceptive processing. A link between migraine and sleep has long been established. Migraine attacks are common during REM sleep periods and many patients find sleeping to be the preferred method to abort an attack. Narcolepsy is a disorder of the sleep-wake cycle with a prevalence of approximately 0.05% in the general population (Aldrich, 1990). It

is characterised by excessive daytime somnolence, overwhelming episodes of sleep, disturbed nocturnal sleep, hypnagogic hallucinations, sleep paralysis, and cataplexy (Aldrich, 1990). The orexinergic system has been linked to the pathophysiology of narcolepsy and it is widely accepted that dysfunction of the hypothalamic orexinergic systems and a loss of orexinergic cells, possibly as a result of an autoimmune disorder, play a causative role (Peyron et al., 2000).

It has been shown that narcoleptic patients have a greatly increased prevalence of migraine. In a study of 68 narcoleptic patients 64% of women and 35% of men were found to suffer from migraine attacks (Dahmen et al., 1999) fulfilling all the International Headache Society (IHS) criteria (Headache Classification Committee of the International Headache Society, 2004). In contrast, the life time prevalence of migraine in the general population is in the range of 16–25% for woman and 7–8% in men (Breslau et al., 1991; Rasmussen et al., 1991; Rasmussen and Olesen, 1992; Stewart et al., 1995; MacGregor et al., 2003; Bigal et al., 2004). The increased prevalence of migraine in narcoleptic patients was later confirmed in a larger study, with 44% of women and 23% of men suffering from migraine (Dahmen et al., 2003).

One interesting finding is the late onset of migraine in narcoleptic patients, demonstrating that narcolepsy appears to put people at an increased risk for migraine compared to the general population (Gobel and Soyka, 1992). The neuroanatomical base of both disorders may involve the brainstem, lesions in the region of the periaqueductal gray (PAG) and dorsal raphe nucleus (DRN) combined with activation of the serotonergic DRN and noradrenergic locus coeruleus all point to a role of the brainstem in migraine (Raskin et al., 1987; Weiller et al., 1995; Afridi and Goadsby, 2003; Afridi et al., 2005b). Cells in these regions play a critical role in rapid eye movement (REM) sleep, a regulatory disturbance of which is thought to underline narcolepsy (Aldrich, 1990; Datta, 1997).

One common pathway, which may provide a link between the two disorders, is the serotonergic system. Pontogeniculo-occipital spikes, an electrophysiological feature of REM sleep can be inhibited by serotonergic mechanisms (Horner et al., 1997).

Hypothalamic orexinergic projections innervate the serotonergic DRN and the densest projections in the brain stem terminate in the noradrenergic LC (Peyron et al., 1998). LC orexinergic synapses are consistent with Gray type I, excitatory synapses (Eccles, 1964) in agreement with the stimulatory orexin B mediated input to the locus coeruleus (LC) (Horvath et al., 1999c).

The orexinergic projections to the DRN, an important nucleus involved in the modulation of pain sensation (Wang and Nakai, 1994) and the sleep-wake cycle (Sakai and Crochet, 2001; Monti et al., 2002), implicate it in the pharmacology of both disorders. OX_1 receptors and to a lesser extent OX_2 receptors have been localised to serotonergic neurons in the DRN (Wang et al., 2005) providing evidence that orexin can directly excite DRN serotonergic neurons and thus may be involved in the modulation of the descending and ascending serotonergic inhibitory and excitatory pathways. It has been shown that both orexin A and B excite DRN serotonergic neurons as well as GABAergic interneurons (Brown et al., 2002; Liu et al., 2002). Thus the orexinergic system can directly excite or indirectly inhibit serotonergic DRN neurons, consistent with a modulatory role.

Further evidence for a possible role of the orexinergic system in the pathophysiology of episodic brain disorders such as migraine is provided by genetic association studies in cluster headache. The 1246 G>A polymorphism of the OX_2 gene (HCRT2) is significantly associated with an increased risk of cluster headache. Patients homozygous for the G allele, in comparison to the remaining genotypes are 5 fold more likely to develop the disorder (Rainero et al., 2004). The hypothalamus is clearly implicated in the pathophysiology of cluster headache (Goadsby, 2002b) and the same may be true of migraine. The orexinergic system provides a novel descending pathway through which

the hypothalamus could modulate numerous processes including sensory processing of pain at various levels exerting both excitatory and inhibitory effects.

Direct evidence for a role of the orexinergic system in the modulation of migraine has not yet been investigated. However in an animal model of trigeminovascular activation, activation of the OX_1 and OX_2 receptor in the posterior hypothalamus has been shown to differentially modulate nociceptive dural input to the TNC (Bartsch et al., 2004b). Activation of the OX_1 receptor elicits an anti-nociceptive effect whereas OX_2 receptor activation elicits a pro-nociceptive effect. Experimental evidence indicates that regulation of autonomic and neuroendocrine functions as well as nociceptive processing is closely coupled in the hypothalamus (Buijs and Van Eden, 2000) and recent data points to the involvement of orexinergic mechanisms (Smart, 1999). Thus the orexinergic system is a posterior hypothalamic mechanism that is involved in central pain modulating of dural input and could be a possible link between the pain of primary neurovascular headaches and the symptomatology that is suggestive of a hypothalamic dysfunction in migraine (Overeem et al., 2002).

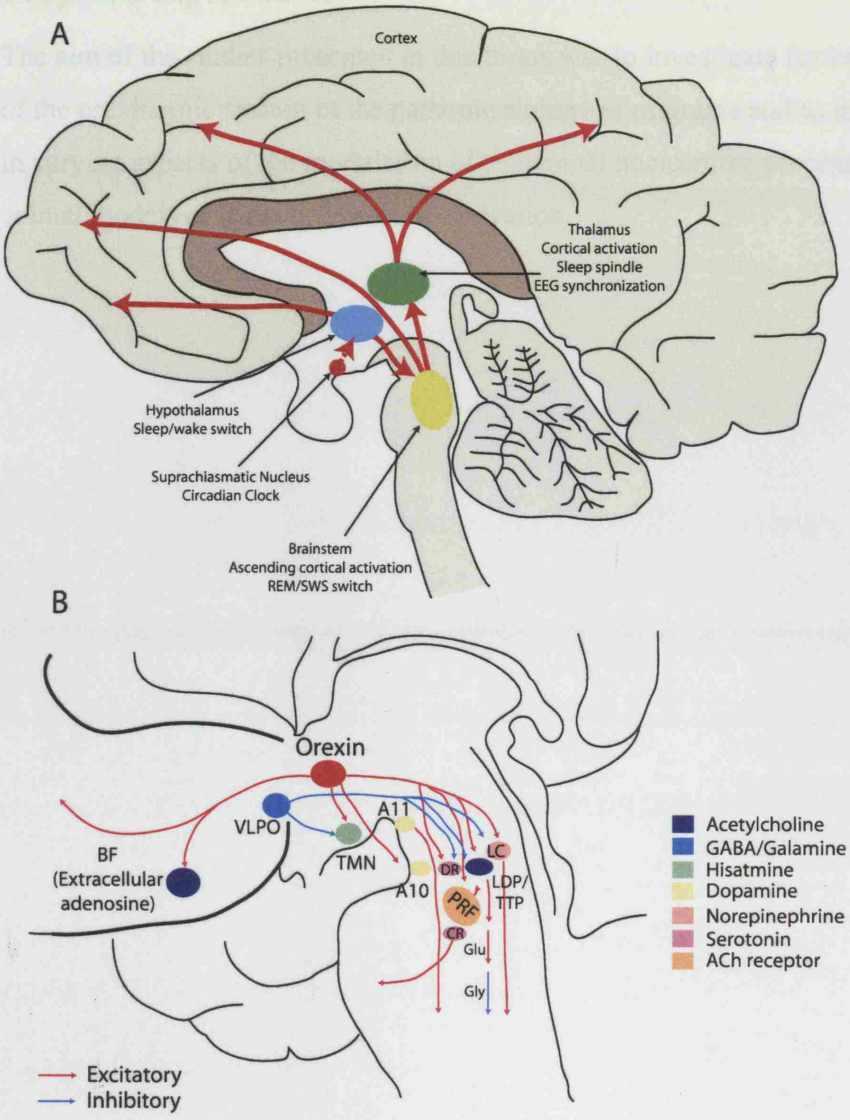

Figure 17: Hypothalamic and brainstem sleep/wake regulation systems, in relation to narcolepsy and its pharmacological treatment.

(A) Distinct roles of the brainstem, thalamus, hypothalamus and cortex for control of vigilance. (B) The sleep-promoting GABAergic/galaninergic neurons in the ventrolateral preoptic area (VLPO) and the wake-promoting orexin neurons in the lateral hypothalamus. Both of these systems innervate the noradrenergic locus coeruleus (LC), serotonergic dorsal raphe nucleus (DRN) and histaminergic tuberomammilary nucleus (TMN) all areas implicated in the pathophysiology of episodic brain disorders such as migraine. BF, basal forebrain cholinergic nuclei; LDT/PPT, laterodorsal tegmental nuclei/pedunculopontine tegmental nuclei; CR, caudal raphe; PRF, pontine reticular formation; Ach, acetylcholine; NE, norepinephrine; GLY, glycine; GLU, glutamate; SWS, slow-wave sleep; REM, rapid eye movement (Mignot et al., 2002a).

Proposed experiments

The aim of the studies presented in this thesis was to investigate further the involvement of the orexinergic system in the pathophysiology of migraine and to investigate their role in varying aspects of the modulation of trigeminal nociceptive processing in different animal models of trigeminovascular activation.

Chapter 2 - General Materials and Methods

Animals

The animals used in the experiments reported in this thesis were cats (n = 14) and Sprague-Dawley rats (n = 70). Both male and female cats were used (supplied by the Denny Brown Laboratories, Institute of Neurology, London, UK) and male rats (supplied by B&K Universal, UK). All animals were maintained on a 12-hour light/dark cycle, with food and water freely available in compliance with UK Home Office regulations. All experiments were conducted under a project and personal licence issued by the UK Home Office under the Animals (Scientific Procedures) Act 1986.

Cat

Anaesthesia and Maintenance

Cats were initially anaesthetized with α-chlorolose 60 $mgkg^{-1}$ intraperitoneal, and supplemented with 20 $mgkg^{-1}$ α-chlorolose in a solution of 2-hydroxy-β-cyclodextrin intravenously when required (Storer et al., 1997). Gaseous halothane (Halothane BP 100%, Rhodia Organique Fine Ltd., Avonmouth, Bristol, BS11 9YF) was administered throughout surgery at 0.8–2.0% and discontinued at the completion of surgery. The need for supplementary anaesthesia was assessed via cardiovascular and respiratory parameters and papillary reaction to noxious pinching of the forepaw. During muscular paralysis the absence of gross fluctuations of blood pressure and heart rate were used to determine the need for supplementary anaesthesia (Wolfensohn, S. and Loyd, M. 1998). Body temperature was continuously monitored and maintained within normal physiological parameters via a rectal thermometer and homoeothermic blanket system (Harvard Instruments, UK). The cat was then endotracheally intubated with a tracheal tube (5.5 mm internal diameter, Portex Ltd., UK) and ventilated to maintain normal physiological parameters. The left femoral artery and vein were exposed and separated using blunt dissection and cannulated with polythene cannulae (external diameter, 1.3 mm, Portex Ltd, UK) to allow continuous measurement of blood pressure and heart rate and the administration and withdrawal of fluids and drugs, respectively. Patency of cannulae was confirmed by backflow of blood into a heparinised syringe and maintained

when required by administration of small amounts of heparinised isotonic saline (10 $unitsml^{-1}$, Multiparin, CP Pharmaceuticals, UK). Arterial blood gas parameters were measured at regular intervals (GEM Premiere 3000, Instrumentation Laboratory, UK) during the experiment and maintained within the normal physiological parameters, see table 16. The animals were then placed in a stereotaxic frame (Model 1600 stereotaxic frame, David Kopf Instruments, USA) for further cranial surgery. The eyes were covered in a lubricating ointment (Lacrilube®, Allergan Ltd., UK) to prevent drying of the cornea. During superior sagittal sinus stimulation a neuromuscular blocking agent, gallamine triethiodide (Concord Pharmaceuticals Ltd., UK) was administered intravenously (6–20 $mgkg^{-1}$) to prevent twitching artefact.

Surgical techniques

In order to stimulate the trigeminal primary afferents in the cat the superior sagittal sinus (SSS) and the surrounding dura mater was isolated and stimulated.

Superior sagittal sinus isolation

A midline incision was made in the skin covering the dorsal surface of the skull and a midline circular craniotomy of no more than 2 cm in diameter was drilled (Dental drill, MF-Perfecta with 945 hand piece, W & H, UK) in the presence of cooling saline to prevent any damage due to overheating. The dura mater along each side of the SSS and the underlying falx was then incised and polythene film (Polypropylene film, 0.18 mm thickness, Goodfellow Cambridge Ltd., UK) inserted to protect the underlying cortex. A brain well was then constructed using dental acrylic (Self curing cold acrylic, Vertex, UK) and filled with isotonic saline to prevent drying of SSS. The animals were then maintained under anaesthesia for 24 hours to recover from surgery. For SSS stimulation the well was drained and two platinum hook electrodes were carefully placed under the SSS and gently lifted. The well was then refilled with liquid paraffin (Sigma-Aldrich, UK) to prevent dehydration of the sinus and isolation of the underlying cortex.

Superior sagittal sinus stimulation

In order to activate trigeminal primary afferents in the cat the SSS was hooked onto a pair of bipolar stimulating electrodes connected to a Grass S88 stimulator (Grass Instrumentation, USA). The SSS was then stimulated via a stimulus isolation unit using square wave 250 μs pulses, every three seconds, 130–150 V for two hours. The electrodes were then removed and the animal left to rest for one hour to allow optimal Fos activation (Hoskin and Goadsby, 1999).

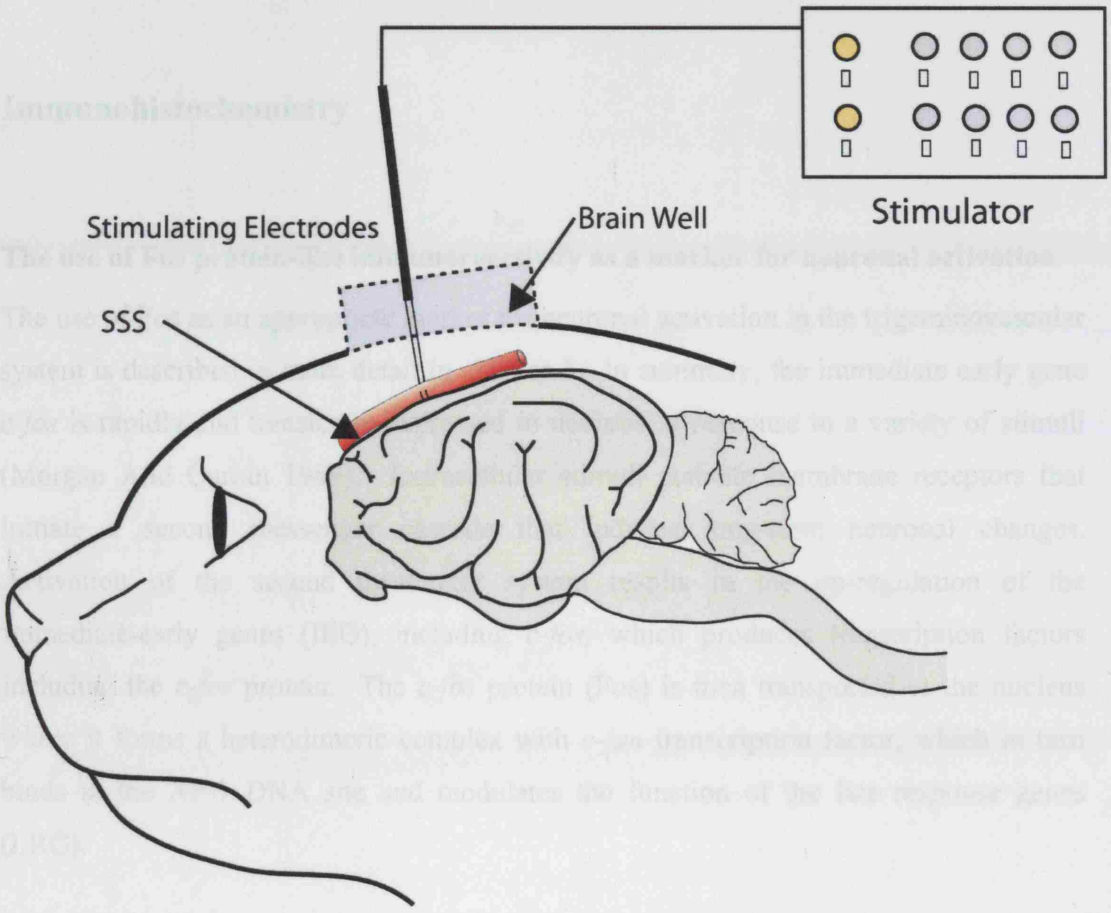

Figure 18: Cat experimental setup.

SSS, superior sagittal sinus

Perfusion and fixation

At the conclusion of experiments animals were perfused transcardially. They received 0.5 ml heparin (Heparin [mucous] injection B.P., 1000 IU) and 0.5 ml sodium nitrite (1%) immediately prior to the infusion into the left cardiac ventricle. Saline, 1.0–1.5 L (0.9%), followed by 2 L of paraformaldehyde (4%, Sigma-Aldrich, UK) and finally 0.6 L of sucrose (30%, BDH, UK) were infused via a mechanical pump (Model 505S, Watson Marlow ltd., UK). Following the perfusion, the brain and spinal cord were removed and stored in 30% sucrose at 4 °C, until used for immunohistochemistry.

Immunohistochemistry

The use of Fos protein-like immunoreactivity as a marker for neuronal activation

The use of Fos as an appropriate marker for neuronal activation in the trigeminovascular system is described in more detail in chapter 3. In summary, the immediate early gene *c-fos* is rapidly and transiently expressed in neurons in response to a variety of stimuli (Morgan And Curran 1989). Extracellular stimuli activate membrane receptors that initiate a second messenger cascade that induces long-term neuronal changes. Activation of the second messenger system results in the up-regulation of the immediate-early genes (IEG), including *c-fos,* which produces transcription factors including the *c-fos* protein. The *c-fos* protein (Fos) is then transported to the nucleus where it forms a heterodimeric complex with *c-jun* transcription factor, which in turn binds to the AP-1 DNA site and modulates the function of the late response genes (LRG).

There are a number of different events that can induce *c-fos* expression:

1. Neurotropic factors.
2. Neurotransmitters.
3. Depolarisation.
4. Increase of $Ca2^{+}$ influx and elevation of intracellular/intranuclear calcium.

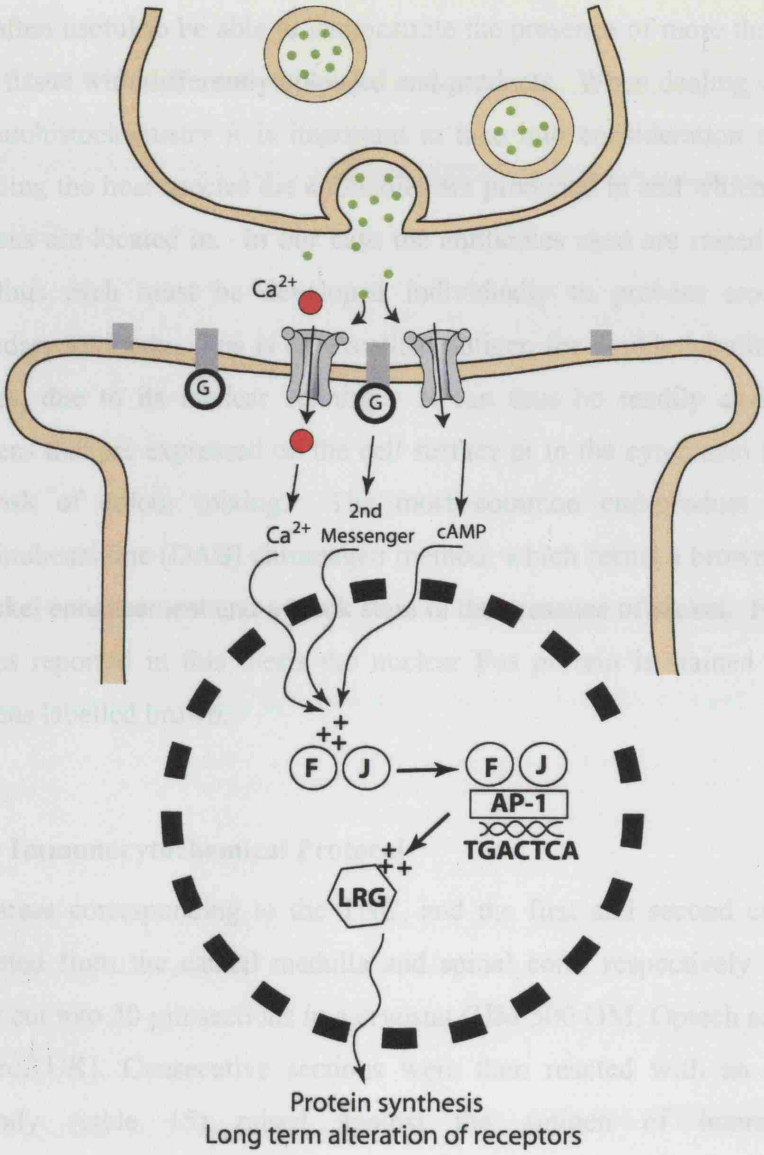

Figure 19: The induction of *c-fos*.

The immediate early gene *c-fos* is rapidly and transiently expressed in neurons in response to a variety of stimuli (Morgan And Curran 1989). Extracellular stimuli activate membrane receptors that initiate a second messenger cascade that induces long-term neuronal changes. Activation of the second messenger system results in the up-regulation of the immediate-early genes (IEGs), including *c-fos,* which produces transcription factors including the *c-fos* (F) protein. The *c-fos* protein (Fos) is then transported to the nucleus where it forms a heterodimeric complex with the *c-jun* (J) transcription factor, which in turn binds to the AP-1 DNA site and modulates the function of the late response genes (LRG).

The use of double labelling immunohistochemistry

It is often useful to be able to demonstrate the presence of more than one antigen in the same tissue with differently coloured end-products. When dealing with double labelling immunohistochemistry it is important to take into consideration a number of factors, including the host species the antibodies are produced in and which tissue structures the antigens are located in. In our case the antibodies used are raised in the same species and thus each must be developed individually to prevent cross reactivity of the secondary antibody. Fos is an excellent antigen for double labelling or co-localisation studies, due to its nuclear staining. It can thus be readily co-localised with many antigens that are expressed on the cell surface or in the cytoplasm for example, without the risk of colour mixing. The most common end-product used is the 3, 3'-diaminobenzidine (DAB) chromagen method, which forms a brown stain in the absence of nickel enhancement and a black stain in the presence of nickel. For the purpose of the studies reported in this thesis the nuclear Fos protein is stained black and the other antigens labelled brown.

Basic Immunocytochemical Protocol

The areas corresponding to the TNC, and the first and second cervical regions were dissected from the caudal medulla and spinal cord, respectively and frozen, prior to being cut into 30 μm sections in a cryostat (HM 500 OM, Optech scientific instruments, Oxford, UK). Consecutive sections were then reacted with an appropriate primary antibody (table 15) raised against the antigen of interest using standard immunocytochemical methods:

1. The sections were placed in netwells and rinsed in phosphate buffer (PB, Sigma, UK).
2. Sections were then washed in 50% Alcohol (Vector, UK) for 30 minutes on a rotating table.
3. Sections were then washed in 3% H_2O_2 (Vector, UK) for a further 30 minutes.

4. Incubated in 10% normal goat serum (NGS, Vector, UK), made up with 0.1 M PB, for 1 hour.
5. Incubated for 1 hour at room temperature then transferred to the fridge at 4°C overnight with the primary antibody, diluted in phosphate buffered goat serum (PBG; 0.1% Bovine serum albumin, 2% NGS, 0.2% Triton-X100 in PB).
6. Washed in PB for three separate 10 minute washes on a rotating table.
7. Incubated in an appropriate secondary antibody (table 15), diluted in PBG, for 2 hours at room temperature.
8. Wash in PB three times for 10 minutes on a rotating table.
9. Incubated with Extravidin Horseradish peroxidase (Vector, UK), diluted in PBG, for 2 hours at room temperature.
10. Washed in PB three times for 10 minutes on a rotating table.
11. Incubated with 20 mls of 3, 3'diaminobenzidine tetra hydrochloride dihydrate (DAB), either with or without nickel enhancement, for 15 minutes.
12. Sections were placed in a fresh 20 ml solution of DAB and 20 µl of glucose oxidase was added to initiate the chromagenic reaction.
13. The DAB reaction was interrupted by washing the sections three times for 5 minutes in PB, once the sections had reached the required staining level.
14. The reaction was then repeated using an antibody raised against a different antigen of interest.
15. Washed in PB, then dH_20 and mounted onto gelatinised coated slides and allowed to air dry.
16. Slides were then dehydrated through increasing concentrations of alcohols, cleared in xylene and cover-slipped.

Table 14: Antibodies used in this thesis and their source and concentration.

Antigen	Primary	Secondary	Tertiary	Chromagen
c-fos	Fos Ab (1:8,000)	Goat anti Rabbit (Vector, 1:200)	EHP (Vector, 1:1,000)	DAB (+Ni)
Ox A	Orexin A Ab (Pheonix, 1: 4,000)	Goat anti Rabbit (Vector, 1:200)	EHP (Vector, 1:600)	DAB (-Ni)
Ox B	Orexin B Ab (Pheonix, 1: 3,000)	Goat anti Rabbit (Vector, 1:200)	EHP (Vector, 1:600)	DAB (-Ni)

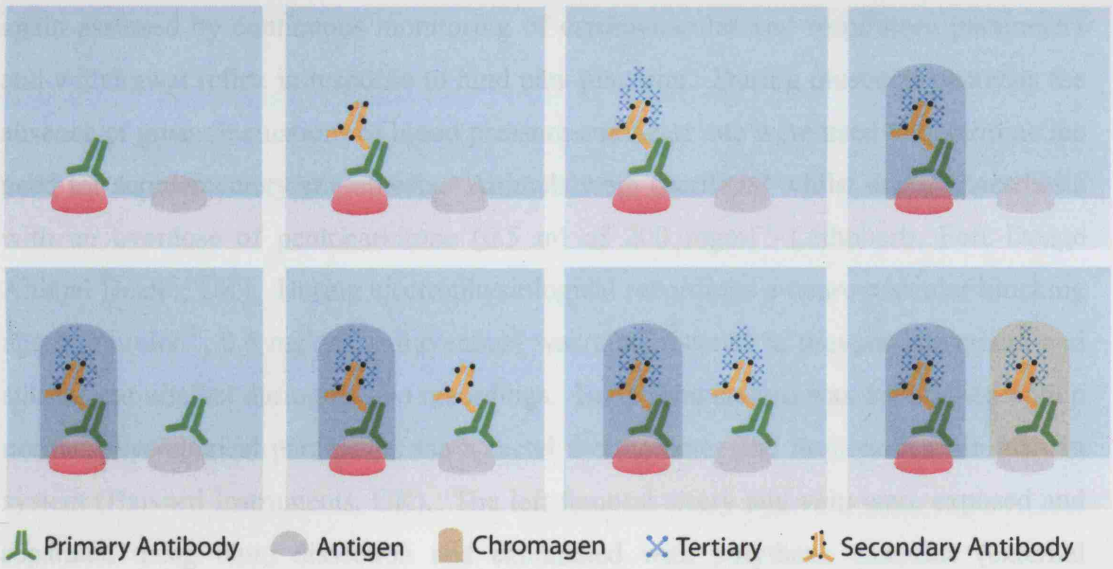

Figure 20: Basic immunohistochemistry double labelling protocol.

The primary antibody directed against the antigen of interest is applied and incubated over night at 4 °C to allow binding, a secondary antibody raised against the host of the first antibody is then applied resulting in a multiplication of bound antibody. A suitable labelled avidin complex is then applied and this further enhances the staining. The tissue is then developed in a suitable chromagen of a specified coloured end-product.

Immunocytochemical Analysis

All analyses on sections were carried out under blinded conditions using a Carl Zeiss Axioplan microscope and Axiocam MRc5 camera. The detailed analyses are explained in the individual studies.

Rat

Anaesthesia and Maintenance

Anaesthesia was initially induced with intraperitoneal administration of pentobarbitone sodium (Sigma-Aldrich, UK) 60 $mgkg^{-1}$, and maintained by intravenous injections of α-chloralose 20 $mgkg^{-1}$ in a solution of 2-hydroxy-β-cyclodextrin or pentobarbitone sodium 10 $mgkg^{-1}$ through the cannulated left femoral vein. Depth of anaesthesia was again assessed by continuous monitoring of cardiovascular and respiratory parameters and withdrawal reflex in response to hind paw pinching. During muscular paralysis the absence of gross fluctuations of blood pressure and heart rate were used to determine the need for supplementary anaesthesia. Animals were sacrificed whilst under anaesthesia with an overdose of pentobarbitone (0.5 ml of 200 $mgml^{-1}$ Lethobarb, Fort Dodge Animal Health, UK). During electrophysiological recordings a neuromuscular blocking agent (Pavulon®, 0.4 $mgkg^{-1}$, intravenous) was administered to prevent movement and subsequent artefact during *in vivo* recordings. Body temperature was maintained within normal physiological parameters via a rectal thermometer and homoeothermic blanket system (Harvard Instruments, UK). The left femoral artery and vein were exposed and separated using blunt dissection and cannulated with polythene cannulae (external diameter, 0.96 mm, Portex Ltd., UK) to allow continuous measurement of blood pressure and heart rate and the administration and withdrawal of fluids and drugs, respectively. Patency of cannulae was confirmed by backflow of blood into a heparinised syringe and maintained when required by administration of small amounts of heparinised isotonic saline (10 $unitsml^{-1}$, Multiparin, CP Pharmaceuticals, UK). Arterial blood gas parameters were measured at regular intervals (GEM Premiere 3000, Instrumentation Laboratory, UK) during the experiment and maintained within the normal physiological parameters (table 15). The trachea was exposed and cannulated

using polythene tubing (external diameter, 2.7 mm, Portex Ltd., UK) and the animal artificially ventilated (Small Rodent Ventilator - model 683, Harvard Instruments, UK) with oxygen-enriched air, with end-tidal CO_2 (Capstar - 100, CWE Inc., USA) maintained within normal physiological parameters (table 15).

Table 15: Standard arterial blood gas values for animals breathing air.

	pH	pCO_2	pO_2	BP (mmHg)	Temp (°C)
Cat	7.35–7.45	3.8–5.3	11–12.5	120	38.1–39.2
Rat	7.35–7.45	3.8–5.3	11–12.5	84–134	36–40

(Flecknell, 1996; Wolfensohn and Lloyd, 2001)

Middle meningeal artery exposure

A midline incision was made in the skin covering the dorsal surface of the skull and the skin and masseter muscle retracted to expose the underlying parietal bone. For the intravital microscopy studies a small cranial window, approximately 5 x 5 mm is drilled using a dental drill (MF-Perfecta with 945 hand piece, W & H, UK) in the presence of cooling saline to prevent any damage due to overheating. The drilling can cause dilation of the dural blood vessels, therefore, the experimental procedure was only started after an hours rest, in order that the dural vessel diameter would normalise. Any bleeding from the skull was halted with bone wax (Ethicon, UK) and the closed cranial window bathed in warm mineral oil (Sigma-Aldrich, UK) to prevent dehydration. For the electrophysiological experiments an identical procedure was followed except that the cranial window was opened by gently peeling away the thinly drilled bone. All surgery in the rat took place with the aid of a dissecting microscope (PZM-BS, WPI, UK & Opmi 99, Zeiss, UK)

Electrode placement and stimulation in the rat

For the electrophysiological experiments a bipolar stimulating electrode (NE-200x, Clark Electromedical Instruments, UK) was placed on the dura mater either side of the MMA using a micromanipulator (Narishige, UK). In order to activate trigeminal primary afferents in the rat electrophysiological experiments the bipolar stimulating electrode was connected to a Grass S88 stimulator (Grass Instrumentation, USA). The MMA was then stimulated via a stimulus isolation unit using electrical square wave stimuli, 0.5–0.6 Hz, of 0.5–2 ms duration up to a maximum of 18 v. This was used as a search stimulus, until a trigeminal neuron could be consistently and reliably recorded from, at which time the stimulus intensity (voltage) was adjusted down to just supra-maximal levels, so as not to over stimulate the neuron.

For the neurogenic vasodilation experiments a bipolar stimulating electrode (NE-200x, Clark Electromedical Instruments, UK) was placed on the surface of the thin cranial window approximately 2–4 mm from a branch of the MMA using a micromanipulator (Narishige, UK). The electrode was positioned carefully so that it was neither over the MMA or depressing the skull, thus preventing any blood flow impairment. The electrode was again connected to a Grass S88 stimulator and the surface of the cranial window was stimulated at 5 Hz, 1 ms for 10 s, with increasing voltage until maximal dilation was observed. Subsequent electrically induced responses in the same animal were then evoked using that voltage (Williamson et al., 1997b; Akerman et al., 2002a). CGRP induced dilation was achieved via the administration of CGRP (Tocris, UK) 1 μgkg^{-1} intravenous bolus injection via the cannulated femoral vein. This dose of CGRP has been shown repeatedly to produce maximal vessel dilation (Williamson et al., 1997b; Akerman et al., 2002a).

Trigeminal nucleus caudalis exposure

In the rat, electrophysiological recordings of the convergent MMA and facial receptive field responsive neurons were made from the trigeminal nucleus caudalis (TNC) at the level of the cervico-medullary junction. The skin and muscles of the dorsal neck were incised and separated. The bone of the first cervical vertebrae was exposed and partially drilled away (Dental drill, MF-Perfecta with 945 hand piece, W & H, UK) on the

ipsilateral side to the stimulating electrode to expose the underlying brain stem and dura mater. The atlanto-occipital membrane and underlying dura was incised (ophthalmic scissors, Fine Scientific Tools, F.S.T., UK) and removed to expose the brain stem at the level of the caudal medulla.

Periaqueductal gray exposure

For the microinjection electrophysiology experiments a small bore hole was drilled in the skull above the stereotaxic co-ordinates of the periaqueductal gray (PAG) (Dental drill, MF-Perfecta with 945 hand piece, W & H, UK) in the presence of cooling saline to prevent any damage due to overheating. The edge of the superior sagittal sinus and adjacent dura mater was pierced to allow penetration of the multi-barrelled microinjection unit (UMP7, Microdata Instruments, USA). Stereotaxic co-ordinates for the ventrolateral PAG (vlPAG) were taken from the atlas of Paxinos & Watson (Paxinos and Watson, 1998): 1.36 mm rostral and 4.0 mm dorsal from the interaural point, 0.5–0.8 mm left of the midline.

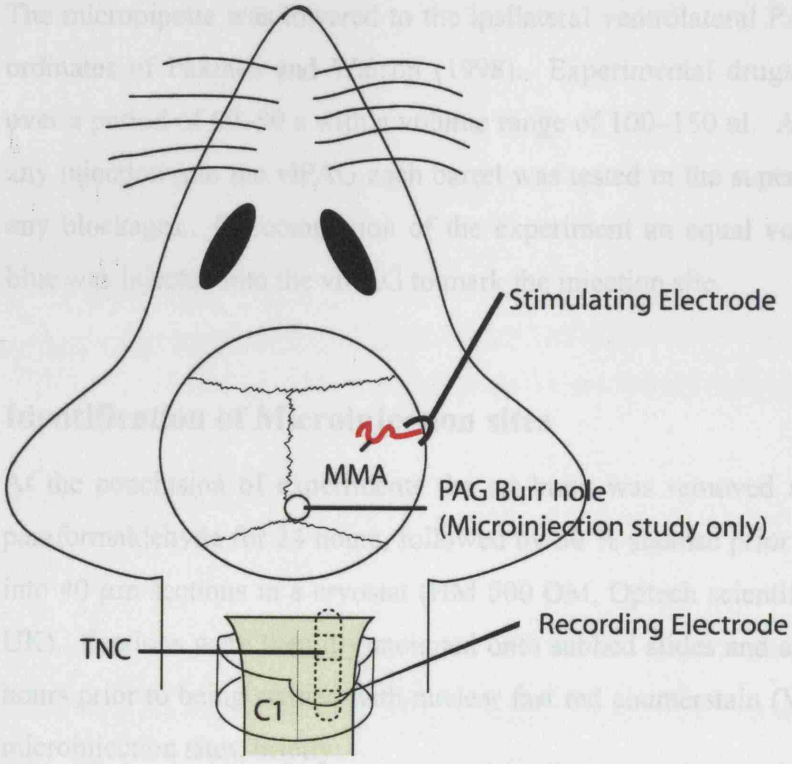

Figure 21: Rat Surgical setup.

Drug administration

Intravenous

For the intravenous electrophysiological study (chapter 5) and the intravital microscopy study (chapter 4) the delivery of experimental compounds was via the cannulated femoral vein. The cannulae were always flushed with saline first, several minutes before administering the different compounds. The effect of intravenous injection of the various compounds on blood pressure was constantly monitored and control vehicle injections were carried out.

Microinjection

For the microinjection study (chapter 6) the microinjection of test and control drugs were carried out using a multi-barrelled glass capillary pipette (UMBP7, Microdata Instruments, USA) pulled to provide a tip diameter no greater than 100 μm, figure 22. The micropipette was lowered to the ipsilateral ventrolateral PAG according to the co-ordinates of Paxinos and Watson (1998). Experimental drugs were pressure injected over a period of 60–90 s with a volume range of 100–150 nl. At least one hour prior to any injection into the vlPAG each barrel was tested in the superior colliculus to test for any blockages. On completion of the experiment an equal volume of pontamine sky blue was injected into the vlPAG to mark the injection site.

Identification of Microinjection sites

At the conclusion of experiments the rat brain was removed and post-fixed in 10 % paraformaldehyde for 24 hours, followed by 30 % sucrose prior to being frozen and cut into 40 μm sections in a cryostat (HM 500 OM, Optech scientific instruments, Oxford, UK). Sections were then dry mounted onto subbed slides and allowed to air dry for 24 hours prior to being stained with nuclear fast red counterstain (Vector, UK) to visualise microinjection sites, briefly:

1. Slides were rinsed in tap water for 3 minutes.
2. Slides were covered completely in nuclear fast red and incubated for 3–5 minutes to obtain the desired intensity.
3. Slides were then washed in dH_20 for 2 x 1 minute.
4. Sections were then dehydrated through increasing concentrations of alcohol, cleared in xylene and cover-slipped.

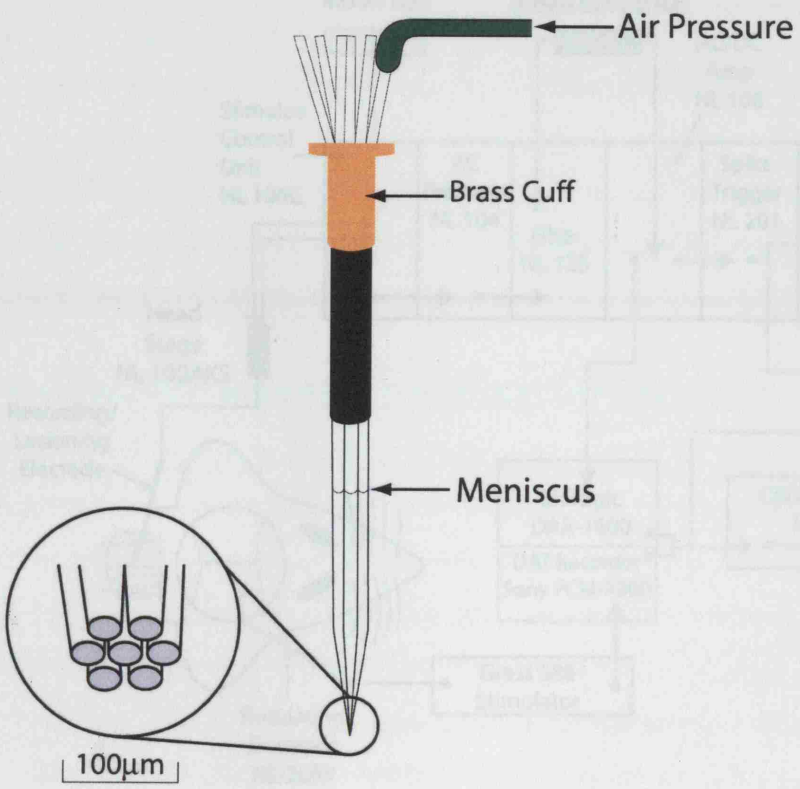

Figure 22: Multibarrelled micropipette for periaqueductal gray microinjection.

Electrophysiology

Recording electrode placement

Following the exposure of the TNC a tungsten microelectrode with an impedance of 0.5 MΩ and a tip diameter of 0.5 µm (World precision Instruments, WPI, UK) was slowly

lowered into the region of the cervico-medullary junction at 5 μm increments with a hydraulic micro-stepper (David Kopf Instruments, USA). Neurons encountered were continuously tested for convergent input from the ophthalmic dermatome of the cutaneous receptive field and the dura mater surrounding the MMA.

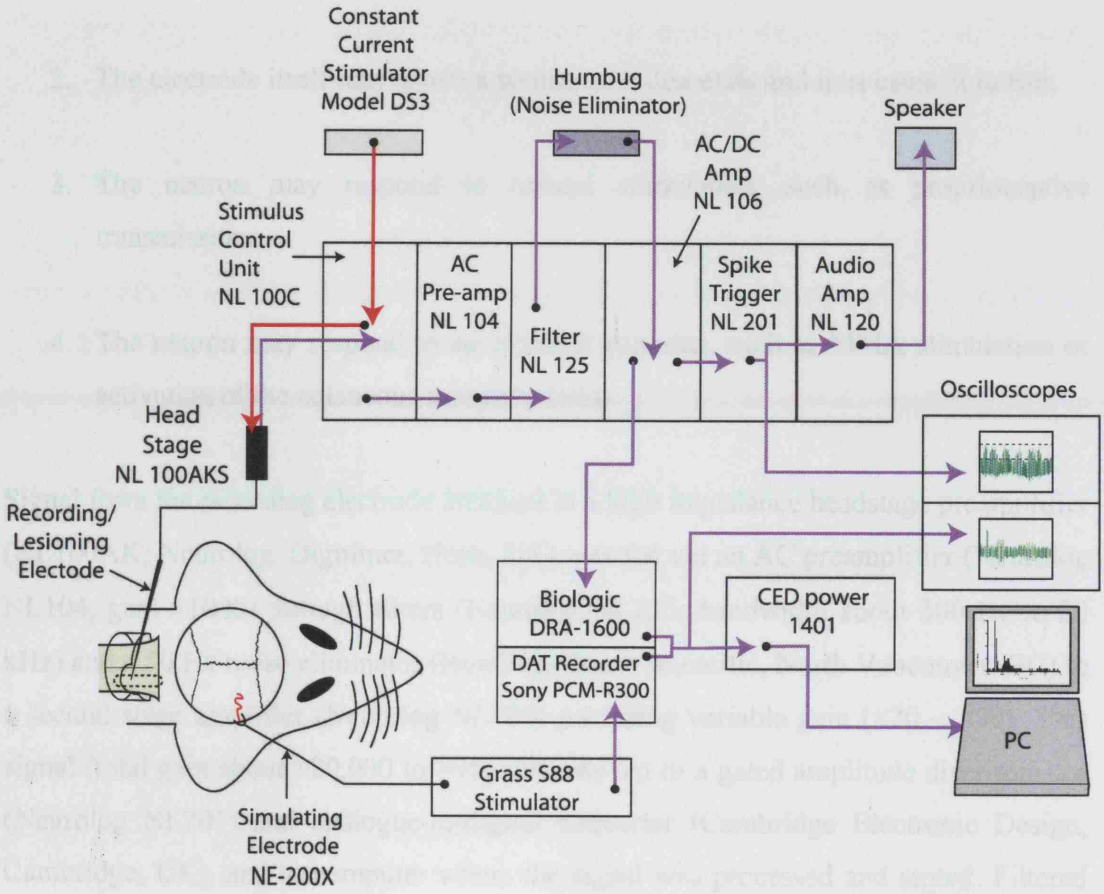

Figure 23: Electrophysiology setup and wiring.

Schematic diagram of the preparation and equipment used in the electrophysiology experiments. A recording electrode is lowered into the TCC, and the electrical signal is fed through a series of amplifiers and filters to a pair of oscilloscopes and a personal computer for analysis. A bipolar stimulating electrode is placed on the middle meningeal artery and connected to a Grass S88 stimulator. At the conclusion of the experiment the animal is terminated with a lethal injection of pentobarbitone sodium and the stimulus control unit is switched to stimulate mode. The constant current stimulator is then activated resulting in a lesion at the tip of the recording electrode. NL, Digitimer neurolog product number; NE, Clark Electromedical product.

Electrophysiological recording and signal processing

As the electrode is lowered into the tissue, unit activity is encountered under one of four conditions:

1. Some neurons are spontaneously active.

2. The electrode itself may injure a neuron as it descends and thus cause it to fire.

3. The neuron may respond to natural stimulation, such as proprioceptive transmission.

4. The neuron may respond to an artificial stimulus, such as MMA stimulation or activation of the cutaneous receptive field.

Signal from the recording electrode attached to a high impedance headstage preamplifier (NL100AK; Neurolog, Digitimer, Herts, UK) was fed via an AC preamplifier (Neurolog NL104, gain ×1000) through filters (Neurolog NL125; bandwidth about 300 Hz to 20 kHz) and a 50 Hz noise eliminator (Humbug, Quest Scientific, North Vancouver, BC) to a second-stage amplifier (Neurolog NL106) providing variable gain (×20 – ×90). This signal (total gain about ×20,000 to ×95,000) was fed to a gated amplitude discriminator (Neurolog NL201) and analogue-to-digital converter (Cambridge Electronic Design, Cambridge, UK), and to computer where the signal was processed and stored. Filtered and amplified electrical signals from action potentials were fed to a loudspeaker via a power amplifier (Neurolog NL120) for audio monitoring, and were displayed on analogue and digital-storage oscilloscopes (Goldstar, LG Precision, Korea; Metrix Electronics, Chauvin Arnoux, Paris, France) to assist the isolation of single unit activity from adjacent cell activity and noise.

Analysis of electrophysiological data

The signal parameter of interest is the spike frequency and its variation with time and with respect to the applied stimulus. If the electrode picks up the activity of a cluster of units, they can be discriminated by exploiting the characteristic neural elements, resulting in different heights of spike amplitude. The purpose of the studies reported in this thesis was not dependant on individual unit responses. Original signals were stored on a digital tape recorder (PCM-R300, Sony, UK). To record the occurrence of individual spikes the amplified signal was fed into a window discriminator, which produces a single pulse of given height and duration in response to each action potential whose height falls within a pre-set window. To ensure a consistency the window discriminator is adjusted for each unit to provide a spontaneous train of activity ranging from 40–60 Hz. The output of the window discriminator is then connected through an interface and displayed on a personal computer. The data is then displayed in two forms:

1. Post-stimulus histograms (PSTH), where the x-axis represents time after an applied stimulus that is repeatable. The time is divided into a pre-set number of bins of a predefined duration in milliseconds (ms). The Y-axis represents the number of spikes that occurs within each bin.

2. Peri-stimulus histograms, where the firing rate of spikes measured in Hz is continuously plotted on the Y-axis against time on the X-axis. Allowing an average of the action potentials to be obtained from multiple sweeps or collections.

The data reported was analysed using the commercially available software Spike2 v5 (CED, UK).

Identification of recording sites

In order to verify the location of recording sites within the TNC electrical lesions were made via the recording electrode at the completion of each experiment. An electrical current of 10 μA was passed through the electrode for 15 s using a constant current generator (Model DS3, Digitimer, Hertfordshire, UK). The animal was then terminated with a lethal dose of pentobarbitone sodium and the region of the spinal cord dissected out. The spinal cord was then stored in a solution of 10% formaldehyde containing potassium hexacyanoferrate (III), which stains the remaining iron deposits from the electrode black. The tissue was then frozen on a cryostat (HM 500 OM, Optech scientific instruments, Oxford, UK) and cut into 50 μm sections which were dry mounted on to gelatinised coated slides and counterstained with nuclear fast red (Vector, UK) as previously described to allow anatomical localisation of the lesion site.

Characterisation of neurons

TNC neurons with convergent input from the dura mater and facial receptive field were identified. The cutaneous receptive field was assessed in all three divisions (figure 24) of the trigeminal innervation and identified as the electrode was lowered in the spinal cord. The receptive field was characterised for non-noxious (gentle brushing), noxious (heavy pinch painful when applied to humans) and noxious thermal stimulation of the facial skin (heating the receptive field to 52 °C with a contact thermal stimulator) and mapped onto a 1:1 drawing of the rat's head (figure 24). Once a neuron sensitive to stimulation of the ophthalmic dermatome of the trigeminal nerve was identified it was tested for convergent input from the dura mater in response to electrical stimulation and the mechanosensitive threshold of the dura mater, as measured by von Frey filaments (Stoelting Company, Illinois. U.S.A). Neurons were then classified as low-threshold mechanoreceptors (LTM) that responded to innocuous stimulation, wide-dynamic range (WDR) that respond to both noxious and non-noxious stimuli or nociceptive specific (NS) that respond to only noxious input (Hu et al., 1981).

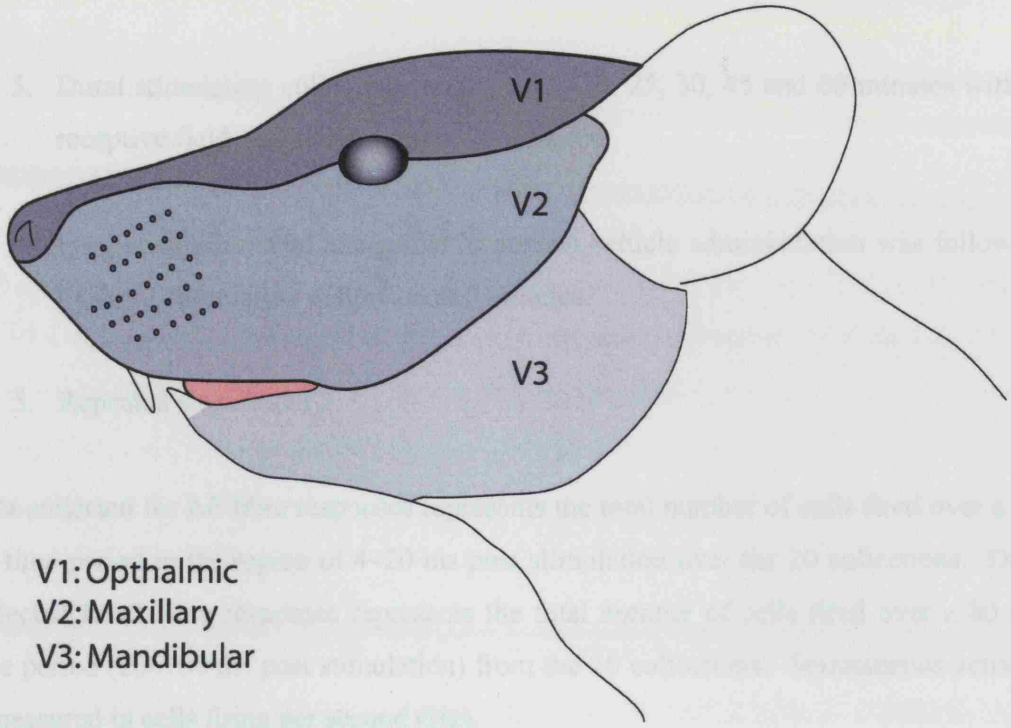

Figure 24: 1:1 drawing of the rat's head, for receptive field characterisation and mapping.

Experimental protocol

Trains of 20 stimuli were delivered at five minute intervals to assess the baseline response to dural electrical stimulation. Responses were analysed using post-stimulus histograms with a sweep length of 100 ms and a bin width of 200 μs that separated Aδ-fibre and C-fibre activated responses in relation to their conduction velocities. An interval of spontaneous activity was recorded for 120–180 seconds preceding any dural stimulation from the peri-stimulus histogram. Once a neuron with convergent inputs from the dura and ophthalmic dermatome of the trigeminal nerve was identified responses were tested using the following protocol:

1. Three baseline collections of dural stimulation and a single receptive field characterisation.

2. Experimental drug or control vehicle administration.

3. Dural stimulation collections at 5, 10, 15, 20, 25, 30, 45 and 60 minutes with a receptive field characterisation at 20 minutes.

4. Further experimental antagonist or control vehicle administration was followed by dural stimulation collection at 5 minutes.

5. Repeated steps 2 and 3.

Data collected for Aδ-fibre responses represents the total number of cells fired over a 10 ms time period in the region of 4–20 ms post stimulation over the 20 collections. Data collected for C-fibre responses represents the total number of cells fired over a 80 ms time period (20–100 ms post stimulation) from the 20 collections. Spontaneous activity is measured in cells firing per second (Hz).

Data Analysis

Intravital microscopy

The effects of electrical stimulation and CGRP administration on dural vessel diameter were calculated as a percentage increase from the pre-stimulation baseline diameters. The nature of the experimental set-up, where the magnification of the dural vessel visualised was different in each animal by virtue of selecting an appropriate target vessel, made it impossible to standardise the dural vessel measurement, therefore, the dural vessel diameter were measured in percentage change from baseline. The typical vessel diameter measured ranges from 120–150 μm. All data are expressed as mean ± SEM. Statistical analysis was performed using an ANOVA for repeated measures with Bonferroni *post-hoc* correction for multiple comparisons followed by Student's paired *t*-test. To compare the effect of orexin A only and orexin A and $CGRP_{8-37}$ an independent

samples *t*-test was used (SPSS v12.0). Significance was assessed at the $P < 0.05$ levels (Field, 2005).

Electrophysiology studies

Measurement of the distance between the MMA stimulating site and the cervico-medullary recording site (25–30 mm), including 1 ms for the central synaptic delay, allowed the calculation of neuronal conduction velocities. Neurons were then classified as receiving input from Aδ-fibres, latency of 4–20 ms or C-fibres, latency of greater than 20 ms. Data collected from units with Aδ-fibre input represents the total number of cells fired over a 10 ms time period in the region of 4–20 ms post stimulation over the 20 collections. Data collected from units with C-fibre input represents the total number of cells fired over an 80 ms time period (20–100 ms post stimulation) from the 20 collections. Spontaneous activity is measured in cells firing per second (Hz). Effects of drug intervention were analysed using an ANOVA for repeated measures with Bonferroni *post-hoc* correction for multiple comparisons followed by Student's paired *t*-test (SPSS v12.0), using the average of the three baselines for comparisons. When the assumption of sphericity with regards to the factor of repeats was violated, adjustments were made for the degrees of freedom and *P* values according to the Greenhouse-Geisser correction. Significance was assessed at the $P < 0.05$ levels (Field, 2005).

Chapter 3 – Hypothalamic neurons that contain orexin A and B express *c-fos* in response to superior sagittal sinus stimulation in the cat

Introduction

Fos expression as a tool to model aspects of migraine pathophysiology

The immediate early gene *c-fos* is rapidly and transiently expressed in response to several forms of stimuli, including extra cellular stimuli and intracellular 2nd messenger systems. *c-fos* mRNA accumulates reaching its peak about 30–40 minutes post stimulus. The gene encodes the nuclear protein Fos, and levels peak about 2 hours post stimulation, figure 19.

Expression of the gene can be measured via northern blot analysis (Ashmawi et al., 2003) or *in situ* hybridization (Nakagawa et al., 2003) and the protein is normally visualised using immunocytochemical techniques (Benjamin et al., 2004).

In the field of migraine research Fos-ir, thus offers a method to identify subpopulations of neurons activated in response to noxious stimuli and thus identify related nociceptive pathways. The majority of studies have employed this technique to map neuronal activation throughout the trigeminovascular system, thus greatly enhancing our understanding of the pathophysiology of migraine (Kaube et al., 1993b; Strassman et al., 1994b; Goadsby and Hoskin, 1997; Sugimoto et al., 1998; Hoskin et al., 1999). One unique property of Fos and other related proteins is their ability to respond to polysynaptic activation, providing a method for mapping functional pathways. This property has been utilised to map neuronal activation in higher structures involved in the ascending and descending modulatory control of migraine, including the periaqueductal gray (Hoskin et al., 2001; Keay et al., 2002) and hypothalamus (Malick et al., 2001; Benjamin et al., 2004).

Fos expression as a model of trigeminovascular activation has also enabled the investigation of different established and experimental anti-migraine compounds as well as neurotransmitter pathways involved in the activation of *c-fos* within the trigeminocervical complex (TCC).

Electrical stimulation of the pain producing structures of the head including the superior sagittal sinus (SSS) and direct stimulation of the trigeminal ganglion, both established methods of trigeminovascular activation have been utilised to investigate the effect of a variety of compounds on Fos expression. The 5-$HT_{1B/1D}$ receptor agonists zolmitriptan (Hoskin and Goadsby, 1998) and eletriptan (Knyihar-Csillik et al., 2000) have both been shown to reduce Fos-ir in the TCC, whereas the less lipophilic sumatriptan was unable to reduce Fos expression (Hoskin and Goadsby, 1998) unless the blood brain barrier was disrupted (Kaube et al., 1993a). Taken together the evidence suggested a peripheral as well as central site of action for the triptans a fact that seems now established. The NMDA receptor (MK-801) and the GluR5 Kainate receptor ([3S,4aR,6S,8aR]-6-[4-carboxyimidazol-1-ylmethyl] decahydroisoquinoline-3-carboxylic acid) antagonists both inhibit Fos expression in this model of trigeminovascular activation (Classey et al., 2001; Filla et al., 2002) implicating their receptor systems in the pathophysiology of migraine.

The second major method of activation of the trigeminovascular system is the use of chemical stimulation of the dura mater with irritant or inflammatory compounds. Capsaicin administration is an established method for trigeminovascular activation. As with electrical stimulation, Fos expression has been shown to be reduced by 5-$HT_{1B/1D}$ receptor agonists such as sumatriptan (Mitsikostas et al., 2002) as well as specific 5-HT_{1F} agonists (Mitsikostas et al., 1999a) in response to capsaicin. This is also the case for the NMDA receptor antagonist MK-801 (Mitsikostas et al., 1998) and the non-NMDA glutamate receptor antagonists (Mitsikostas et al., 1999b), as well as the barbiturate butalbital (Cutrer et al., 1999).

Infusion of the nitric oxide donor glyceryltrinitrate (GTN) has been shown to cause a headache similar to migraine in sufferers after a delay of 4–5 hours (Iversen et al., 1989). Similarly GTN infusion leads to *c-fos* expression within the TCC (Tassorelli and Joseph, 1995a) indicating that nitric oxide donors can activate the trigeminovascular system. It has also been demonstrated that GTN activates neurons within the TCC that express or are in close proximity to processes containing nitric oxide synthase (NOS)

(Tassorelli and Joseph, 1995b), suggesting a possible role of NOS in migraine pathophysiology. Administration of the NOS-Inhibitor L-NAME has been shown to significantly decrease Fos expression in both the capsaicin- and electrical- induced models (Hoskin et al., 1999; Offenhauser et al., 2005), supporting the evidence for a role of NO in the pathophysiology of migraine.

Limitations of the Fos model.

As with any models of the constituent parts of migraine the use of Fos expression has certain limitations highlighted by the failure of the NK-1 receptor antagonists to translate into the clinical environment (Goldstein et al., 1997; Moskowitz and Mitsikostas, 1997; Goldstein et al., 2001; May and Goadsby, 2001) despite consistently blocking Fos expression in the TCC (Shepheard et al., 1995; Polley et al., 1997). It is important to realise that induction of *c-fos* to quantifiable levels requires a strong consistent stimulation that may not be physiological (Bullitt et al., 1992; Lima and Avelino, 1994). It must also be remembered that *c-fos* is not expressed in all neurons as with the dorsal root and trigeminal ganglion cells (Hunt et al., 1987), thus lack of Fos expression does not equate to lack of neuronal activity. One final limitation of the model is seen via direct activation of the antinociceptive descending pathways which elicits Fos expression in spinal neurons even in the absence of any nociceptive input (Bett and Sandkuhler, 1995). Thus any nociceptive stimulation engaging these systems will result in a subpopulation of Fos expression as a result of antinociceptive processes and not the stimulation method studied. The current model has however greatly advanced our understanding of the pathophysiology and underlying pharmacology of the trigeminovascular system establishing itself as one of the most effective experimental methods for the study of the pathophysiology of the brain process likely to be involved in migraine.

Previous studies have demonstrated that stimulation of the pain producing structures of the dura mater including the SSS results in a significant up-regulation of Fos expression in the supra-optic and posterior hypothalamic nuclei of the cat (Benjamin et al., 2004).

A further non-significant increase was observed in the caudal lateral hypothalamic nuclei. All three nuclei play an important role in a variety of different functions including the sleep wake cycle, the biological clock and pain processing (Danguir and Nicolaidis, 1980; Lumb and Cervero, 1989; Lumb, 1990; Saper, 1990; Cai et al., 1999; Buijs and Van Eden, 2000; Abrahamson et al., 2001; Overeem et al., 2002; Dodick et al., 2003).

The posterior and lateral hypothalamus contain the only orexin synthesising neurons in the entire brain and from here they project throughout the entire length of the brain and spinal cord, including the other hypothalamic nuclei as described in chapter 1 (Sakurai et al., 1998; Trivedi et al., 1998; Chen et al., 1999; Cutler et al., 1999; Date et al., 1999; Harrison et al., 1999; Horvath et al., 1999c; van den Pol, 1999; Date et al., 2000; Hervieu et al., 2001; Marcus et al., 2001).

Recent research has implicated the orexinergic system in a variety of functions including sleep, feeding, energy homeostasis and most recently nociceptive processing. The orexins have been shown to project to multiple neuronal systems, many of which are involved in nociceptive processing (Peyron et al., 1998; Trivedi et al., 1998; Cutler et al., 1999; van den Pol, 1999; Marcus et al., 2001; Mintz et al., 2001; Zhang et al., 2001; Zhang et al., 2002a; Zhang et al., 2002b, 2004). Robust innervation of the hypothalamus, PAG and lamina I, II and X of the spinal cord demonstrate anatomical evidence for a potential role in the modulation of nociceptive processing.

Direct evidence for the involvement of the orexinergic system in the modulation of migraine has not yet been investigated. However in an animal model of trigeminovascular nociception, activation of the OX_1 or OX_2 receptor in the posterior hypothalamus has been shown to modulate differentially nociceptive dural input to the TNC (Bartsch et al., 2004b). Activation of the OX_1 receptor elicits an anti-nociceptive effect whereas OX_2 receptor activation elicits a pro-nociceptive effect. Experimental evidence indicates that regulation of autonomic and neuroendocrine functions as well as nociceptive processing is closely coupled in the hypothalamus (Buijs and Van Eden,

2000) and recent data points to the involvement of orexinergic mechanisms (Smart, 1999). Thus the orexinergic system is a posterior hypothalamic pathway that may be involved in central pain modulation and could be a possible link between the pain of primary neurovascular headaches and the symptomatology that is suggestive of a hypothalamic dysfunction in migraine (Overeem et al., 2002).

To further investigate the possible involvement of the orexinergic system in the pathophysiology of migraine we utilised an animal model of trigeminovascular activation, via stimulation of the superior sagittal sinus (SSS) in the cat. This model has previously been shown to demonstrate neuronal activation throughout the trigeminovascular system and higher structures including the hypothalamus (Benjamin et al., 2004). The aim of this study was to investigate if stimulation of the SSS results in the activation of orexinergic neurons in the hypothalamus resulting in the up-regulation of Fos-ir in the posterior and lateral nuclei.

Methods

Animals

Fourteen cats weighing 2.8 ± 0.3 kg were studied. All animals reported had normal physiological variables (mean ± SE): blood pressure, 118 ± 10 mmHg, and respiratory parameters, pH 7.38 ± 0.19, pCO_2 4.29 ± 0.32, throughout the study.

Surgical procedures

Following the preparatory surgery, detailed in the general material and methods chapter, a 24 hour rest period was imposed during which time the animal was kept in the stereotaxic frame, anaesthesia was maintained with α-chloralose, and physiological variables maintained within normal limits. In order to activate trigeminal primary afferents in the cat the SSS was stimulated via a Grass S88 stimulator (Grass Instrumentation, USA) using square wave 250 μs pulses, every three seconds, 130–150 V for two hours. The electrodes were then removed and the animal left to rest for a further hour to allow optimal Fos activation (Hoskin and Goadsby, 1999). Sham animals underwent the above procedure with the omission of the stimulation and control animals underwent cannulation and perfusion only.

Stimulation parameters

- Control: anaesthetised and perfused only; $n = 3$.

- Sham: SSS hooked onto stimulating electrodes for 2 hours, with no electrical stimulation. Electrodes removed and animal allowed to rest for 1 hour; $n = 3$.

- Stimulated: SSS hooked onto stimulating electrodes for 2 hours, with square wave 250 μs pulses, every 3 seconds, 130–150 V. Electrodes removed and animal allowed to rest for 1 hour; $n = 8$.

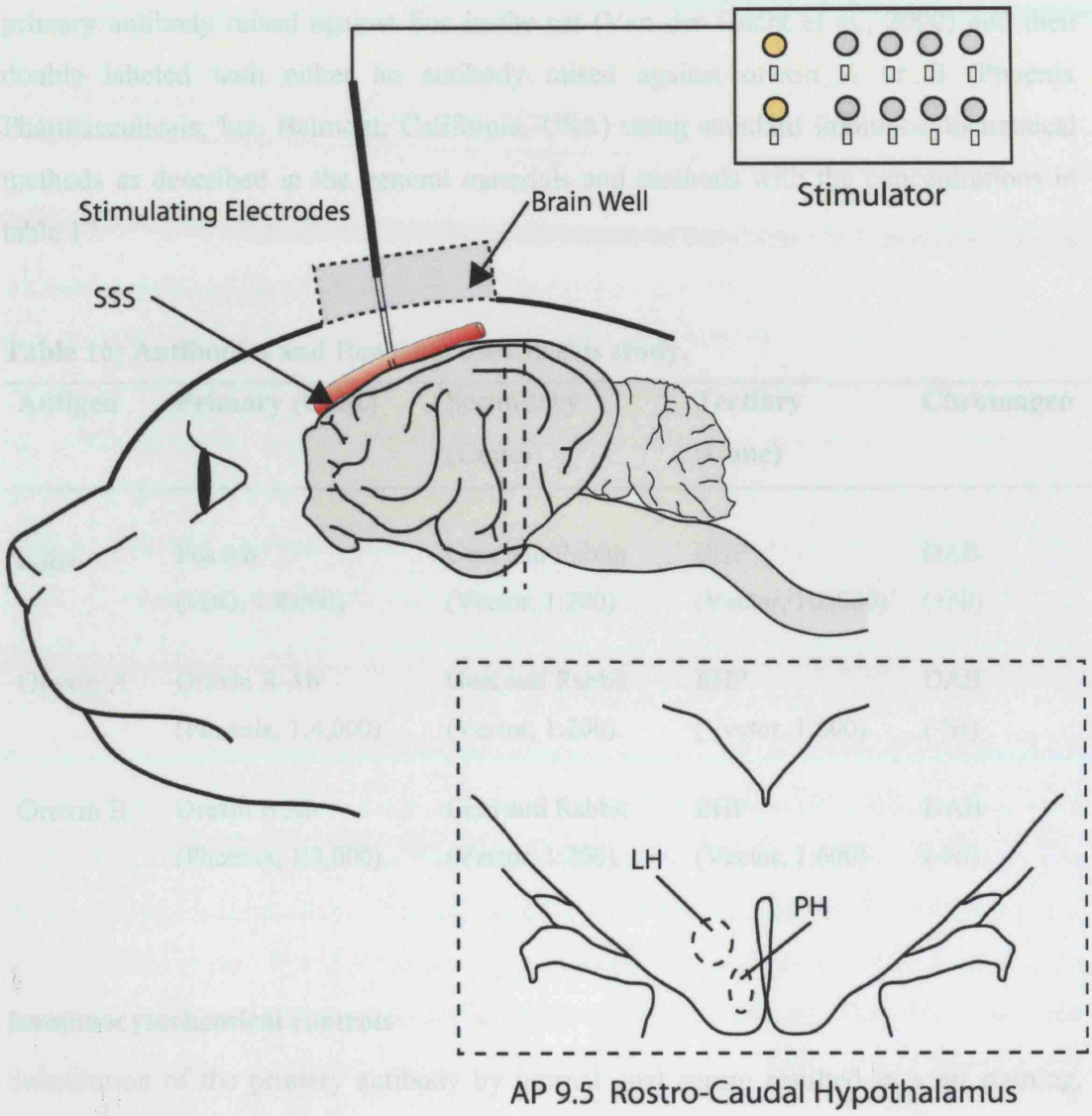

Figure 25: Experimental setup and hypothalamic dissection in the cat.
LH, lateral hypothalamic nuclei; PH, posterior hypothalamic nuclei

Immunocytochemistry

At the conclusion of the experiment the animal was perfused and the brain and spinal cord removed and stored as described in the general material and methods. The areas corresponding to the lateral and posterior hypothalamic nuclei (figure 25) were dissected out and frozen, prior to being cut into 30 μm sections using a cryostat. The sections were then rinsed in phosphate buffer (PB) and consecutive sections reacted with a

primary antibody raised against Fos in the cat (Van der Gucht et al., 2000) and then double labeled with either an antibody raised against orexin A or B (Phoenix Pharmaceuticals, Inc. Belmont, California, USA) using standard immunocytochemical methods as described in the general materials and methods with the concentrations in table 17.

Table 16: Antibodies and Reagents used in this study.

Antigen	Primary (Conc)	Secondary (Conc)	Tertiary (Conc)	Chromagen
c-fos	Fos Ab (vDG, 1:8,000)	Goat anti Rabbit (Vector, 1:200)	EHP (Vector, 1:1,000)	DAB (+Ni)
Orexin A	Orexin A Ab (Phoenix, 1:4,000)	Goat anti Rabbit (Vector, 1:200)	EHP (Vector, 1:600)	DAB (-Ni)
Orexin B	Orexin B Ab (Phoenix, 1:3,000)	Goat anti Rabbit (Vector, 1:200)	EHP (Vector, 1:600)	DAB (-Ni)

Immunocytochemical controls

Substitution of the primary antibody by normal goat serum resulted in a no staining. Omission of one of the various incubation steps abolished the immunocytochemical staining completely indicating method specificity.

Anatomical identification

Anatomical localisation was confirmed under a light microscope (Zeiss, Axioplan Microscope) using an appropriate atlas of the cat CNS for reference (Snider and Niemer, 1964).

Immunohistchemical staining was examined at the levels corresponding to the lateral and posterior hypothalamus. Fos immunoreactivity was distinguishable from orexin A and B staining by cellular location: the nucleus was always labelled an intense black locating the fos protein, whereas immunopositive neurons staining brown indicated the presence of orexin A or B. Sections were mounted and cover-slipped before undergoing blinded analysis using a Carl Zeiss Axioplan microscope and Axiocam MRc5 camera.
For counting and statistical analysis cells were only considered fos-positive if they stained as a black oval structure and conformed to the established criteria (Hammond et al., 1992), where the cell must be distinguishable from the background through the range of 400 x, 200 x, 100 x, and 50 x magnification under the light microscope. Each Fos-positive cell was counted as one and a tally of fos-positive counts was made for both areas of interest over 5 randomly selected sections. Cells were considered orexin-positive if the cell body stained brown and was clearly distinguishable from the background. Orexin-positive fibres were not counted for quantitative analysis.

The total numbers of Fos, orexin only and fos and orexin double labelled cells were counted. Data derived from the Fos protein counts were quantified, the data from Fos protein studies is quantifiable, but not necessarily evenly distributed or conforming to a clear interval scale. For this reason non-parametric statistics were used, control/sham and stimulated groups were compared using the Kruskal-Wallis analysis of variance and data are presented as medians with the interquartile ranges (SPSS v12.0). Significance was assessed at the $P < 0.05$ levels (Field, 2005).

Results

Fos protein expression in control and sham animals

Control or 2 hour of SSS sham-stimulated animals demonstrated little or no Fos expression in the posterior and lateral hypothalamic nuclei (table 17) in agreement with previous studies (Benjamin et al., 2004).

The effect of stimulation on Fos protein expression

Following 2 hour SSS stimulation and a 1 hour rest period, fos protein-like immunoreactivity was seen throughout the lateral and posterior hypothalamic nuclei at different levels. The lateral hypothalamic nuclei demonstrated a significant increase in fos-immunoreactivity from median 0; interquartile range (0–1 Fos-positive nuclei) in the control animals to median 11; interquartile range (6–16 Fos-positive nuclei) in the stimulated animals ($H(2) = 36.98$, $P < 0.01$; figure 26–28). The posterior hypothalamic nucleus demonstrated a much more robust increase in fos-immunoreactive nuclei increasing from median 3; interquartile range (1–4 Fos-positive nuclei) to median 25; interquartile range (21–37 Fos-positive nuclei) in the stimulated animals ($H(2) = 39.96$, $P < 0.01$; figure 26–28)

Table 17: Median number of Fos-positive neurons per section, data represents the median (interquartile range) number of fos positive nuclei counted for 5 randomly selected sections in the posterior and lateral hypothalamic nuclei for control ($n = 3$), sham ($n = 3$) and stimulated ($n = 8$) animals.

Nuclei	Control	Sham	Stimulated
Posterior	3 (1–4)	4 (2–6)	25 (21–37)
Lateral	0 (0–1)	0 (0–2)	11 (6–16)

Orexin A and B distribution

Orexin A and B positive cell bodies were seen throughout the posterior and lateral hypothalamic nuclei. Although no co-localisation was carried out for the peptides, orexin A and B demonstrated a similar staining pattern in agreement with previous studies (Wagner et al., 2000; Zhang et al., 2001, 2002b). The vast majority of the orexin-positive neurons were seen in the lateral hypothalamic nuclei located dorsal and lateral to the fornix, orexin-positive fibres were more sparsely distributed. The posterior hypothalamic nuclei demonstrated a similarly sparse distribution of orexin-positive fibres but the level of orexin-positive neurons was much lower than that of the lateral hypothalamic nuclei (figure 26–28).

Distribution of Orexin and Fos positive neurons

Fos immunoreactivity was restricted to neuronal nuclei and demonstrated a black stain. Orexin positive soma and dendrites were identifiable by a brown stain as a result of the omission of the nickel from the chromagen reaction. A neuron displaying a black nucleus and a brownish cytoplasm characterised a double-labelled neuron (figure 27, 28).

Posterior Hypothalamic nuclei

Forty eight percent of the orexin-positive (A and B) neurons in the PH demonstrated fos double-labelling as a result of SSS stimulation. Fos immunoreactivity was not confined to orexin-positive neurons with a large proportion of fos-positive neurons not expressing either orexin A or B (figure 27, 28).

Lateral Hypothalamic nuclei

In contrast to the PH, only 21% of orexin-positive (A and B) nuclei in the LH were double-labelled for Fos as a result of SSS stimulation. Again fos immunoreactivity was not confined to only orexin-positive neurons, figure 27, 28. The distribution of both orexin-positive neurons and fos immunoreactivity was consistent with previous reports

(Peyron et al., 1998; Wagner et al., 2000; Zhang et al., 2001, 2002b; Benjamin et al., 2004).

Table 18: Total number of Fos positive nuclei for the posterior and lateral hypothalamic nuclei throughout the 5 randomly selected sections for the stimulated animals (*n* = 8). Followed by the percentage of orexin A and B neurons demonstrating Fos-immunoreactivity.

Hypothalamic Nuclei:	Fos +ve	Fos -ve
Posterior:	135 ± 17	
Orexin A	48 ± 5%	52 ± 5%
Orexin B	48 ± 4%	52 ± 4%
Lateral:	73 ± 18	
Orexin A	20 ± 3%	80 ± 3%
Orexin B	24 ± 5%	76 ± 5%

Data presented as mean ± SEM

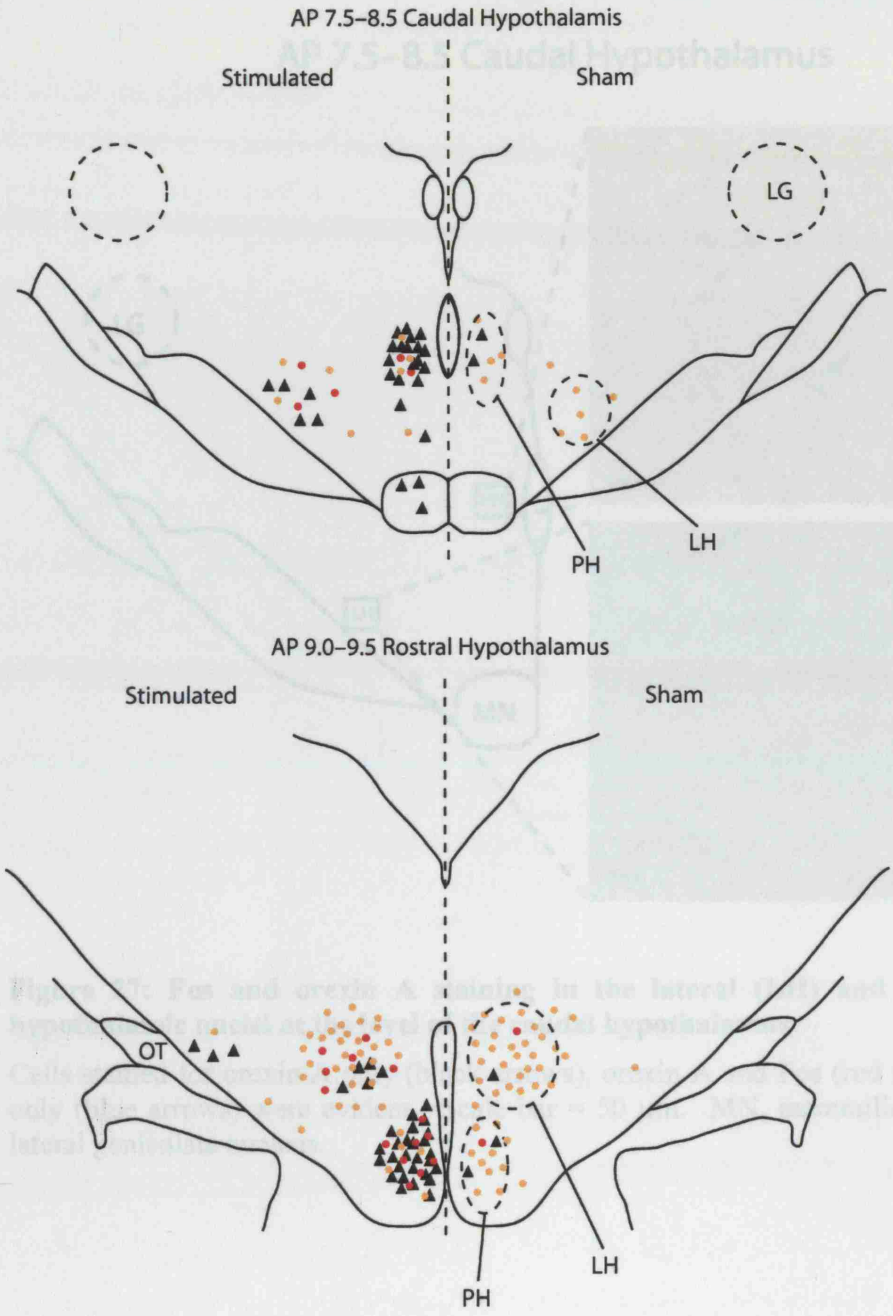

Figure 26: Caudal and Rostral Hypothalamic orexin A, B and Fos expression.

Line drawing of an example of the caudal and rostral hypothalamus, illustrating the number of orexin only labelled neurons (brown circles), fos only immunoreactive neurons (black triangles) and orexin and fos double-labelled cells (red circles) in the posterior and lateral hypothalamic nuclei of the cat. OT, optic tract; LG, lateral geniculate nucleus; PH, posterior hypothalamic nucleus; LH, lateral hypothalamic nucleus.

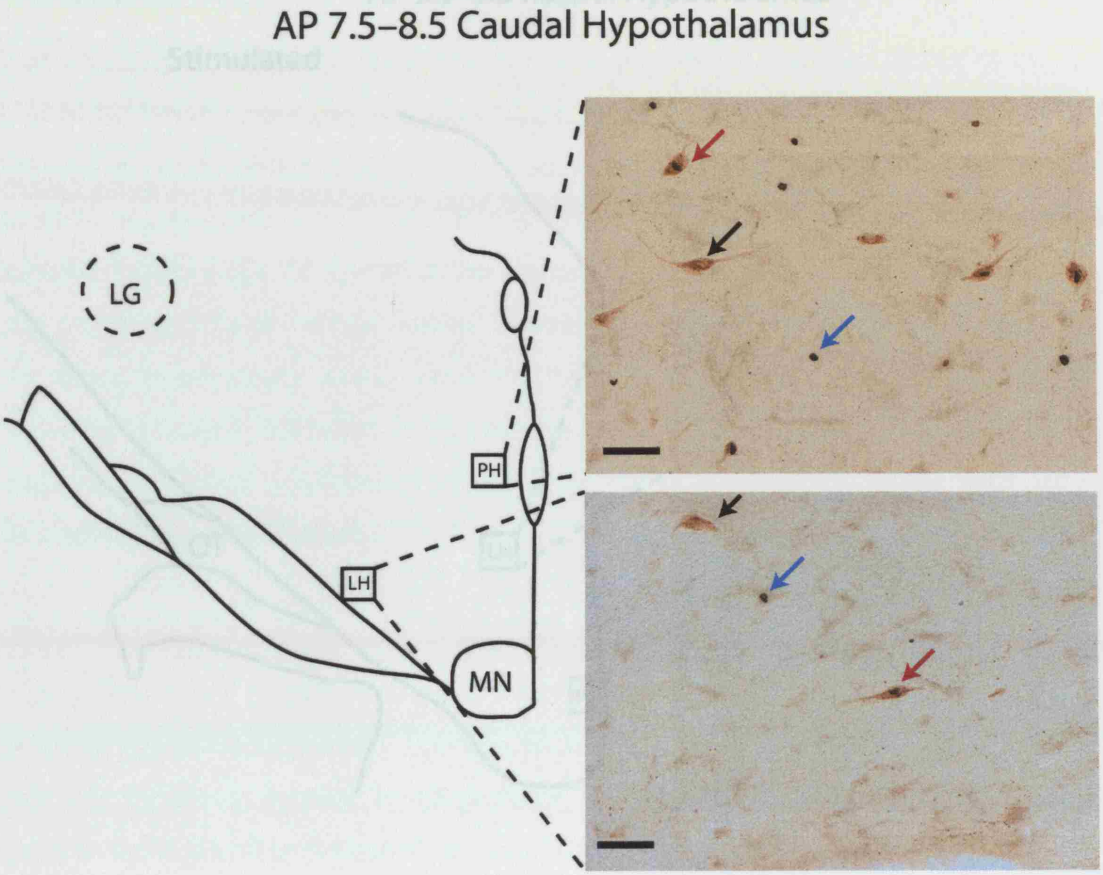

Figure 27: Fos and orexin A staining in the lateral (LH) and posterior (PH) hypothalamic nuclei at the level of the caudal hypothalamus.

Cells stained for orexin A only (black arrows), orexin A and Fos (red arrows), and Fos only (blue arrows) were evident. Scale bar = 50 μm. MN, mammillary nucleus; LG, lateral geniculate nucleus.

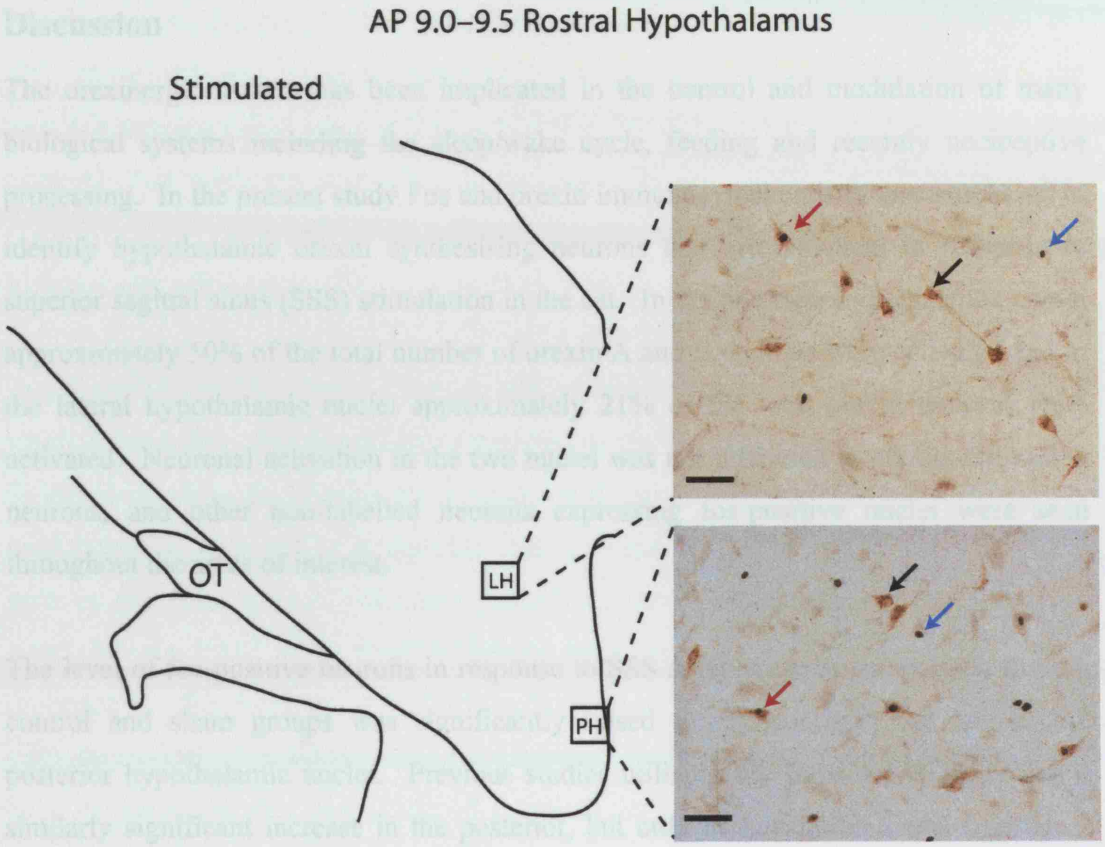

Figure 28: Fos and orexin B staining in the lateral (LH) and posterior (PH) hypothalamic nuclei at the level of the rostral hypothalamus.

Cells stained for orexin B only (black arrows), orexin B and Fos (red arrows), and Fos only (blue arrows) were evident Scale bar = 50 μm. OT, optic tract.

Discussion

The orexinergic system has been implicated in the control and modulation of many biological systems including the sleep/wake cycle, feeding and recently nociceptive processing. In the present study Fos and orexin immunocytochemistry was combined to identify hypothalamic orexin synthesising neurons that are activated in response to superior sagittal sinus (SSS) stimulation in the cat. In the posterior hypothalamic nuclei approximately 50% of the total number of orexin A and B neurons were activated and in the lateral hypothalamic nuclei approximately 21% of the total orexin neurons were activated. Neuronal activation in the two nuclei was not restricted to orexin expressing neurons, and other non-labelled neurons expressing fos-positive nuclei were seen throughout the areas of interest.

The level of fos-positive neurons in response to SSS stimulation in comparison to both control and sham groups was significantly raised throughout both the lateral and posterior hypothalamic nuclei. Previous studies utilising the same model identified a similarly significant increase in the posterior, but only demonstrated a non-significant increase in the lateral hypothalamic nuclei (Benjamin et al., 2004).

This study demonstrates that activation of the trigeminovascular system results in activation of a subset of orexin synthesising neurons in the hypothalamus. It has been shown that the sensory fibres innervating the cranial vessels arise from neurons which have their cell bodies within the trigeminal ganglion. Sensory inputs from the dural blood vessels (such as the superior sagittal sinus and middle meningeal artery) synapse on second order neurons in the trigeminocervical complex. These in turn project to the higher structures including the thalamus and hypothalamus for processing.

Afferent and efferent fibres connect the hypothalamus to a variety of structures including the spinal cord. Although the hypothalamus is not traditionally associated with nociceptive processing it does receive a direct ascending pathway from the dorsal horn, and in particular the trigeminal nucleus caudalis in the rat sends direct projections to the posterior and lateral hypothalamic nuclei (Iwata et al., 1992). In turn descending

inhibitory pathways project from the cortex, via the hypothalamus and terminate on the TNC and spinal cord, either via direct projections or via synapses in the periaqueductal gray and nucleus raphe magnus (Millan, 2002). Experimentally it has been shown that chemical and electrical activation of the posterior and lateral hypothalamus elicits inhibitory effects (Carstens et al., 1983; Carstens, 1986; Manning and Franklin, 1998; Yaksh, 1999; Leone et al., 2001; Leone et al., 2003).

One limitation of this study is that we are unable to determine whether the activated neurons form part of an ascending or descending pathway, or indeed a mixture of both. Evidence points to the possible involvement of the orexinergic system in the descending modulation of pain and it is possible that a subset of orexinergic neurons activated perform this role. Direct orexinergic projections link the hypothalamus and the spinal cord and the PAG, both possible mechanisms for the modulation of nociceptive processing. Bingham et al. (2001) postulated a novel descending orexin driven inhibitory system, that plays a role in maintaining basal nociceptive threshold and it has been demonstrated that destruction of the posterior hypothalamus in the rat results in transient hyperalgesia (Millan et al., 1983).

Microinjection of orexin A and B into the posterior hypothalamus results in differential responses of trigeminal neurons to electrical stimulation of the dura mater in the rat, with orexin A demonstrating an antinociceptive response and orexin B facilitating the response (Bartsch et al., 2004b). It is therefore possible that a subset of orexin synthesising neurons activated in the PH and LH in response to SSS stimulation may form part of a novel descending modulatory pathway that is activated as a result of trigeminovascular activation.

In relation to the primary headache syndromes, including migraine and cluster headache, there is considerable evidence that the hypothalamus plays an important role in the pathophysiology of these disorders (Zurak, 1997; May et al., 1998a; May et al., 1999b; Peres et al., 2001; Leone et al., 2003). The orexinergic system is one possible pathway that is known to influence a variety of hypothalamic functions that are predictive of a

hypothalamic dysfunction in migraine including the circadian rythmicity of attacks and the presence of premonitory symptoms up to 48 hours prior to onset (Date et al., 1999; Horvath et al., 1999c; Smart and Jerman, 2002; Ferguson and Samson, 2003). This study is the first to demonstrate that nociceptive activation of the trigeminovascular system reliably activates a subset of orexinergic neurons in the PH and LH and may therefore provide a direct link between the pain of primary headaches and the autonomic and neuroendocrine abnormalities found in the disorder (Smart, 1999).

Chapter 4 – Orexin 1 but not orexin 2 receptor activation attenuates neurogenic dural vasodilation in an animal model of trigeminovascular nociception

Introduction

Whilst migraine is now considered to be a disorder of the brain (Goadsby et al., 2002b) there are features of the innervation of the dural vasculature that can help in understanding its pathogenesis. It has been recognised for some time that most of the intracranial structures, including the dura mater and blood vessels, are pain-producing, especially when electrical stimulation is utilised (Penfield, 1932, 1934; Penfield and McNaughton, 1940; Wolff, 1948; McNaughton and Feindel, 1977). The trigeminal ganglion is psudo-unipolar and as a result of this one is able to study central and peripheral projections in relation to migraine. Intravital microscopy relies upon the reaction of dural blood vessels as an indication of trigeminal nerve activation from a peripheral perspective, and given that dural blood vessel distension is painful in humans (Ray and Wolff, 1940) and trigeminal nerve activation causes dural blood vessel dilation (Williamson et al., 1997a) it enables us to model some aspect of the migraine attack.

Intravital microscopy uses a thinned closed cranial window combined with a video microscopy device that allows the visualisation and measurement of cranial (dural and pial) blood vessels in real time, figure 29 (Williamson et al., 1997a, b; Petersen et al., 2004; Gozalov et al., 2005; Petersen et al., 2005b; Petersen et al., 2005a). Electrical stimulation of the cranial window causes a reproducible dural and pial blood vessel dilation via activation of the trigeminal nerve, thought to be via the release of CGRP from pre-synaptic trigeminal nerve endings, that dilates dural blood vessels (Williamson et al., 1997a; Akerman et al., 2002b; Petersen et al., 2004). Inhibition of neurogenic dural vasodilation (NDV) has proved successful in predicting anti-migraine efficacy with numerous compounds including the triptans, 5-$HT_{1B/1D}$ receptor agonists, dihydroergotamine (DHE) and CGRP receptor antagonists all able to inhibit neurogenic dural vasodilation (Williamson et al., 1997a, b; Williamson et al., 2001a; Akerman et al., 2002b; Petersen et al., 2004). Interestingly, the neurokinin 1 (NK1) receptor antagonists were unable to inhibit NDV (Williamson et al., 1997a), as well as demonstrating similarly poor results in clinical trials (Goldstein et al., 1997; Goldstein et al., 2001). Other compounds that have demonstrated the ability to inhibit NDV are μ-opioid receptor agonists (Williamson et al., 2001b), neuronal nitric oxide synthase inhibitors

(Akerman et al., 2002a), and the non steroidal anti-inflammatory, indomethacin (Akerman et al., 2002b).

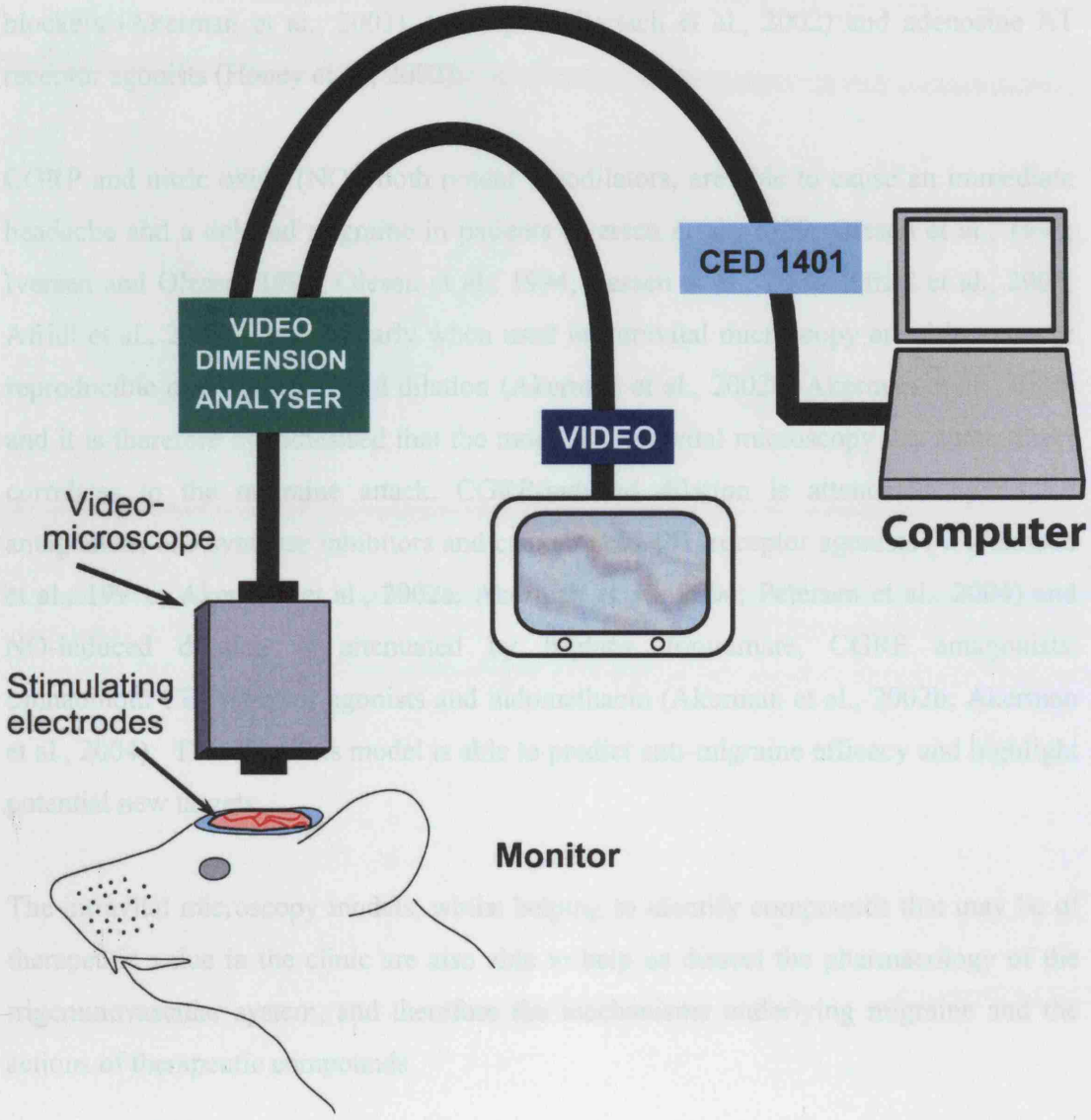

Figure 29: Overview of the intravital set-up in the rat.

The magnified image of the dural artery is displayed on a monitor and recorded. The diameter of the blood vessel is constantly measured via the video dimension analyser. A second output from the video dimension analyser passes to the CED 1401, which converts the signal to enable on-line analysis via the Spike 2 v5 software on the computer.

There are also a series of compounds that are able to inhibit neurogenic dural vasodilation, and represent potential targets in the clinic, cannabinoid CB_1 receptor agonists (Akerman et al., 2004), P/Q, N and L-type voltage-dependent calcium channel blockers (Akerman et al., 2003), nociceptin (Bartsch et al., 2002) and adenosine A1 receptor agonists (Honey et al., 2002).

CGRP and nitric oxide (NO), both potent vasodilators, are able to cause an immediate headache and a delayed migraine in patients (Iversen et al., 1989; Olesen et al., 1993; Iversen and Olesen, 1994; Olesen et al., 1994; Lassen et al., 2002; Afridi et al., 2004; Afridi et al., 2005b) and similarly when used in intravital microscopy are able to cause reproducible dural blood vessel dilation (Akerman et al., 2002b; Akerman et al., 2004) and it is therefore hypothesised that the model of intravital microscopy has some direct correlates to the migraine attack. CGRP-induced dilation is attenuated by CGRP antagonists, NO synthase inhibitors and cannabinoid CB_1 receptor agonists (Williamson et al., 1997b; Akerman et al., 2002a; Akerman et al., 2004; Petersen et al., 2004) and NO-induced dilation is attenuated by triptans, topiramate, CGRP antagonists, cannabinoid CB_1 receptor agonists and indomethacin (Akerman et al., 2002b; Akerman et al., 2004). Therefore this model is able to predict anti-migraine efficacy and highlight potential new targets.

The intravital microscopy models, whilst helping to identify compounds that may be of therapeutic value in the clinic are also able to help us dissect the pharmacology of the trigeminovascular system, and therefore the mechanisms underlying migraine and the actions of therapeutic compounds.

The purpose of this study was therefore to investigate the effect of varying doses of orexin A and B on neurogenic and CGRP induced dural vasodilation to investigate their potential as anti-migraine therapeutic targets. The study also investigated the receptor pharmacology of any response by utilising the novel OX_1 receptor antagonist SB-334867 and the CGRP receptor antagonist CGRP $_{8-37}$.

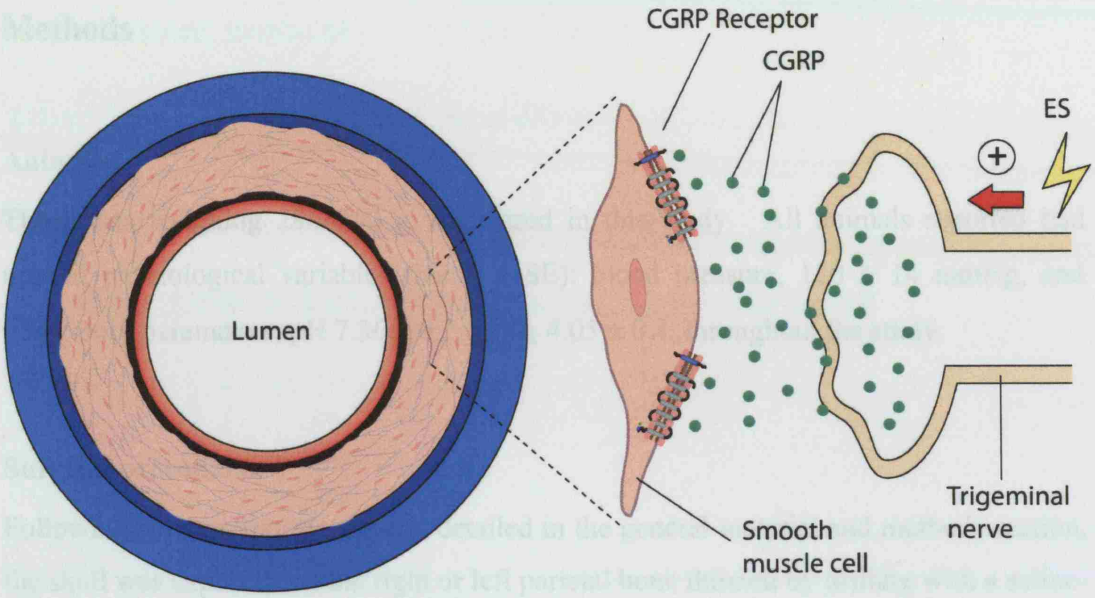

Figure 30: Summary of neurogenic dural vasodilation.

The diagram shows a schematic representation of a dural artery innervated by a trigeminal sensory nerve. Electrical stimulation (ES) causes CGRP release from the pre-junctional activated trigeminal neurons. CGRP activates CGRP receptors in the smooth muscle of the dural artery causing the vessel to dilate.

Methods

Animals

Thirty rats weighing 280–350 g were used in this study. All animals reported had normal physiological variables (mean ± SE): blood pressure, 110 ± 14 mmHg, and respiratory parameters, pH 7.36 ± 0.2, pCO_2 4.05 ± 0.4, throughout the study.

Surgical procedures

Following the preparatory surgery, detailed in the general material and methods section, the skull was exposed and the right or left parietal bone thinned by drilling with a saline-cooled drill until the blood vessels of the dura mater were clearly visible through the intact skull.

Stimulation parameters

Neurogenic dural vasodilation (NDV) was achieved by electrical stimulation of the cranial window as described in the general material and methods section. In brief, the surface of the cranial window was stimulated at 5 Hz, 1 ms for 10 s (Grass Stimulator S88, Grass Instrumentation) with increasing voltage until maximal dilation was observed. Subsequent electrically induced responses in the same animal were then evoked using that voltage (Williamson et al., 1997b; Akerman et al., 2002a). The reproducibility of this vasodilator response to electrical stimulation has been demonstrated previously using consecutive saline-controlled stimuli (Akerman et al., 2002b). CGRP induced dilation was achieved via the administration of CGRP (Tocris Cookson Ltd., UK) 1 μgkg^{-1} intravenous bolus injection via the cannulated femoral vein. This dose of CGRP has been shown repeatedly to produce maximal vessel dilation (Williamson et al., 1997b; Akerman et al., 2002a).

Experimental protocol

Effect of orexin on evoked dural vessel dilation

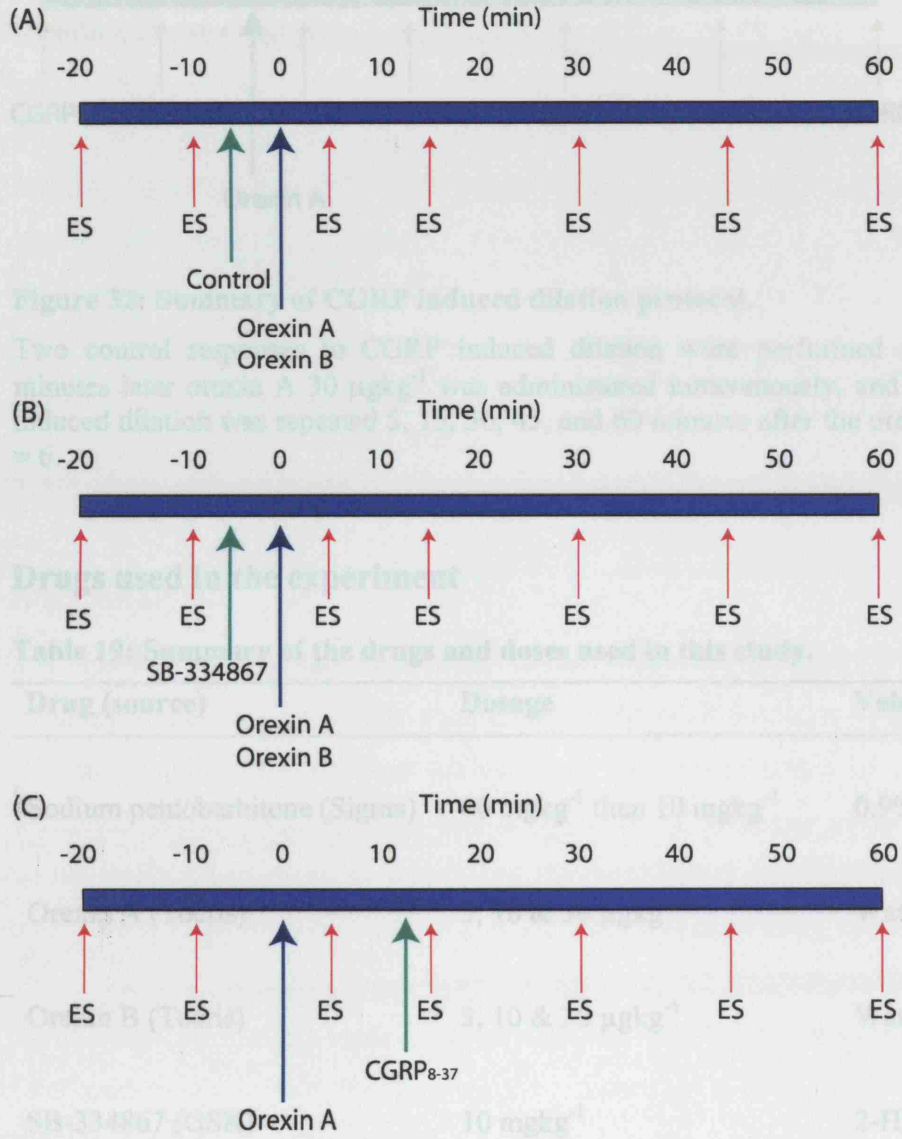

Figure 31: Summary of electrical stimulation protocol.

Two control responses to electrical stimulation (ES) were performed at least 10 minutes prior to intervention, then electrical stimulation was repeated at 5, 15, 30, 45 and 60 minutes following intervention. (A) Effect of orexin A (n = 8) and B (n = 7) on NDV, (B) Effect of orexin A (n = 6) and B (n = 6) on NDV following pre-treatment with the Ox_1 receptor antagonist SB-334867, and (C) Effect of orexin A and $CGRP_{8-37}$ (n = 6) on NDV.

Effect of orexin A on CGRP evoked dural vessel dilation

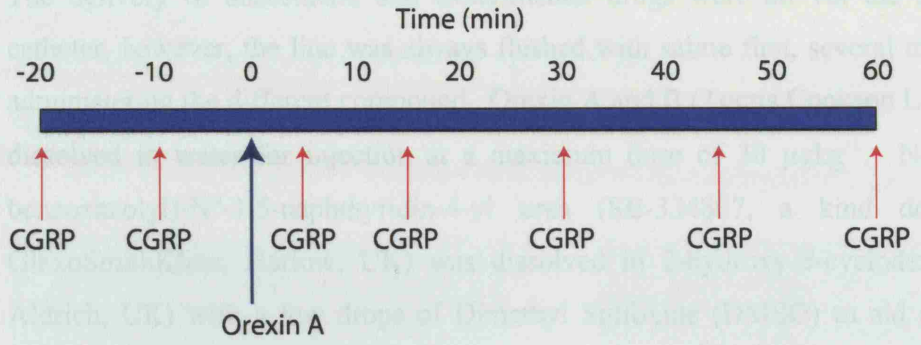

Figure 32: Summary of CGRP induced dilation protocol.

Two control responses to CGRP induced dilation were performed and at least 10 minutes later orexin A 30 μgkg^{-1} was administered intravenously, and then the CGRP induced dilation was repeated 5, 15, 30, 45, and 60 minutes after the orexin treatment, $n = 6$.

Drugs used in the experiment

Table 19: Summary of the drugs and doses used in this study.

Drug (source)	Dosage	Vehicle
Sodium pentobarbitone (Sigma)	60 $mgkg^{-1}$ then 10 $mgkg^{-1}$	0.9% Saline
Orexin A (Tocris)	3, 10 & 30 μgkg^{-1}	Water for injection
Orexin B (Tocris)	3, 10 & 30 μgkg^{-1}	Water for injection
SB-334867 (GSK)	10 $mgkg^{-1}$	2-HβC & DMSO
CGRP (Tocris)	1 μgkg^{-1}	dH_20 & Saline
$CGRP_{8-37}$ (Tocris)	300 μgkg^{-1}	0.9% Saline

2-HβC: 2-hydroxy-β-cyclodextrin; DMSO: Dimethyl Sulfoxide

The delivery of anaesthetic and experimental drugs were all via the same femoral catheter, however, the line was always flushed with saline first, several minutes before administering the different compound. Orexin A and B (Tocris Cookson Ltd., UK) were dissolved in water for injection at a maximum dose of 30 μgkg^{-1}. N-(2-Methyl-6-benzoxazolyl)-N''-1,5-naphthyridin-4-yl urea (SB-334867, a kind donation from GlaxoSmithKline, Harlow, UK) was dissolved in 2-hydroxy-β-cyclodextrin (Sigma-Aldrich, UK) with a few drops of Dimethyl Sulfoxide (DMSO) to aid solubility and injected at a dose of 10 $mgkg^{-1}$. CGRP (Tocris Cookson Ltd., UK) was initially dissolved in distilled water, aliquotted and frozen. Subsequent dilutions were made in 0.9% saline before injection at a dose of 1 μgkg^{-1}. $CGRP_{8-37}$ was dissolved in 0.9% saline for injection at a dose of 300 μgkg^{-1}. All drugs were made fresh on the morning of an experiment.

Data Analysis

The effects of electrical stimulation and CGRP administration on dural vessel diameter were calculated as a percentage increase from the pre-stimulation baseline diameters. The nature of the experimental set-up, where the magnification of the dural vessel visualised was different in each animal by virtue of selecting an appropriate target vessel, made it impossible to standardise the dural vessel measurement, therefore, the dural vessel diameter were measured in percentage change from baseline. The typical vessel diameter measured ranges from 120–150 μm. All data are expressed as mean ± SEM. Statistical analysis was performed using an ANOVA for repeated measures with Bonferroni *post-hoc* correction for multiple comparisons followed by Student's paired *t*-test. To compare the effect of orexin A only and orexin A and $CGRP_{8-37}$ an independent samples *t*-test was used (SPSS v12.0). Significance was assessed at the $P < 0.05$ levels (Field, 2005).

Results

Effect of electrical stimulation of the cranial window

Electrical stimulation 50–300 μA produced reproducible dural blood vessel dilation of 136 ± 9% (n = 35), fig 32.

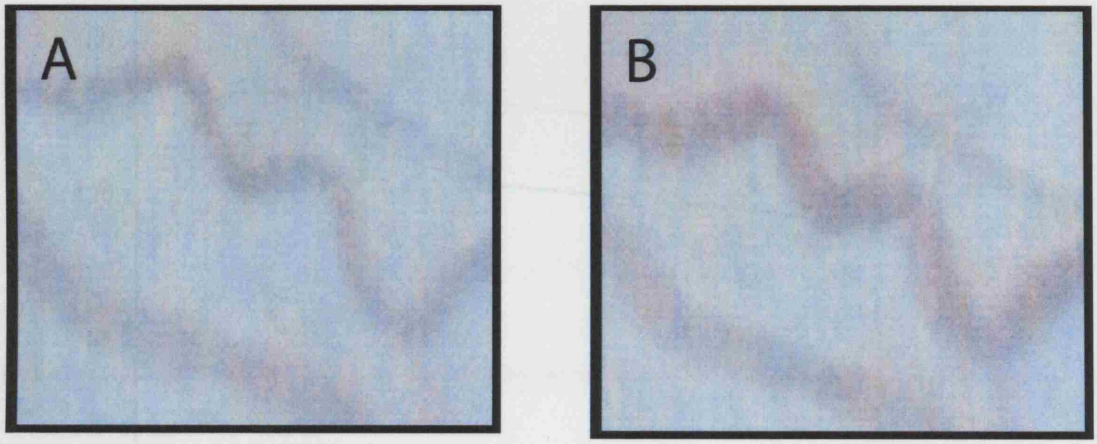

Figure 33: An example of the video-microscope images of a meningeal blood vessel. Baseline diameter before electrical stimulation (A), and the dilated blood vessel 30 seconds post stimulation (B)

Effect of orexin A on neurogenic dural vasodilation

Orexin A given intravenously at 3 and 10 μgkg^{-1} did not significantly attenuate the response to electrical stimulation of the cranial window (figure 34), but had a significant effect at 30 μgkg^{-1} ($F_{2.4,16.6}$ = 16.4, P < 0.001; figure 35). Orexin A produced its maximum effect after 15 minutes, reducing the neurogenic dural vasodilation by 60% (t_7 = 7.1, n = 8, P < 0.001). Pre-treatment with SB-334867 the selective OX_1 receptor antagonist 5 minutes prior to orexin A administration blocked the observed reduction in neurogenic dural vasodilation ($F_{2.4,11.9}$ = 2.08, P = 0.16), indicating the orexin A response was most likely mediated through the OX_1 receptor, figure 35. Addition of $CGRP_{8-37}$ 13 minutes post orexin A produced a significant decrease in neurogenic dural vasodilation at the 15 minute time point when compared to orexin A only (t_5 = 3.5, n =

6, $P < 0.005$; figure 35) and baseline ($F_{5,25} = 142.4$, $P < 0.001$; figure 35). Control vehicle injection demonstrated no significant effect.

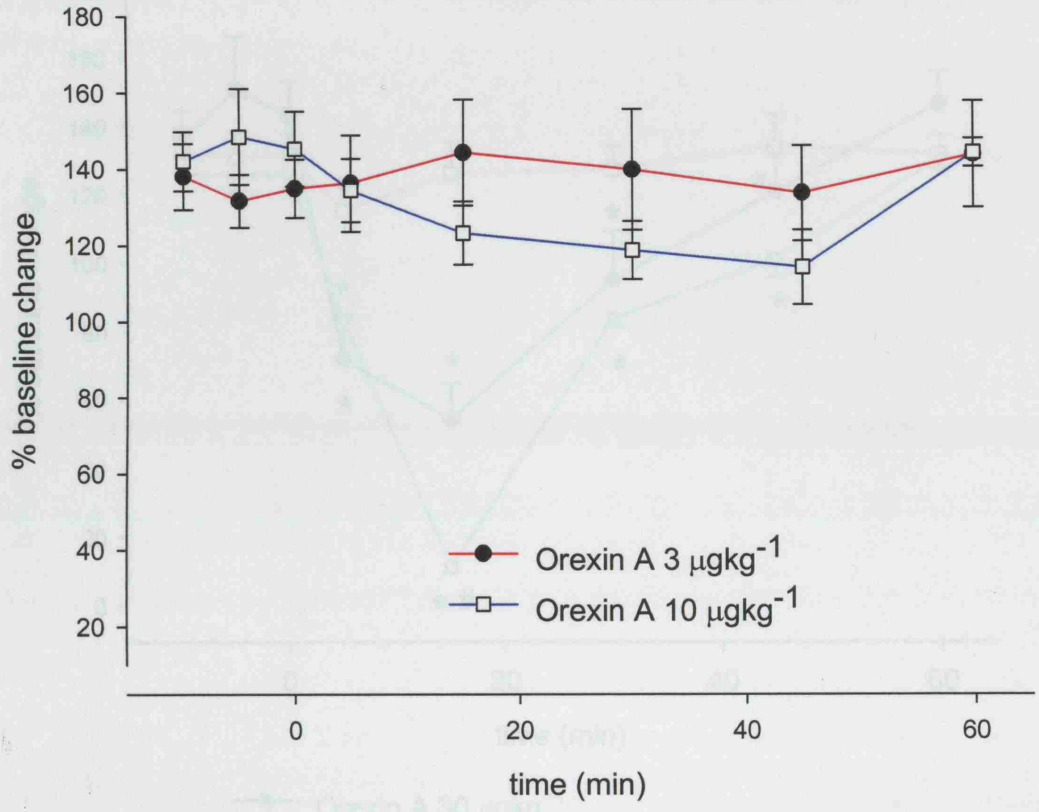

Figure 34: Effects of orexin A 3 and 10 μgkg^{-1} on neurogenic vasodilation.

Following control responses to electrical stimulation rats were injected with orexin A at 3 or 10 μgkg^{-1} ($n = 6$) and electrical stimulation repeated after 5, 15, 30, 45 and 60 minutes. No significant effect is seen.

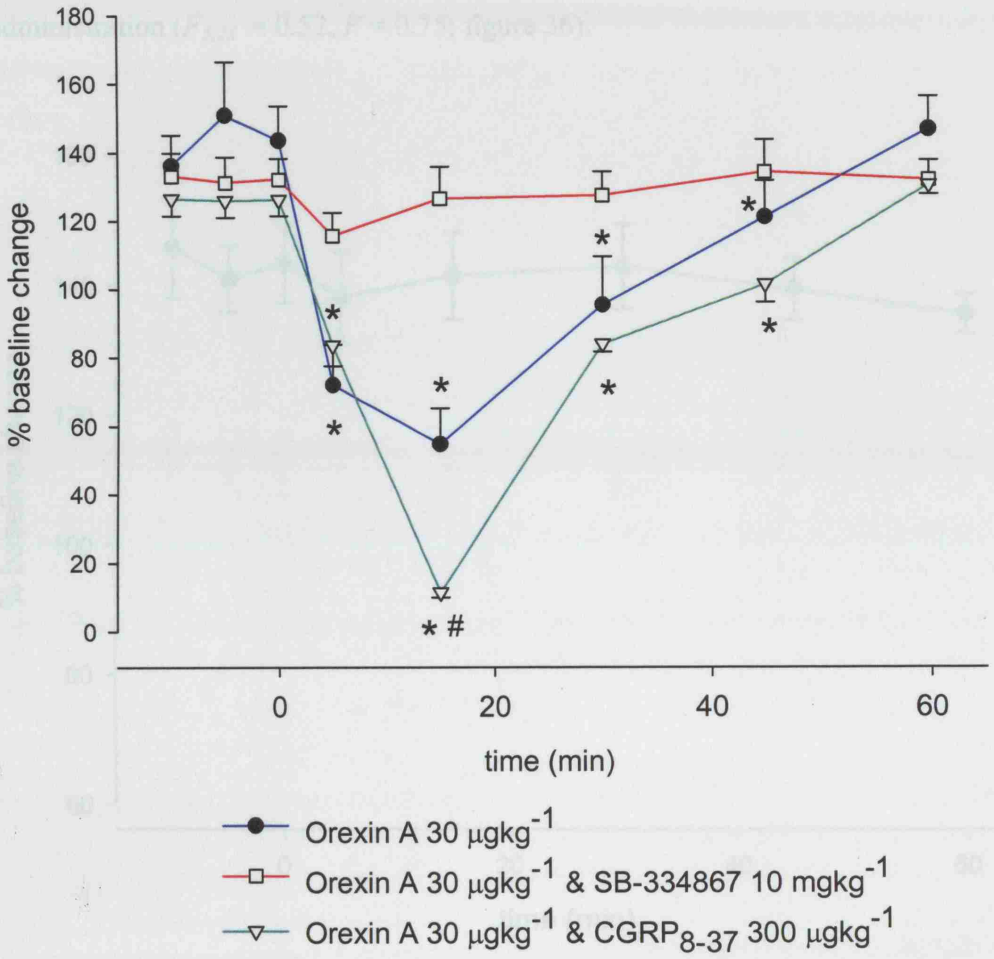

Figure 35: Effects of orexin A 30 μgkg^{-1} on neurogenic dural vasodilation and the effects of pre-treatment with SB-334867 and co-administration of CGRP$_{8-37}$.

Following control responses to electrical stimulation rats were injected with either orexin A at 30 μgkg^{-1} (n = 8), orexin A 30 μgkg^{-1} and CGRP$_{8-37}$ 300 μgkg^{-1} (n = 6), or pretreated with SB-334867 10 mgkg^{-1} 5 min prior to orexin A injection (n = 6) and electrical stimulation repeated after 5, 15, 30, 45 and 60 minutes. Inhibition of neurogenic dural vasodilation is seen in response to orexin A and this is reversed by the OX_1 receptor antagonist SB-334867. CGRP$_{8-37}$ further inhibits the neurogenic dural vasodilation in the presence of orexin A.

*P < 0.05 significance compared to the control response.

#P < 0.05 significance compared to orexin A inhibition.

Effects of Orexin A on CGRP induced dural vasodilation

CGRP administration (1 μgkg^{-1}) produced a reproducible dural blood vessel dilation of 145 ± 7% (n = 6). Intravenous administration of orexin A at 30 μgkg^{-1}, which inhibited neurogenic dural vasodilation had no effect on dural vasodilation in response to CGRP administration ($F_{5,25}$ = 0.52, P = 0.75; figure 36).

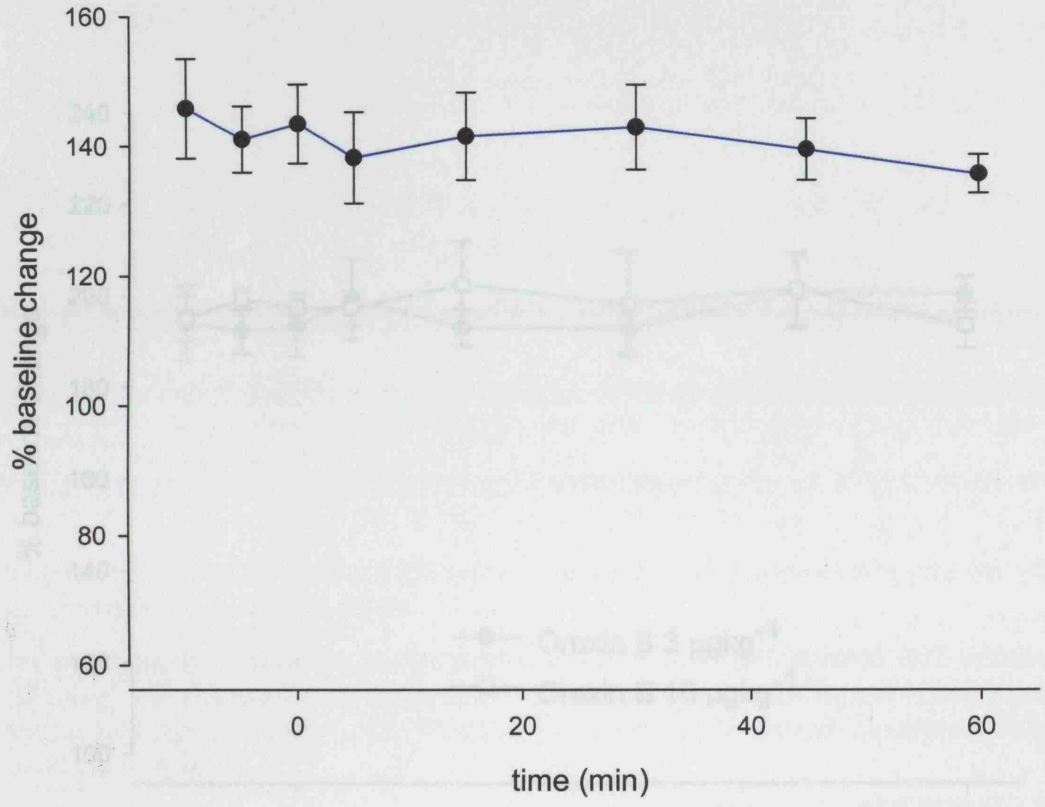

Figure 36: Effects of orexin A 30 μgkg^{-1} on CGRP 1 μgkg^{-1} induced vasodilation.
Following control responses to CGRP administration rats were injected with orexin A at 30 μgkg^{-1} and CGRP injection repeated after 5, 15, 30, 45 and 60 minutes. Overall no significant effect of orexin A on CGRP induced vasodilation was seen.

Effects of Orexin B on neurogenic dural vasodilation

Orexin B given intravenously at 3 and 10 μgkg^{-1} (n = 7) had no effect on neurogenic dural vasodilation, figure 37. Orexin B given intravenously at 30 μgkg^{-1} (n = 7) elicited

a non-significant decrease in neurogenic dural vasodilation ($F_{3.1,18.8}$ = 0.86, P = 0.48; figure 38). Pre-treatment with SB-334867 followed 5 minutes later by orexin B 30 μgkg^{-1} (n = 6) elicited a slight increase in neurogenic dural vasodilation, however, this was not significant from baseline ($F_{1.9,9.5}$ = 1.63, P = 0.26; figure 38). Grouped comparisons of orexin B and orexin B post SB-334867 showed no significant difference between the two treatments. Control vehicle injections demonstrated no significant effect.

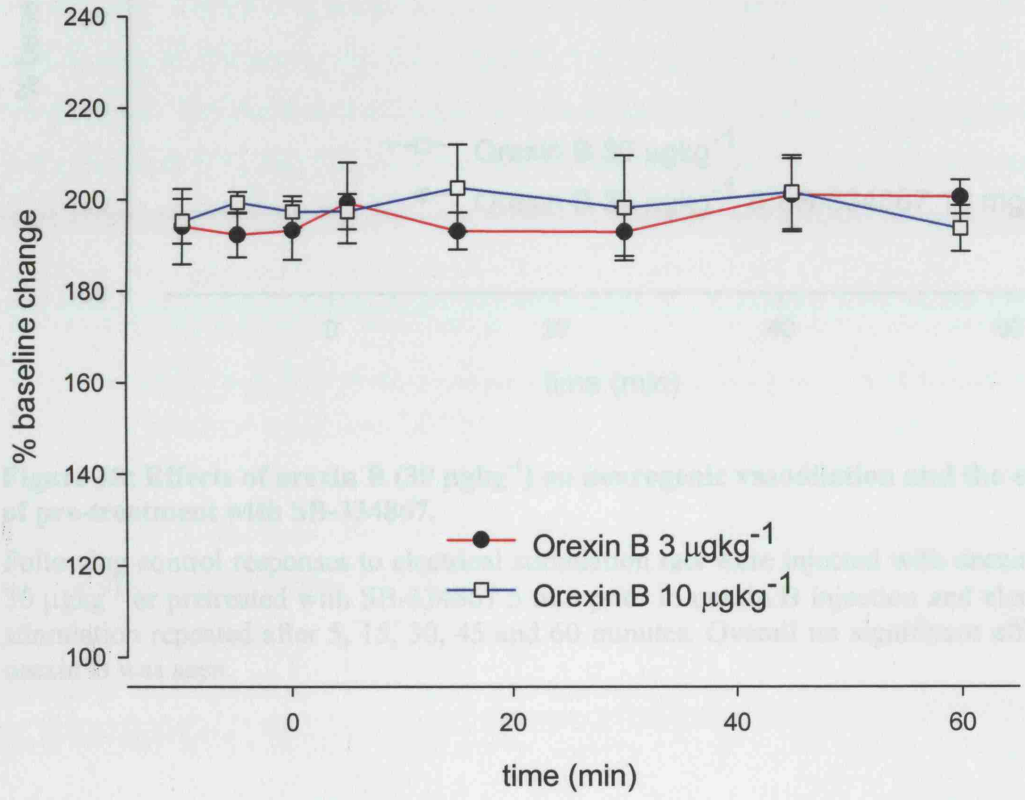

Figure 37: Effects of orexin B (3 and 10 μgkg^{-1}) on neurogenic vasodilation.

Following control responses to electrical stimulation rats were injected with orexin B at 3 or 10 μgkg^{-1} and electrical stimulation repeated after 5, 15, 30, 45 and 60 minutes. No significant effect is seen.

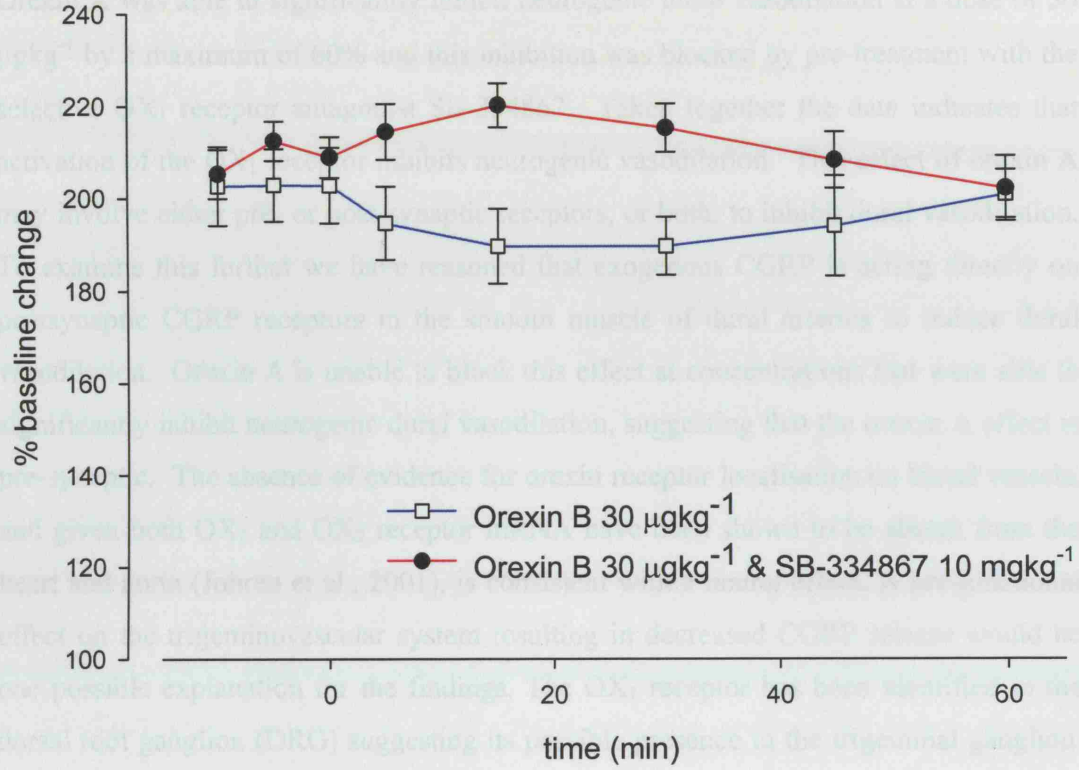

Figure 38: Effects of orexin B (30 μgkg^{-1}) on neurogenic vasodilation and the effects of pre-treatment with SB-334867.

Following control responses to electrical stimulation rats were injected with orexin B at 30 μgkg^{-1} or pretreated with SB-334867 5 min prior to orexin B injection and electrical stimulation repeated after 5, 15, 30, 45 and 60 minutes. Overall no significant effect of orexin B was seen.

Discussion

Orexin A was able to significantly inhibit neurogenic dural vasodilation at a dose of 30 μgkg^{-1} by a maximum of 60% and this inhibition was blocked by pre-treatment with the selective OX_1 receptor antagonist SB-334867. Taken together the data indicates that activation of the OX_1 receptor inhibits neurogenic vasodilation. This effect of orexin A may involve either pre- or post-synaptic receptors, or both, to inhibit dural vasodilation. To examine this further we have reasoned that exogenous CGRP is acting directly on postsynaptic CGRP receptors in the smooth muscle of dural arteries to induce dural vasodilation. Orexin A is unable to block this effect at concentrations that were able to significantly inhibit neurogenic dural vasodilation, suggesting that the orexin A effect is pre-synaptic. The absence of evidence for orexin receptor localisation on blood vessels, and given both OX_1 and OX_2 receptor mRNA have been shown to be absent from the heart and aorta (Johren et al., 2001), is consistent with a neural effect. A pre-junctional effect on the trigeminovascular system resulting in decreased CGRP release would be one possible explanation for the findings. The OX_1 receptor has been identified in the dorsal root ganglion (DRG) suggesting its possible presence in the trigeminal ganglion. The CGRP receptor antagonist $CGRP_{8-37}$ when administered at the point of maximal inhibition (60% of baseline response) with orexin A, further significantly inhibits neurogenic dural vasodilation (11% of baseline response) suggesting that orexin A does not completely block the pre-synaptic release of CGRP.

Orexin B was unable to significantly alter neurogenic dural vasodilation at all three doses studied. At the 30 μgkg^{-1} dose a non-significant trend to a reduction in the dilator response was observed, possibly as a result of an effect at the OX_1 receptor. In the presence of orexin B, pre-treatment with the selective OX_1 receptor antagonist SB-334867, whilst still having no significant effect, caused a slight increase in dural vessel dilation as a result of electrical stimulation. The experimental model utilised in this study results in dilation of the dural blood vessels under examination and as such there is an upper physiological limit to the level of dilation achievable, therefore one is unable to rule out a possible effect of orexin B either with or without SB-334867 pre-treatment.

Orexin A injected into the hypothalamus has been shown previously to significantly inhibit cell firing in the trigeminocervical complex (TCC) in response to dural electrical stimulation and noxious thermal stimulation of the facial skin in the rat (Bartsch et al., 2004b). The level of inhibition achieved by intravenous administration of orexin A at a dose of 30 μgkg^{-1} in our model of trigeminovascular activation indicates a potent ability to influence the trigeminovascular system directly. As previously reported the ability to inhibit neurogenic vasodilation has been used to identify potential migraine therapy targets, such as sumatriptan (Williamson et al., 1997a). OX_1 receptor activation causes an inhibition comparable with that of other acute attack treatments, and as such may be considered a putative target for migraine medicine development.

The trigeminal ganglion is psudo-unipolar, with its afferent fibres innervating the dural blood vessels in the periphery and centrally projecting to the trigeminal nucleus caudalis (TNC). The pharmacology of the peripheral and central branches of the trigeminal ganglion in general match each other, thus work demonstrating an effect on the neuronal mechanisms involving the dural blood vessels may also apply to the central neuronal mechanisms in the TNC. Numerous compounds including the triptans, $5\text{-}HT_{1B/1D}$ receptor agonists (Williamson et al., 1997c; Boers et al., 2000, 2004) and the CGRP receptor blockers (Williamson et al., 1997b; Storer et al., 2004) are able to inhibit the activation of both the central and peripheral branches of the trigeminal ganglion. The data presented suggests the possibility that OX_1 receptor agonists may also be able to inhibit neurons in the TNC directly.

The current study demonstrates that orexin A is able to inhibit neurogenic dural vasodilation via activation of the OX_1 receptor. This effect is most likely pre-junctional acting on the trigeminovascular system resulting in decreased but not complete blockade of CGRP release. The data compliment electrophysiological work in the rat demonstrating that OX_1 receptor activation in the hypothalamus is able to inhibit neuronal firing in the TNC in response to electrical stimulation of the dura mater and noxious thermal stimulation of the facial receptive field (Bartsch et al., 2004b). The widespread distribution of the orexins and their receptors throughout the CNS including

the hypothalamus, periaqueductal gray and lamina I, II and X of the spinal cord (Peyron et al., 1998; Trivedi et al., 1998; van den Pol, 1999), which are all areas involved in nociceptive processing, provide the possibility for further research into the role of the orexins in neuronal systems potentially involved in migraine and cluster headache. Orexins may provide some part of the link between some of the remarkable triggering and behavioural manifestations of migraine, such as those involved in eating, and the disorder of sensory control mechanisms that is so characteristic of the condition.

Chapter 5 – Orexin 1 receptor activation modulates dural nociceptive input to the trigeminal nucleus caudalis in the rat, an intravenous electrophysiological study

Introduction

The pathophysiology of migraine remains to be fully elucidated; it is clear however that activation of the trigeminovascular system as described in the general introduction underpins the neural substrate of the pain in primary headache syndromes such as migraine (Goadsby et al., 2002a). The nociceptive inflow from the meninges to the spinal cord is relayed in the trigeminocervical complex (TCC), before ascending via second order neurons to higher structures including the thalamus and hypothalamus. The ability to record the activation of these second order neurons in the TCC and hence attempt to find compounds that can inhibit their activation is of prime importance to the identification of anti-migraine therapeutic targets.

An important characteristic of the second order trigeminal neurons is the convergent input from the dural structures including the middle meningeal artery (MMA), the ophthalmic dermatome of the cutaneous receptive field, and the cervical afferents innervating the neck area (Piovesan et al., 2003; Bartsch, 2005). It is this convergence that is considered to be the underlying mechanism for the referred pain reported following deep tissue injury (Bolton et al., 2005). With particular relevance to the convergence of trigeminal afferents is the pathology of migraine headache which is characterised by attacks of head pain, sensitivity to sensory information and allodynia of the facial skin (Selby and Lance, 1960; Burstein et al., 2000). It is currently considered that the dural blood vessels and their neural connectivity with the trigeminocervical complex play a fundamental role in the perception of these symptoms (Goadsby et al., 2002b). An increased understanding of the mechanisms and the pharmacological profile of these neurons has major implications for the pathophysiology and treatment of migraine.

The orexins as described in the general introduction have recently been linked with a role in the modulation of nociceptive processing (Bingham et al., 2001; Yamamoto et al., 2002; Cheng et al., 2003; Kajiyama et al., 2005; Watanabe et al., 2005) and a possible role in migraine pathophysiology (Bartsch et al., 2004b). The previous intravital study raised the possibility of a central effect of the orexins acting directly on

trigeminal neurons in the TNC. The purpose of this study was to examine the effect of the orexin receptor activation in the modulation of nociceptive processing by examining the effect of orexin A and B on dural nociceptive input to the TNC and to dissect out the receptor pharmacology of any response by utilising the novel OX_1 receptor antagonist SB-334867 (GlaxoSmithKline, Harlow, UK). The responses of neurons in the TNC were examined in relation to dural stimulation and nociceptive and non-nociceptive activation of the cutaneous facial receptive field. To test for any sensitisation of the dural structures resulting from repeated electrical stimulation mechanical von Frey thresholds of the dura surrounding the MMA were tested at regular intervals.

Material and methods

Animals

Eighteen rats weighing 270–310 g were used in this study. All animals reported had normal physiological variables (mean ± SE): blood pressure, 115 ± 4 mmHg, and respiratory parameters, pH 7.35 ± 0.2, pCO_2 4.1 ± 0.4, throughout the study.

Surgical procedures

Following the preparatory surgery, detailed in the general material and methods section, the skull was exposed and the right or left parietal bone thinned and removed, a partial C1 laminectomy was performed and the underlying dura mater dissected to reveal the spinal cord. A stimulating electrode was placed on the dura mater surrounding the MMA and a recording electrode lowered into the cervico-medullary junction until a neuron responsive to dural and ophthalmic facial receptive field stimulation was located.

Experimental Protocols

Trains of 20 stimuli at 0.6 Hz were delivered at five minute intervals to assess the baseline response to dural electrical stimulation. Responses were analysed using post-stimulus histograms with a sweep length of 100 ms and a bin width of 200 μs, that separated Aδ-fibre and C-fibre activated responses in relation to their conduction velocities. An interval of spontaneous activity was recorded for 120–180 seconds preceding any dural stimulation from the peri-stimulus histogram.

Once a neuron with convergent inputs from the dura mater and ophthalmic dermatome of the trigeminal nerve was identified responses were tested using the following protocol. (1) Three baseline collections of dural stimulation and a single receptive field characterisation. (2) Orexin A, B or control vehicle intervention. (3) Dural stimulation collections at 5, 10, 15, 20, 25, 30, 45 and 60 minutes with a receptive field

characterisation at 20 minutes. (4) SB-334867 or control vehicle pre-treatment followed by dural stimulation collection at 5 minutes. (5) Repeated steps 2 and 3.

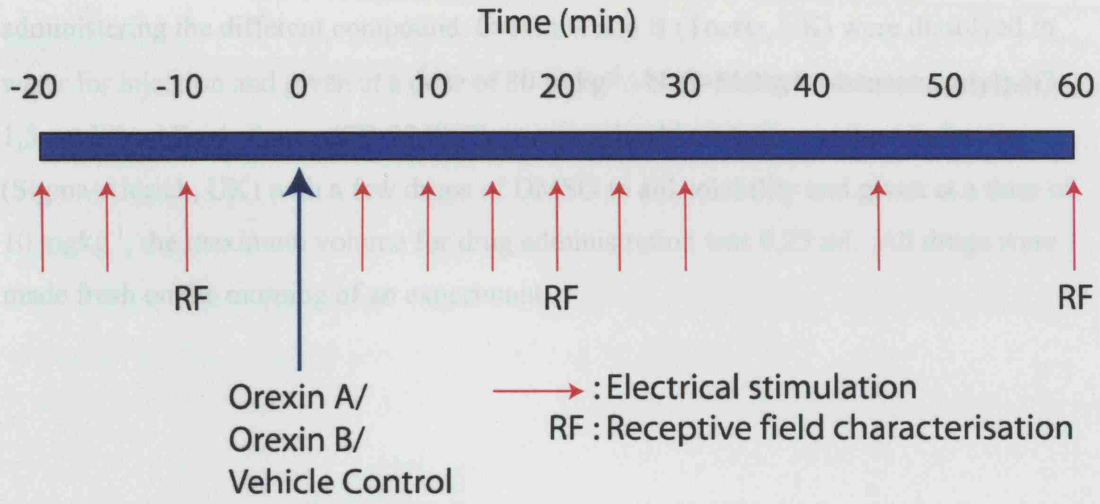

Figure 39: Intravenous orexin electrophysiology protocol.

Data Analysis

Data collected for Aδ-fibre responses represents the total number of cells fired over a 10 ms time period in the region of 4–20 ms post stimulation over the 20 collections. Data collected for C-fibre responses represents the total number of cells fired over a 80 ms time period (20–100 ms post stimulation) from the 20 collections. Spontaneous activity is measured in cells firing per second (Hz). Effects of drug intervention were analysed using an ANOVA for repeated measures with Bonferroni *post-hoc* correction for multiple comparisons followed by Student's paired *t*-test (SPSS v12.0), using the average of the three baselines for comparisons. When the assumption of sphericity with regards to the factor of repeats was violated, adjustments were made for the degrees of freedom and *P* values according to the Greenhouse-Geisser correction. Significance was assessed at the $P < 0.05$ levels (Field, 2005).

Drugs

The delivery of anaesthetic and experimental drugs were all via the same femoral catheter, however, the line was always flushed with saline first, several minutes before administering the different compound. Orexin A and B (Tocris, UK) were dissolved in water for injection and given at a dose of 30 μgkg^{-1}. N-(2-Methyl-6-benzoxazolyl)-N''-1,5-naphthyridin-4-yl urea (SB-334867) was dissolved in 2-hydroxy-β-cyclodextrin (Sigma-Aldrich, UK) with a few drops of DMSO to aid solubility and given at a dose of 10 $mgkg^{-1}$, the maximum volume for drug administration was 0.25 ml. All drugs were made fresh on the morning of an experiment.

Results

Recordings were made from 23 neurons all of which were WDR responsive to dural MMA stimulation and had cutaneous receptive fields restricted to the ophthalmic and maxillary dermatome (figure 40A) of the trigeminal nerve. Neurons were found in deep layers (laminae V and VI) of the dorsal horn at the level of the cervico-medullary junction at a depth of 500–950 μm (figure 40B) and electrode placement was confirmed in 15 animals via an electrolytic lesion in the TNC (figure 40C). Neurons with Aδ-fibre inputs had latency to activation after dural stimulation of 15 ± 0.7 ms, while neurons with C-fibre inputs had latency to activation of 44 ± 2 ms. The baseline spontaneous firing rate for the cohort of neurons studied was 35 ± 2 Hz.

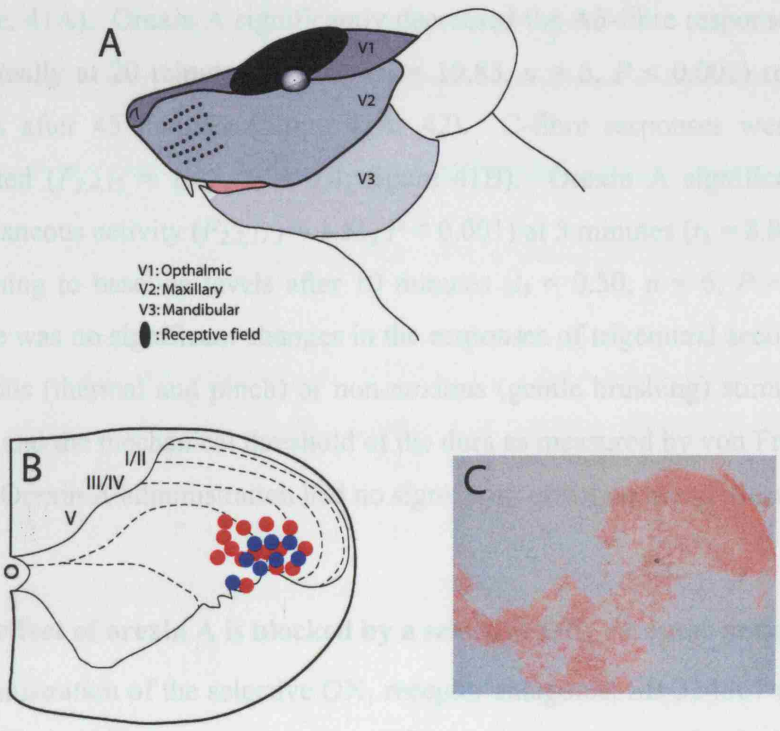

Figure 40: Example of a facial receptive field location and recording sites within the trigeminal nucleus caudalis.

(A) Cutaneous receptive field **(B)** Summary of the locations of lesion sites (red circles) in the TNC indicating the location of the recording electrode for 15 WDR neurons used in this study. Blue circles represent recording sites constructed from microdrive readings. **(C)** An example of the lesion site identified within the dorsal horn.

Effects of Orexin A on responses to dural stimulation

Orexin A was given at the highest dose used in the previous study (chapter 4) as this was the only dose that had a significant effect on neurogenic dural vasodilation when given intravenously. Therefore it was felt that due to the difference in the two experimental models, namely that in this study we were investigating the central effects of orexin A, it was felt that the higher dose would provide more adequate central nervous system penetration. The effect of intravenous administration of orexin A 30 μgkg^{-1} on the response to dural MMA and receptive field stimulation was assessed in 6 animals. Orexin A, which has equal affinity for the OX_2 receptor as orexin B, but 30–100 times more affinity for the OX_1 receptor, significantly inhibited the response of Aδ-fibre neurons to dural electrical stimulation over the 60 minutes ($F_{1.9,9.8} = 21.93$, $P < 0.001$; figure. 41A). Orexin A significantly decreased the Aδ-fibre response at 15 minutes and maximally at 20 minutes by 30% ($t_5 = 19.83$, $n = 6$, $P < 0.001$) returning to baseline levels after 45 minutes (figure 41A, 42). C-fibre responses were not significantly affected ($F_{2.4,12} = 1.02$, $P = 0.4$; figure 41B). Orexin A significantly decreased the spontaneous activity ($F_{2.2,11.1} = 1.51$, $P < 0.001$) at 5 minutes ($t_5 = 8.86$, $n = 6$, $P < 0.001$) returning to baseline levels after 10 minutes ($t_5 = 0.50$, $n = 6$, $P = 0.64$; figure 41C). There was no significant changes in the responses of trigeminal second order neurons to noxious (thermal and pinch) or non-noxious (gentle brushing) stimulation of the facial skin, and the mechanical threshold of the dura as measured by von Frey filaments (figure 43). Orexin A administration had no significant effect on blood pressure.

The effect of orexin A is blocked by a selective OX_1 receptor antagonist

Administration of the selective OX_1 receptor antagonist SB-334867 at 10 $mgkg^{-1}$ had no significant effect on Aδ- or C-fibre responses to dural MMA stimulation. Administration of SB-334867 5 minutes prior to orexin A administration blocked the observed inhibition of Aδ-fibre neuronal responses to dural stimulation ($F_{3.5,17.5} = 0.49$, $P = 0.73$; figure 41A) and the decrease in spontaneous activity ($F_{2.4,13.9} = 1.26$, $P = 0.32$; figure 41C). SB-334867 administration had no significant effect on blood pressure.

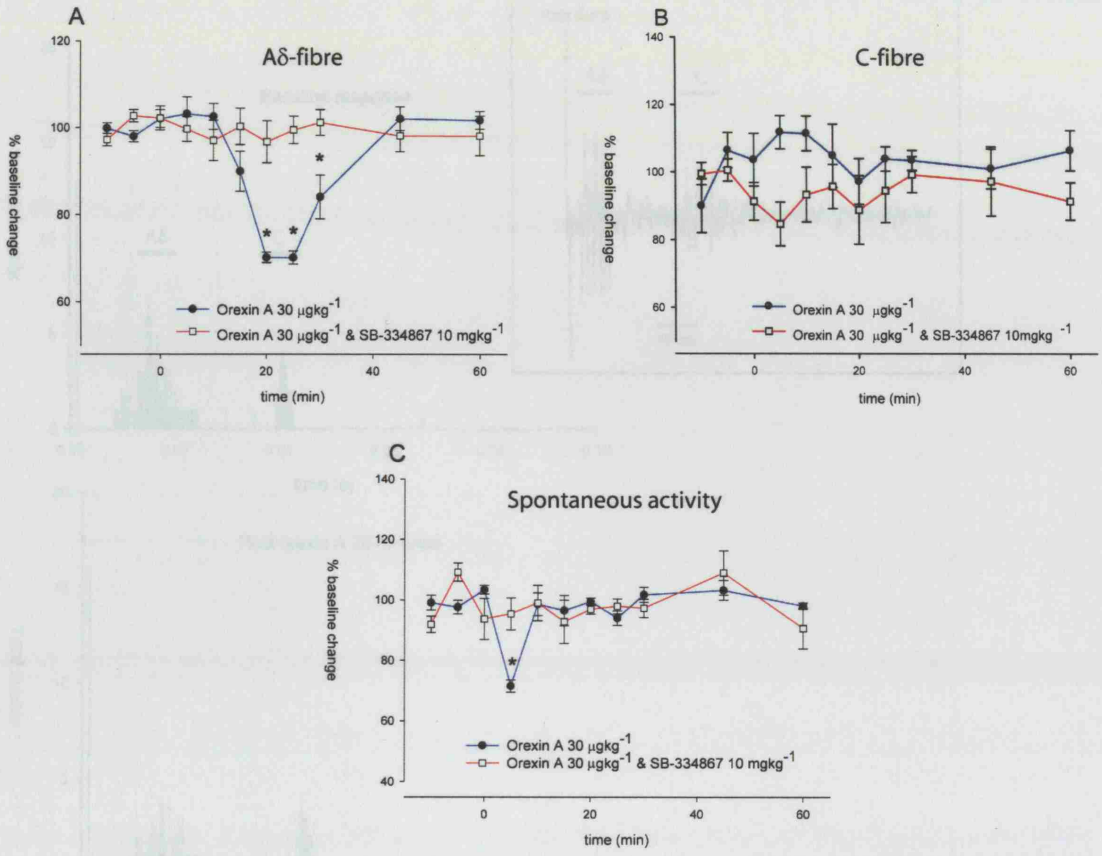

Figure 41: Summary of changes in neuronal responses of trigeminal neurons after orexin A (30 μgkg^{-1}) and orexin A (30 μgkg^{-1}) with SB-334867 (10 mgkg^{-1}).

(A) Aδ-fibres, **(B)** C-fibres **(C)** spontaneous activity. Orexin A inhibited spontaneous activity and Aδ-fibre responses to dural electrical stimulation, but not C-fibre and these effects were blocked by the selective OX_1 receptor antagonist SB-334867.
*$P < 0.05$ significance compared to the control response.

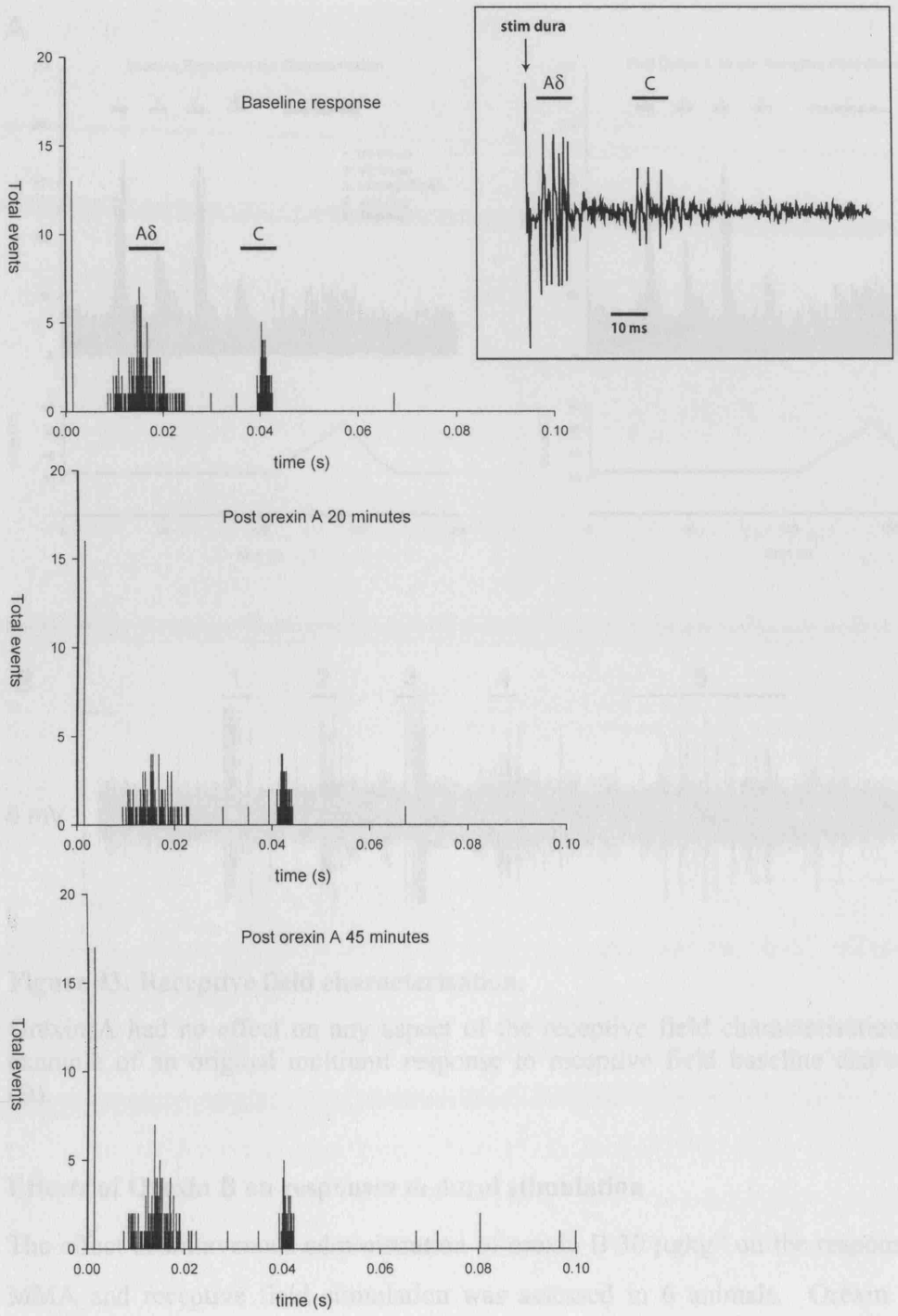

Figure 42: Original post-stimulus histograms of neuronal responses.

Orexin A inhibited Aδ-, but not C-fibre response maximally by 30% after 20 minutes, returning to baseline levels after 45 minutes. Insert shows an original sample trace demonstrating multi unit responses.

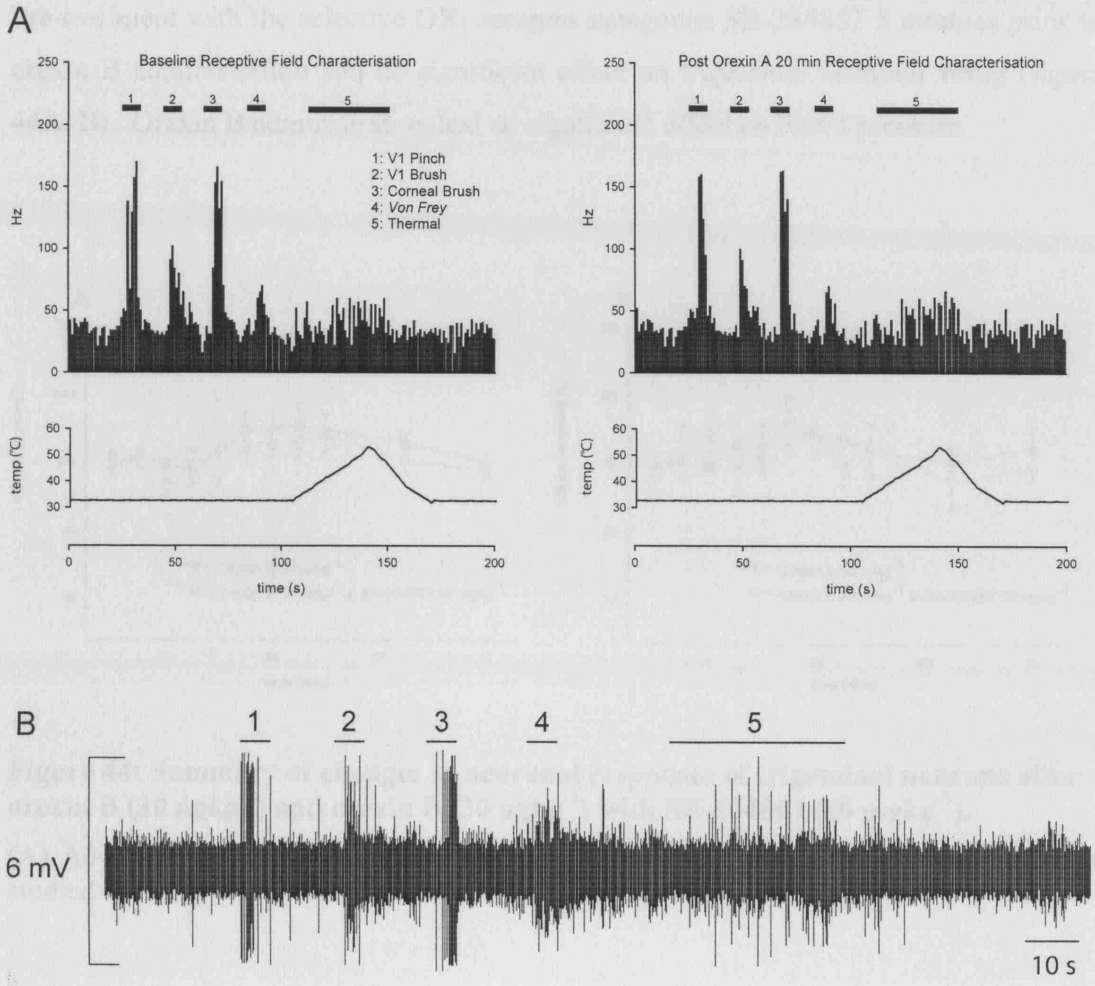

Figure 43: Receptive field characterisation.

Orexin A had no effect on any aspect of the receptive field characterisation (A). An example of an original multiunit response to receptive field baseline characterisation (B).

Effects of Orexin B on responses to dural stimulation

The effect of intravenous administration of orexin B 30 μgkg^{-1} on the response to dural MMA and receptive field stimulation was assessed in 6 animals. Orexin B had no significant affect on the response of Aδ-fibre ($F_{2.6,13.0}$ = 1.54, P = 0.25; figure 44A) or C-fibre ($F_{2.2,11}$ = 1.07, P = 0.46; figure 44B) neurons to dural electrical stimulation over the 60 minutes. Orexin B had no significant effect on spontaneous activity or the receptive field characterisation.

Pre-treatment with the selective OX_1 receptor antagonist SB-334867 5 minutes prior to orexin B administration had no significant effect on trigeminal neuronal firing (figure 44A, B). Orexin B administration had no significant effect on blood pressure.

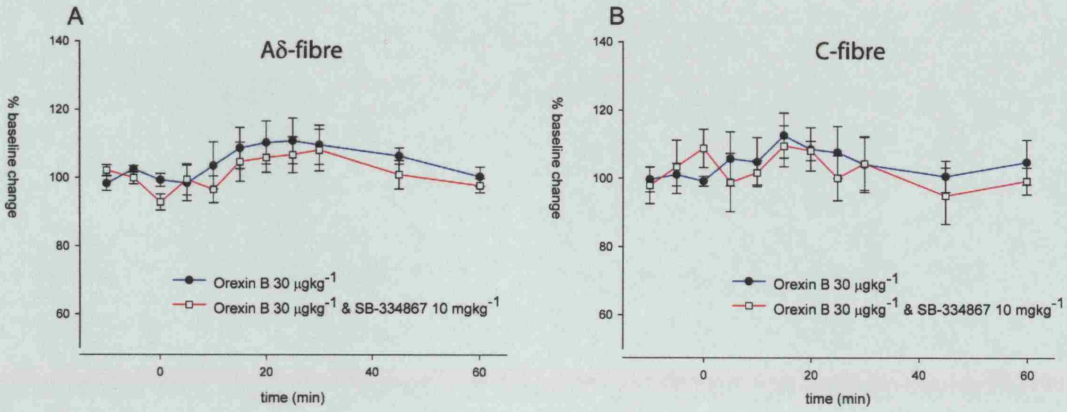

Figure 44: Summary of changes in neuronal responses of trigeminal neurons after orexin B (30 μgkg^{-1}) and orexin B (30 μgkg^{-1}) with SB-334867 (10 $mgkg^{-1}$).

(A) Aδ-fibres, **(B)** C-fibres. Orexin B had no significant effect on any of the aspects studied.

Effects of vehicle control administration on responses to dural stimulation and cutaneous receptive fields

Administration of saline had no significant effect on Aδ- and C- fibre responses to dural stimulation or characterisation of the cutaneous receptive field. Similarly administration of 2-hydroxy-β-cyclodextrin (Sigma-Aldrich, UK) with 2–4 drops of DMSO had no significant effect on Aδ- or C-fibre responses to dural stimulation or characterisation of the cutaneous receptive field. The control vehicles had no significant effect on blood pressure.

Discussion

In the present study it has been demonstrated that intravenous administration of orexin A is able to significantly inhibit the Aδ-fibre responses of TNC neurons to electrical stimulation of the dura mater surrounding the MMA by a maximum of 30%. Orexin A has been shown previously to inhibit significantly cell firing in the TNC following microinjection into the posterior hypothalamus in response to dural electrical stimulation and noxious thermal stimulation of the facial skin in the rat (Bartsch et al., 2004b). Orexin A also inhibits neurogenic dural vasodilation in a model of peripheral trigeminal nerve activation that measures dilation of dural blood vessels in response to electrical stimulation of a closed cranial window (Chapter 4). The selective OX_1 receptor antagonist SB-334867, while having no effect when given alone, was able to block completely the orexin A induced inhibition of Aδ-fibre responses to dural stimulation and the observed decrease in spontaneous activity. Orexin A has a high affinity for the OX_1 receptor and the present study demonstrates that the inhibition of Aδ-fibre responses to dural electrical stimulation and decrease in spontaneous activity is specific to activation of this receptor.

In the current experimental model intravenous administration of orexin B had no effect on any of the aspects studied. This is in contrast to the central administration of orexin B in the hypothalamus, which demonstrated a pro-nociceptive effect (Bartsch et al., 2004b). The lack of effect of orexin B is not unsurprising and is likely to be due to its low lipophilicity resulting in poor brain penetrability. Orexin B is also subjected to a high rate of metabolism in the blood (Kastin and Akerstrom, 1999), resulting in low levels of the intact peptide in the brain following intravenous administration. Orexin A in contrast is highly lipophilic and rapidly enters the brain (Kastin and Akerstrom, 1999) as well as being poorly metabolised in the liver resulting in a relatively long half-life when compared to other peptide hormones (Ehrstrom et al., 2004). Therefore one can speculate that the lack of effect of orexin B in this model is due to the intravenous route of administration rather than a lack of effect in the TNC, perhaps microiontophoretic application directly into the TNC will elucidate its effect in this region more definitively. SB-334867 has been shown to be the most specific of the OX_1 receptor antagonists

developed, demonstrating a 50-fold selectivity over the OX_2 receptor and 100-fold selectivity over other molecular targets including the 5-$HT_{2B/C}$ receptors. Intravenous administration of SB-334867 reversed the orexin A induced inhibition and this is in agreement with its known blood-brain barrier penetrability and *in vivo* activity (Randeva et al., 2001).

This data is in agreement with behavioural studies in which intravenous (Bingham et al., 2001) and intrathecal (Yamamoto et al., 2002; Yamamoto et al., 2003a) administration of orexin A produced analgesic effects; whereas orexin B had no effect (Yamamoto et al., 2002). The widespread distribution of the orexins and their receptors throughout the CNS including the hypothalamus, periaqueductal gray (PAG) and lamina I, II and X of the spinal cord in a variety of experimental animals (Peyron et al., 1998; Trivedi et al., 1998; van den Pol, 1999), all areas involved in nociceptive processing provide the possibility for further research into the role of the orexins in migraine. Intravenous orexin A could be eliciting its effects on a number of structures including the descending inhibitory pathways arising in the cortex and hypothalamus before passing through the PAG and nucleus raphe magnus and terminating in the dorsal horn of the TNC (Messlinger and Burstein, 2000). Other possible sites of action include a direct action via spinal cord mechanisms (Yamamoto et al., 2002) and a proposed effect at the peripheral terminals of primary afferents (Bingham et al., 2001), supported by the ability of orexin A to inhibit neurogenic dural vasodilation in the intravital microscopy model via inhibition of pre-junctional release of calcitonin gene-related peptide from trigeminal neurons (Holland et al., 2005).

The presence of a novel tonic inhibitory orexin drive has been postulated. Bingham *et al.* (2001) demonstrated a pro-hyperalgesic effect of SB-334867 in the carrageenan-induced thermal hyperalgesia test. The presence of direct orexinergic projections from the hypothalamus to the spinal cord (van den Pol, 1999), raise the possibility of an endogenous descending orexin inhibitory drive. This drive is thought to be activated in response to chronic inflammatory nociceptive stimuli as it is not seen in acute nociceptive behavioural studies (Yamamoto et al., 2002). It is reasonable to assume that

the lack of effect of administration of SB-334867 on its own may be due to the acute nociceptive stimuli used in the present study. The dose of SB-334867 must also be considered as it has been reported that SB-334867 only demonstrates *in vivo* effects at concentrations higher than that needed to block the actions of orexin A (Ishii et al., 2004).

This study supports the emerging theory for a role of the orexins in the modulation of nociceptive processing and further highlights the possible anti-migraine therapeutic benefits of manipulating the orexinergic system. The method of administration used in this study does not allow the identification of exact sites of action and further studies are required to clarify this.

Chapter 6 - Orexin 1 and 2 receptor activation in the periaqueductal gray modulates dural nociceptive input to the trigeminal nucleus caudalis in the rat.

Introduction

The electrophysiological basis for studying trigeminal second order neurons is covered in the general introduction and in chapter 6. In summary activation or the perceived activation of the trigeminovascular system is thought to underpin the pain component in migraine (Goadsby et al., 2002b). The psudo-unipolar trigeminal neurons arising from the trigeminal ganglion innervate the pain-producing dural structures and synapse on second order projection neurons within the TNC. An increased understanding of the mechanisms and the pharmacological profile of these second order trigeminal neurons has major implications for understanding the pathophysiology and treatment of migraine. The trigeminal second order neurons receive inputs from a variety of descending modulatory pathways from higher brain and cortical structures. One such pathway originates in the cortex and hypothalamus and passes via the PAG and nucleus raphe magnus to the TNC where it has potent inhibitory effects (Messlinger and Burstein, 2000; Millan, 2002). Therefore, as well as establishing an understanding of the ascending nociceptive pathways an increased understanding of the descending inhibitory systems is of great importance to the pathophysiology and treatment of migraine. The PAG is dealt with in more detail in the general introduction, briefly it is known to play an important role as an anti-nociceptive modulatory structure in animal models of pain (Reynolds, 1969; Behbehani, 1995). Imaging studies have demonstrated migraine specific (Derbyshire et al., 1994; May et al., 1998c) activation of the rostral brainstem including the PAG during spontaneous and triggered migraine attacks, which continued even after headache relief (Weiller et al., 1995; Bahra et al., 2001).

The ventrolateral column of the PAG (vlPAG) selectively receives input from trigeminovascular afferents (Oliveras et al., 1974; Keay and Bandler, 1998; Hoskin et al., 2001) and its stimulation can inhibit trigeminovascular specific nociception (Knight and Goadsby, 2001; Knight et al., 2002; Knight et al., 2003). Interestingly it has also been demonstrated that microinjection of the anti-migraine 5-$HT_{1B/1D}$ receptor antagonist naratriptan into the vlPAG selectively inhibits Aδ- and C-fibre responses to dural

electrical stimulation raising the possibility that the triptans may exert part of their anti-migraine action within the PAG (Bartsch et al., 2004a).

The orexins are two hypothalamic peptides (de Lecea et al., 1998) present in projections throughout the neuroaxis including those to the PAG. The orexinergic system has been implicated in the regulation of many physiological processes including feeding, sleep and the neuroendocrine system (Date et al., 1999; Willie et al., 2001; Backberg et al., 2002). The orexins have also been linked with a possible role in the modulation of nociceptive processing (Peyron et al., 1998; Bingham et al., 2001; Backberg et al., 2002; Yamamoto et al., 2002). The orexinergic system projects to multiple neuronal systems (Peyron et al., 1998) and is a possible mechanism by which the hypothalamus can influence nociceptive processing in the TNC, either directly or via relays in the PAG and nucleus raphe magnus. Bartsch *et al.* (2004) demonstrated that microinjection of orexin A and B into the posterior hypothalamus had differential effects on the modulation of nociceptive meningeal and facial input to the TNC. It has also been shown that destruction of the posterior hypothalamus in rats causes transient hyperalgesia (Millan et al., 1983) indicating a possible role in maintaining basal nociceptive threshold.

The purpose of this study was to investigate further the role of the orexins in nociceptive processing by examining the effect of activation of the OX_1 and OX_2 receptors in the vlPAG on dural nociceptive input to the TNC. The study also aimed to dissect out the receptor pharmacology of any response by utilising the novel OX_1 receptor antagonist SB-334867. Orexin A, B and SB-334867 were microinjected into the vlPAG and the responses of neurons in the TNC were examined in relation to dural stimulation and nociceptive and non-nociceptive activation of the facial receptive field.

Materials and Methods

Animals

Twenty rats weighing 290–330 g were used in this study. All animals reported had normal physiological variables (mean ± SE): blood pressure, 100 ± 16 mmHg, and respiratory parameters, pH 7.4 ± 0.2, pCO2 4.2 ± 0.5, throughout the study.

Surgical procedures

Following the preparatory surgery, detailed in the general material and methods section, the skull was exposed and the right or left parietal bone thinned and removed, a bore hole was then drilled above the coordinates for the ipsilateral vlPAG: 1.36 mm rostral and 0.5–0.7 mm left of the midline (Paxinos and Watson, 1998). A partial C1 laminectomy was performed and the underlying dura mater dissected to reveal the spinal cord. A stimulating electrode was placed on the dura mater surrounding the MMA and a recording electrode lowered into the cervico-medullary junction until a neuron responsive to dural and ophthalmic facial receptive field stimulation was located.

PAG microinjection

A multi-barrelled glass capillary unit with a total tip diameter of no more than 75 μm was stereotaxically positioned at the coordinates for the ipsilateral vlPAG: 1.36 mm rostral and 4.2 mm dorsal from the interaural point, 0.5–0.7 mm left of the midline (Paxinos and Watson, 1998). Experimental drugs, controls and pontamine sky blue were slowly injected over a period of 30–90 seconds in a volume of 100–200 nl.

Experimental Protocols

Trains of 20 stimuli at 0.6 Hz were delivered at five minute intervals to assess the baseline response to dural electrical stimulation. Responses were analysed using post-stimulus histograms with a sweep length of 100 ms and a bin width of 200 μs, that separated Aδ-fibre and C-fibre activated responses in relation to their conduction

velocities. An interval of spontaneous activity was recorded for 120–180 seconds preceding any dural stimulation from the peri-stimulus histogram.

Once a neuron with convergent inputs from the dura mater and ophthalmic dermatome of the trigeminal nerve was identified responses were tested using the following protocol:

1. Three baseline collections of dural stimulation and a single receptive field characterisation.
2. Orexin A, B or control vehicle microinjection.
3. Dural stimulation collections at 5, 10, 15, 20, 25, 30, 45 and 60 minutes with a receptive field characterisation at 20 minutes.
4. SB-334867 or control vehicle microinjection followed by dural stimulation collection at 5 minutes.
5. Repeated steps 2 and 3.

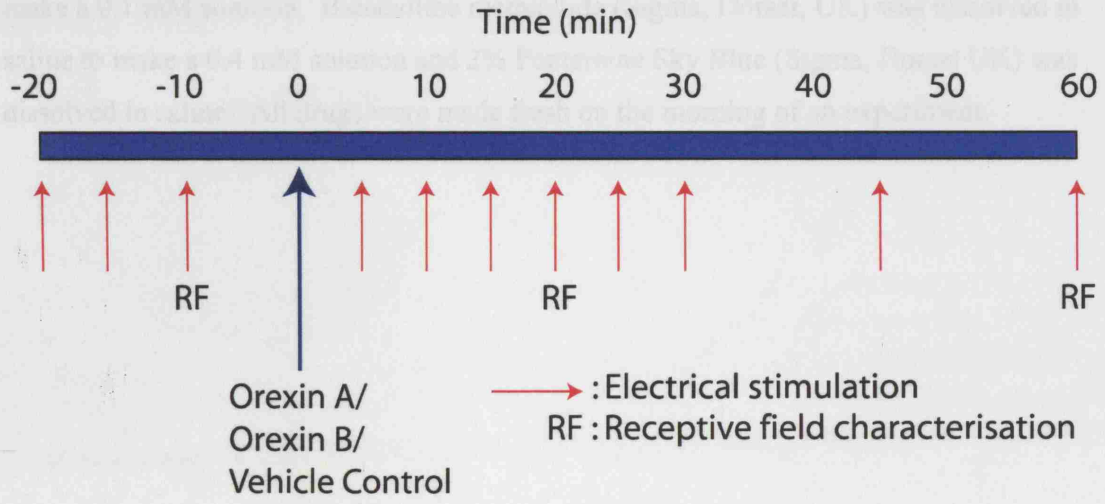

Figure 45: Microinjection orexin electrophysiology protocol.

Data Analysis

Data collected for Aδ-fibre responses represents the total number of cells fired over a 10 ms time period in the region of 4–20 ms post stimulation over the 20 collections. Data collected for C-fibre responses represents the total number of cells fired over a 80 ms time period (20–100 ms post stimulation) from the 20 collections. Spontaneous activity

is measured in cell firing per second (Hz). Effects of drug intervention were analysed using an ANOVA for repeated measures with Bonferroni *post-hoc* correction for multiple comparisons followed by Student's paired *t*-test (SPSS v12.0), using the average of the three baselines for comparisons. When the assumption of sphericity with regards to the factor of repeats was violated, adjustments were made for the degrees of freedom and *P* values according to the Greenhouse-Geisser correction (Field, 2005). Significance was assessed at the $P < 0.05$ levels.

Drugs

The delivery of anaesthetic and neuromuscular blocker was all via the same femoral catheter. Orexin A and B (Tocris Cookson, Bristol, UK) were dissolved in distilled water to make a 0.1 mM solution. N-(2-Methyl-6-benzoxazolyl)-N''-1,5-naphthyridin-4-yl urea (SB-334867, GlaxoSmithKline, Hertfordshire, UK) was dissolved in DMSO to make a 0.1 mM solution. Bicuculline methiodide (Sigma, Dorset, UK) was dissolved in saline to make a 0.4 mM solution and 2% Pontamine Sky Blue (Sigma, Dorset UK) was dissolved in saline. All drugs were made fresh on the morning of an experiment.

Results

Recordings were made from 21 neurons all of which were WDR responsive to dural MMA stimulation and cutaneous receptive fields restricted to the ophthalmic and maxillary dermatome (figure 46A) of the trigeminal nerve. All neurons showed a mechanosensitive dural receptive field that was confined to the vicinity immediately surrounding the MMA or one of its branches (figure 46B). Neurons were found in laminae III to VI of the dorsal horn at the level of the cervico-medullary junction at a depth of 450–950 μm (figure.) and electrode placement was confirmed in 18 animals via an electrolytic lesion in the TNC (figure 47). Microinjection sites were restricted to the area of the vlPAG (figure 47). Neurons with Aδ-fibre inputs had latency to activation after dural stimulation of 16 ± 0.3 ms, while neurons with C-fibre inputs had latency to activation of 52 ± 3 ms. The baseline spontaneous firing rate for the cohort of neurons studied was 41 ± 2 Hz.

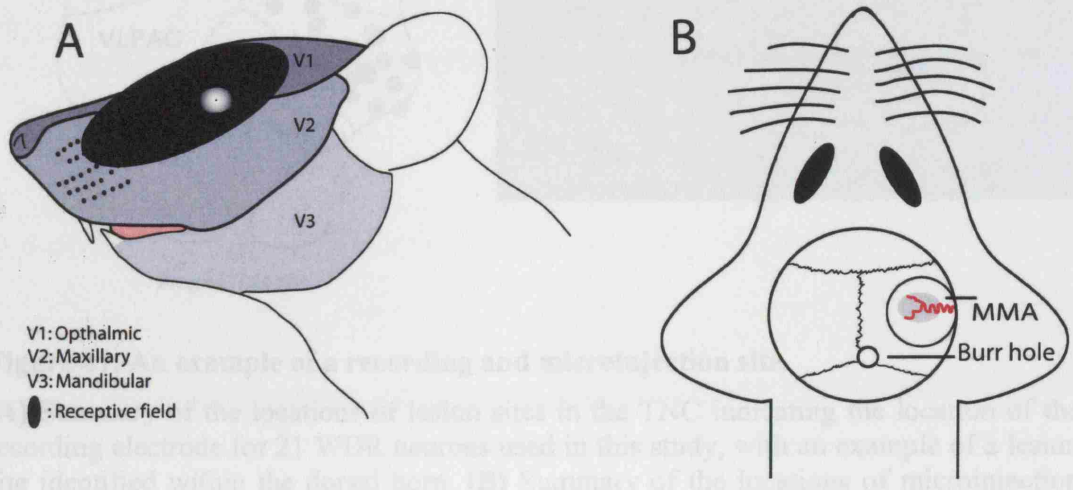

Figure 46: An example of receptive field locations for a convergent trigeminal nucleus caudalis neuron responsive to dural electrical and facial receptive field stimulation.

(A) Cutaneous receptive field **(B)** Mechano-sensitive receptive field restricted to the vicinity of the MMA.

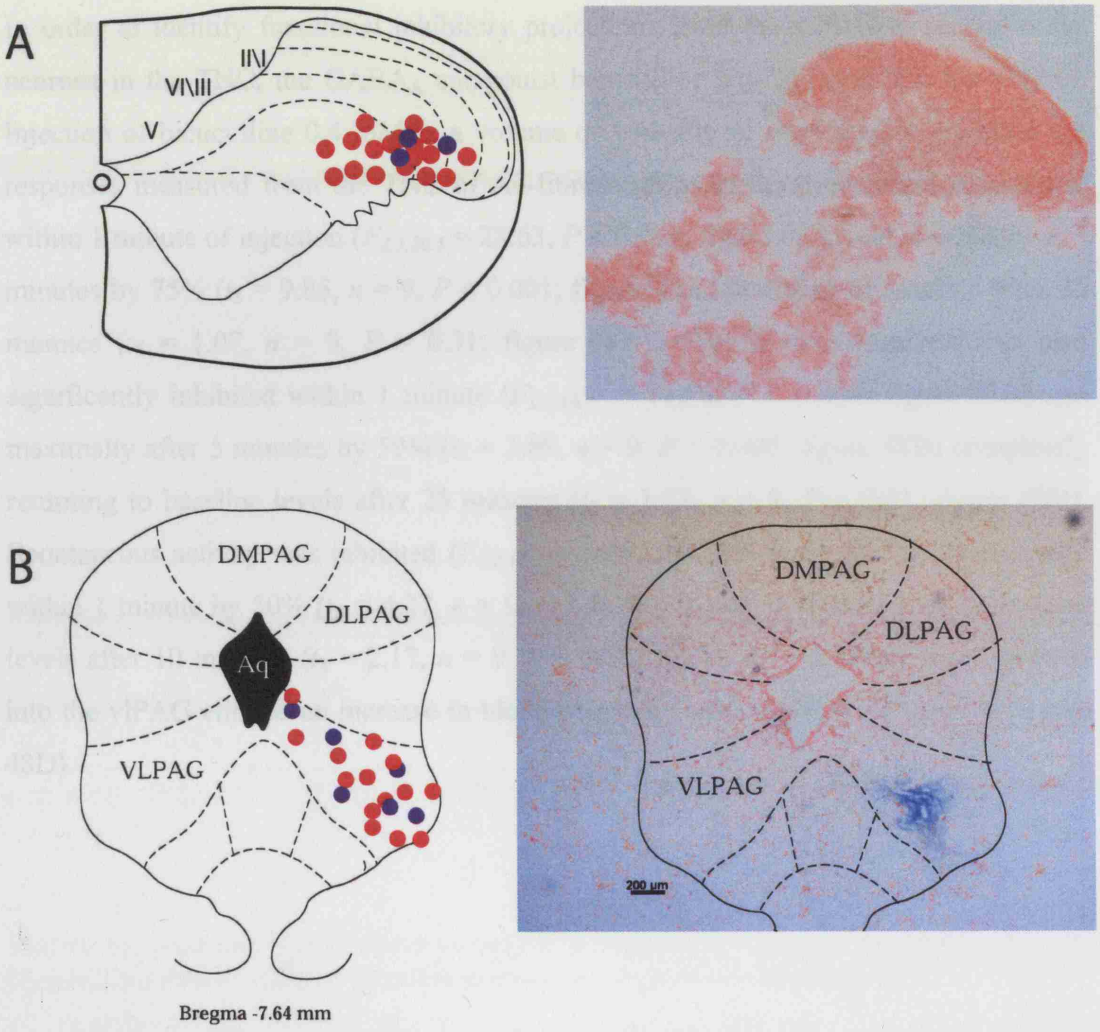

Figure 47: An example of a recording and microinjection site.

(A) Summary of the locations of lesion sites in the TNC indicating the location of the recording electrode for 21 WDR neurons used in this study, with an example of a lesion site identified within the dorsal horn. **(B)** Summary of the locations of microinjection sites in the vlPAG used in this study, with an example of a pontamine sky blue injection (100–200 nl) to demonstrate location and spread of compounds. Red circles, lesion/microinjection site found; blue circles, site recreated from micro drive readings. DMPAG, dorsomedial periaqueductal gray; DLPAG, dorsolateral periaqueductal gray; VLPAG, ventrolateral periaqueductal gray.